



TETRA TECH EM INC.

August 19, 2011

Lynn Nakashima
Department of Toxic Substances Control
Project Manager
700 Heinz Avenue
Berkeley, CA 94710

**Subject: University of California, Berkeley, Richmond Field Station
Response to DTSC Comments on the Technical Memorandum for Well Destructions,
DTSC Site Investigation and Remediation Order I/SE-RAO 07/07-004 Section 5.16**

Dear Ms Nakashima:

Please find enclosed the August 19, 2011 Final Technical Memorandum for Well Destructions. This version updates the version submitted August 25, 2010 and incorporates all the edits requested by your October 4, 2010 letter.

If you have any questions or need further information regarding this submittal, please contact me at 510-302-6283.

Sincerely,



Jason Brodersen

Enclosure

cc: Greg Haet, UC Berkeley
Karl Hans, UC Berkeley
Anthony Garvin, UC Regents
Bill Marsh, Edgcomb Law Group



August 19, 2011

Greg Haet
EH&S Associate Director, Environmental Protection
Office of Environment, Health & Safety
University of California, Berkeley
University Hall, 3rd Floor #1150
Berkeley, CA 94720

**Subject: Technical Memorandum for Well Destructions
Richmond Field Station, Richmond, California**

Dear Mr. Haet:

Tetra Tech EM Inc. (Tetra Tech) was contracted by the University of California (UC) Berkeley to prepare a permanent destruction plan for 18 wells no longer in use at the Richmond Field Station (RFS), in Richmond, California. This application discusses the history and construction specifications of the wells where available, current conditions of the wells, and proposed destruction methods.

Site History

The RFS property is owned by The Regents of the University of California and is located at 1301 South 46th Street in Richmond, California, in western Contra Costa County. RFS is bordered by Meade Street, off Interstate 580, to the north; by South 46th Street to the east; by the East Bay Regional District Bay Trail to the south; and by Meeker Slough and Regatta Boulevard to the west. Prior to UC's purchase of the RFS property, the California Cap Company used the property for manufacturing of explosives from the late 1800s until 1948. In 1950, UC purchased the property primarily for research facilities for the UC Berkeley College of Engineering; later, other campus departments used portions of RFS.

The 170-acre property consists of four main areas:

- 96 acres of uplands, used for academic institutional activities
- Approximately 7.5 acres of tidal salt marsh
- 5.5 acres of marsh-edge habitat and transition area
- Approximately 61 acres south of the East Bay Regional Park District's Bay Trail, known as the outboard area, consisting of tidal mud flats, marsh, and open water

Most of the wells proposed for closure are located in the Geosciences Well Field, located west of Building 300 as shown on Figure 1. This area has not been developed by UC Berkeley or previous site owners, as determined through Sanborn maps and a review of historical aerials. The geology in this area appears to be alternating layers of clays, gravels, and sands (Pouch 1987).

Background Information Research

Tetra Tech conducted exhaustive file reviews and personnel interviews in order to obtain all information available pertaining to the wells proposed for destruction. All wells were inspected and measurements of depth to water and depth to bottom (or obstruction) were recorded in July 2010. A summary of the files reviewed and contacts made is presented below. Information gathered is summarized in the Well Construction Specifications following this section.

- Tetra Tech interviewed staff at UC Berkeley's Office of Environment, Health & Safety, College of Engineering, and RFS. Tetra Tech reviewed all historical information in RFS files, including aerial photographs, Sanborn maps, and documentation related to previous well decommissioning in a nearby former RFS Research Well Field.
- Tetra Tech contacted Linda Vida of the UC Berkeley Water Resources Library. Ms. Vida performed a search of the library's records for information pertaining to the well field. Ms. Vida contacted professors who had performed research at the well field. These contacts included researchers at UC Berkeley, Lawrence Berkeley National Laboratory, Lawrence Livermore National Laboratory, and EMI Schlumberger, Inc. A summary of the information is presented in the following section.
- Tetra Tech reviewed the California Department of Water Resources files; no information regarding the RFS property was identified.
- Tetra Tech contacted EMI Schlumberger, Inc. who leases space in Building 300 and uses some of the wells in the Geosciences Well Field for testing equipment used in cross-well electromagnetic imaging. David Alumbaugh, an advisor to EMI Schlumberger, Inc. and researcher at UC Berkeley, provided information on boreholes drilled prior to 1992 which is included as Attachment 1. Mr. Alumbaugh's information supplemented the information provided in Dimitri Bevc's 1989 (Attachment 2) Master thesis and Gregory Pouch's 1987 Master thesis (Attachment 3).

Well Construction Specifications

Geosciences Well Field

Fifteen of the eighteen wells to be closed are located in the Geosciences Well Field which consists of a total of twenty five existing wells. Ten wells in the well field will remain open for continued use by EMI Schlumberger, Inc. and UC Berkeley researchers. The borings in the geosciences well field have predominantly been used for experiments involving equipment which maps underground geologic features through electro-resistivity and electromagnetic imaging techniques. Most well completion records and boring logs could not be located, have not been confirmed, or are not known. Following is the available information gathered on the installation and use of these wells.

In August and September of 1986, Smitty's Drilling of Oakland drilled two 6-inch, INJ and EXT, and six 4-inch wells, including OBS 5 and 6 (Pouch 1987). These wells were drilled in support of a borehole-to-

surface resistivity experiment performed by Dimitri Bevc for a 1989 Masters thesis. Wells INJ and EXT have metal pipe casing segments at 21.3 to 22.9 meters (m), 38.7 to 40.2 m, and a metal screen segment between 30.5 and 33.5 m (Bevc 1989). These metal segments were connected by individual cables to a current transmitted at ground surface. The well construction for well EXT was included as an appendix to Bevc's research paper. This log indicates that the plastic sections of EXT were surrounded by cement grout. Based on Bevc's descriptions of the wells, it is assumed that INJ has the same construction. Wells OBS 5 and 6 are 4-inch PVC and are screened at the bottoms of the wells as indicated by Pouch's appendices. Pouch's logs note that the screens were placed in gravel filter packs. It is assumed that the plastic casing was grouted into place with cement as the EXT log indicates.

Wells CAS2, RES1, and RES2 were drilled in 1990. In a 1989 memorandum from Professor Don Lippert of the Earth Sciences Division to UC Berkeley's purchasing department, it appears CAS2 (well 2, CAS 1 is well 1 which will remain open) was drilled to 100 feet (See Attachment 4, the wells are referred to as wells 1 through 6, not their current designations; wells 5 and 6 from this memo will remain open). The memorandum specified that the first 20 feet be 4-inch slotted PVC backfilled with gravel. The rest of the casing was to be 4-inch steel which would be cemented into place using the mixture, "90% cement, 10% bentonite, mixed with salt water. For every 100 lbs of cement add 10 lbs of salt and mix with standard drinking water" (Lippert 1989). According to the memorandum, RES1 and RES2 (wells 3 and 4) were to be drilled to a depth of 160 feet. The information provided in Alumbaugh's 1992 paper states that they were drilled to 100 feet. There is no known indication of their final depth. In Professor Morrison's files, drilling notes from Pitcher Drilling Co. were found for four of the six wells drilled in 1990; however, the RES well logs were missing. The Lippert memorandum specifies that the RES wells were to be open at the bottom and starting at the bottom the first 2 feet were to be 4-inch steel casing, followed by 8 feet of 4-inch PVC casing, alternating until the last section which was to be 10 feet of PVC casing. These wells were to be cemented following the specifications outlined above. When these wells were measured for depth in July 2010, an obstruction was encountered at 10 feet bgs. Alumbaugh's 1992 research states that these wells had a series of downhole electrodes grouted in place for the purpose of making crosshole resistivity measurements. This statement was confirmed during an interview with Frank Morrison who recalled the installation of these two wells for use by the Lawrence Livermore National Laboratory researchers.

The remaining wells in the Geosciences Well Field (Mb, RFS#23, RFS#24, RFS#28, SF1, SF2, SF3, and SF4) are of unknown origin. Professor Frank Morrison did not have any recollection of why or when they were drilled. Mike Wilt of EMI Schlumberger, Inc. recalled that the SF wells were shallow borings used to test the conductivity of different muds and cements. He could not recall who was performing this research or a date that the research or drilling occurred. No information was found pertaining to Mb, RFS#23, or RFS#28. RFS#24 is located in the field east of Building 300. No information could be found pertaining to its installation or use except that it was installed between November 2004 and February 2006.

Three other wells

Three of the eighteen wells proposed for destruction are located outside of the Geosciences Well Field.

500- S: This located south of Building 177 well is believed to be one of the wells from the Research Well Field installed in the 1950s as part of a state-funded research project on deep well injection and contaminant transport. The majority of these wells were closed in 2006; however, three wells could not

be located for the closures performed by Stellar and Associates in 2005. Based on its location and construction, this well is believed to be 500-South, one of the previously un-located wells. According to 1954 report by James Hunt, this well was completed in February 1953 to a depth of 104 feet. The specifications of the observations wells from the 1950's well field show that this well has a 6-inch steel slotted casing (from 96-103 feet bgs) with 28 slots each measuring 1/8-inch wide by 6 inches long. These wells had no annular space, filter pack material, or annular pollution seal.

The final two wells (RFS# 25 and RFS# 26) to be closed are large steel-cased wells by Building 175. These wells have been labeled 'two water supply wells' on historic maps and are believed to have been water supply wells for the California Cap Company's operations. RFS facilities personnel stated that as late as the 1980's water was being pumped from one of the wells for irrigation. The pump has been removed and the facilities crew measured the two wells to be steel-cased 30 inches and 20 inches in diameters, and approximately 33 and 36 feet deep.

Well Decommissioning and Destruction Methods

Most of the steel-cased wells will be grouted at the lowest screened interval (that can be reached with the tremie pipe) through approximately 2-inch-diameter steel pipe with a neat cement mixture as specified in the Contra Costa County Health and Safety Division "Annular Seal and Well Destruction Materials". This grout will be allowed to harden before the well casing is ripped with a Mills knife if possible from the grout to 6 feet bgs. If some of the casings are off-set or collapsed preventing advancement of the Mills knife, Contra Costa inspectors will be consulted for approval to grout without perforation, as was the case for the 1950's Research Well Field. A column in Table 1 specifies intervals for high density perforation. This high density perforating will help to re-establish the integrity of fine-grained, low-permeability strata. Finer-grained strata were identified based on available boring logs which are provided in the Attachments following this report.

If fine-grained intervals cannot be identified based on available data, the use of natural gamma logging should be considered.

Following the ripping with the Mills knife, the borings will be tremie-grouted by lowering approximately 2-inch-diameter steel pipe to the depth of the previously-grouted interval, and pumping the wells from the bottom up with well sealing material. Casing material will be removed to ground surface and grout will be brought to the top of the casing.

Wells RFS#25 and RFS#26 are located in Building 175. Based on the layout of the building, there is no access to equipment necessary for overdrilling equipment; therefore, these wells will be grouted to the surface under the supervision of Contra Costa County inspectors.

The shallow PVC-cased wells will be overdrilled and tremie-grouted to surface.

All soil and casing material from the overdrilling process will be containerized and analyzed for waste characterization purposes. A summary of the well construction information and proposed destruction methods is presented in Table 1.

RES1 and RES2 will be considered closed in place given their construction specifications. These two borings were drilled as part of a geolithic study and had no slotting in the casing and were not developed as wells. These borings were used by researchers to hold sensors underground at specific depth intervals. The sensors were lowered into the casings then grouted into place. When these borings were drilled, the researchers specified that the outer grout material be mixed with salt water, as described above. Tetra Tech consulted chemists within Tetra Tech as well as a UC Berkeley professor. Each professional stated that high sodium chloride concentrations are often used to accelerate the curing process and to gain strength and should not affect the long term stability of the grout. They also stated that the salt could potentially corrode the steel casing. According to the design specifications, the casings for RES1 and RES2 were to be 2 feet of steel casing followed by 8 feet of PVC casing, so only 20 percent of the casing is steel. The casing is enclosed in grout on the inside and outside of the casing; therefore, the stability of the borings as a whole are considered intact and comparable to a closed boring, which is in essence, a column of grout. This conclusion is backed up by a 1964 study, "The Effect of Salt in Concrete on Compressive Strength, Water Vapor Transmission, and Corrosion of Reinforcing Steel" which is included as Attachment 5 to this report.

Table. 1. Well Summary and Proposed Well Destruction Methods

WELL NAME	DIAMETER and MATERIAL	TOC to BOTTOM OF WELL (July 2010)	ORIGNIAL DEPTH	YEAR INSTALLED	PROPOSED HIGH DENSITY PERFORATION INTERVAL	PROPOSED DESTRUCTION METHOD
INJ	6" PVC and Steel	106'	131'	1986	80' – 90' & 100-120'	Rip with Mills knife, power grout
EXT	6" PVC and Steel	119.2'	131'	1986	25' – 40' & 90' – 105'	Rip with Mills knife, power grout
OBS5	4" PVC	104.5'	98'	1986	25' - 40' & 105' - bottom	Rip with Mills knife, power grout
OBS6	4" PVC	101.6'	98'	1986	75' - bottom	Rip with Mills knife, power grout
CAS2	4" PVC and Steel	78.8'	98'	1990	25' – 40' & 90' – 105'	Rip with Mills knife, power grout
RES1	4" PVC and Steel	10'	160' or 98'	1990	NA	Overdrill top 10 feet, consider closed in place
RES2	4" PVC and Steel	9.10'	160' or 98'	1990	NA	Overdrill top 10 feet, consider closed in place
Mb	6" PVC	25.75'	Unknown	Unknown	NA	Overdrill casing, grout boring
RFS#23	4" PVC	10.1'	Unknown	Unknown	NA	Overdrill casing, grout boring
RFS#28	4" PVC	10.2'	Unknown	Unknown	NA	Overdrill casing, grout boring
SF1	4" PVC	9.11'	Unknown	Unknown	NA	Overdrill casing, grout boring
SF2	4" PVC	9.3'	Unknown	Unknown	NA	Overdrill casing, grout boring
SF3	4" PVC	9.9'	Unknown	Unknown	NA	Overdrill casing, grout boring
SF4	4" PVC	10'	Unknown	Unknown	NA	Overdrill casing, grout boring
RFS# 24	4" PVC	20.1'	Unknown	Est. 2005	NA	Overdrill casing, grout boring
500-S	6" Steel	110'	104'	1953	20' – 25' & 55' – 60'	Rip with Mills knife, power grout
RFS# 25	30" Steel	32.5'	Unknown	Unknown	NA	Grout to surface
RFS# 26	20" Steel	11'	36'	Unknown	NA	Grout to surface

Groundwater Sample Results

Groundwater sampling results obtained during the first and second round of groundwater sampling as part of the Field Sampling Workplan Phase I groundwater investigation showed very few exceedances of maximum contaminant levels (MCL). These samples were collected from shallow piezometers (less than 20 feet below ground surface) installed in the fall of 2010 and sampled in November 2010 and again in April 2011. These piezometers are shown on Figure 2 along with groundwater contour data from November 2010. This figure shows that the piezometers cover the entire RFS, and provide chemical and groundwater flow data from both upgradient and downgradient of the wells proposed for closure. This information provides sufficient chemical information to close shallow wells proposed for closure without additional sampling.

Results from the analysis of samples collected during previous well closure activities to the Research Well Field by Stellar Environmental Solutions in 2005 detected concentrations of copper and zinc. Neither analyte exceeded the Soluble Threshold Limit Concentration (STLC) or MCL. These samples were also analyzed for poly chlorinated biphenyls (PCB) and volatile organic compounds (VOC), both of which were reported as non-detect. These wells were also sampled for radionuclides; all data was reported as within background ranges.

The 2005 samples helped to characterize groundwater in the central portion of the RFS. Conditions in the deeper groundwater zone in the Geosciences Well Field area are unknown. Therefore, wells OBS6 and EXT will be sampled and analyzed for pesticides, polychlorinated biphenyls (PCB), semi-volatile organic compounds (SVOC), total extractable petroleum hydrocarbons (TPH-e), total purgeable petroleum hydrocarbons (TPH-p), polycyclic aromatic hydrocarbons (PAH), and VOCs. These two wells are located in the northern and southern ends of the Geosciences Well Field. They both have screened intervals that are still exposed (not silted up). The groundwater samples will be collected consistent with the protocols outlined in the Field Sampling Workplan dated June 2, 2010 and will follow the quality control measures for both field work and data analysis as outlined in the accompanying Quality Assurance Project Plan. Prior to sampling, the piezometers will be purged and monitored for stabilized parameters consistent with the Field Sampling Workplan.

If you have any questions or comments regarding this submittal, please call me at (510) 302-6283.






Sincerely,

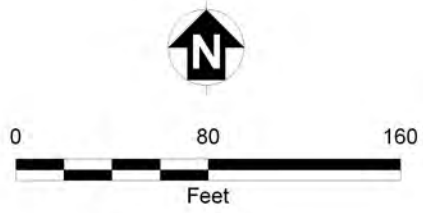


Jason Brodersen, P.G.
Project Manager

FIGURES



-  Geosciences Well
-  Open Well (Not in Use)
-  Building
-  Road Edge and Other Landscape Feature
-  Fenceline

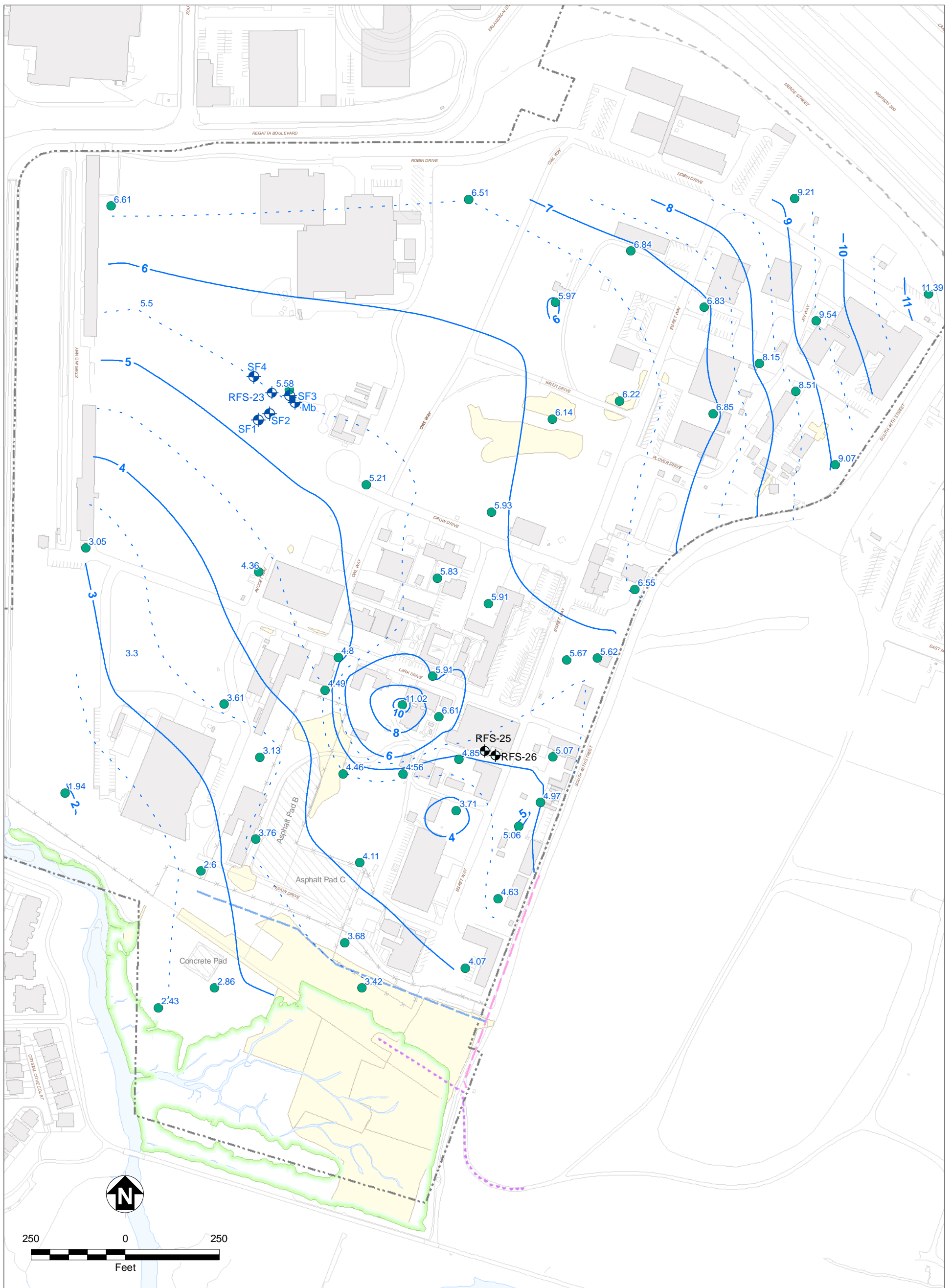


Notes:
Some locations are approximate.



Richmond Field Station
University of California, Berkeley

FIGURE 1
WELLS PROPOSED FOR
CLOSURE AUGUST 2011



- Existing Building
- Asphalt/Concrete Pad
- Remediated Area
- Surface Water
- Marsh Boundary
- Property Boundary
- Approximate Property Boundary
- Roads and Other Landscape Features
- Fenceline
- Shallow Piezometer Location (< 20 ft bgs)
- Biologically Active Permeable Barrier Wall
- Former Seawall (Approximate)
- Slurry Wall
- Groundwater Contour, 1-Foot Interval
- Groundwater Contour, .5-Foot Interval
- Open Well (Not in Use)
- Geosciences Well



**Richmond Field Station
University of California, Berkeley**

**FIGURE 2
SHALLOW GROUNDWATER
ELEVATION CONTOURS,
NOVEMBER 1, 2010**

Note:
bgs below ground surface
ft feet
Groundwater elevations given in ft above mean sea level

ATTACHMENT 1
ALUMBAUGH APPENDIX

Appendix D

The Richmond Well Field and Borehole Logs

This appendix summarizes the well logging information that was obtained during the 1992 Richmond field station experiment. Table A1 provides information on the well field at Richmond Field Station which is shown in Figure 5.1. Through February, 1992 14 wells have been drilled in the 10 acre field west of building 300. These wells were drilled in four separate episodes beginning in 1986.

The first nine wells were drilled in 1986 for a borehole-to-surface resistivity experiment (Bevc and Morrison, 1991). Wells INJ and EXT (not shown in Figure 5.1) are opened through steel-screening to a gravel aquifer at 26-30 m. This screened interval is also used an electrode. There are also two other steel electrodes in each well located 10 m above and below the screened interval. Wells OBS1-6 are plastic-cased observation wells opened only at the bottom of the 30 m casing. These wells were designed for water level measurements although they have also been used as geophysical observation wells.

Wells EMNE and EMSW, which straddle the injection well INJ, were added in 1989 in order to make crosshole EM measurements. These wells are separated by 52 m and penetrate to a depth of 90 m making them the deepest wells in the field. They are sealed at the bottom and are not open to the formation at any point.

In 1990 wells CAS1 and CAS2 were drilled at the southern end of the field (not shown in Figure 5.1) and cased with steel. These wells are designed for experiments involving measurements through steel casing. At this same time two 30m deep wells (RES1 and RES2) were drilled and a series of downhole electrodes grouted in place for the purpose of making crosshole resistivity and MMR measurements. Eight resistivity electrodes, spaced at 3 m intervals, are emplaced in each of these wells beginning at a depth of 9 m.

The most recent set of boreholes (INJ1, EMNW and EMSE) were added in 1992 for the present salt water monitoring experiment. Each of these wells are 70m deep, capped at the bottom and are open to the aquifer at 30m depth.

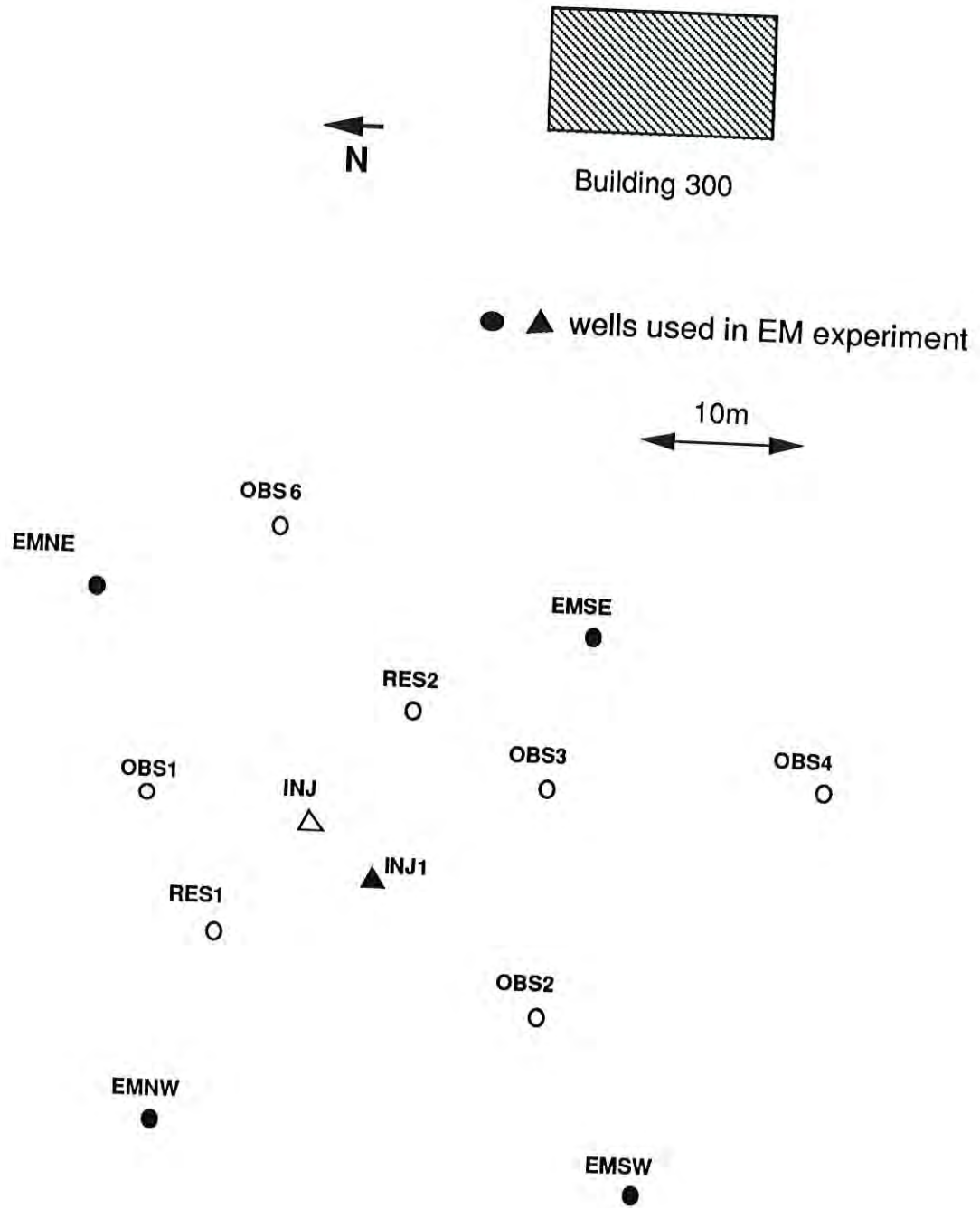


Figure 5.1 - Location map for the building 300 well field at the Richmond Field Station.

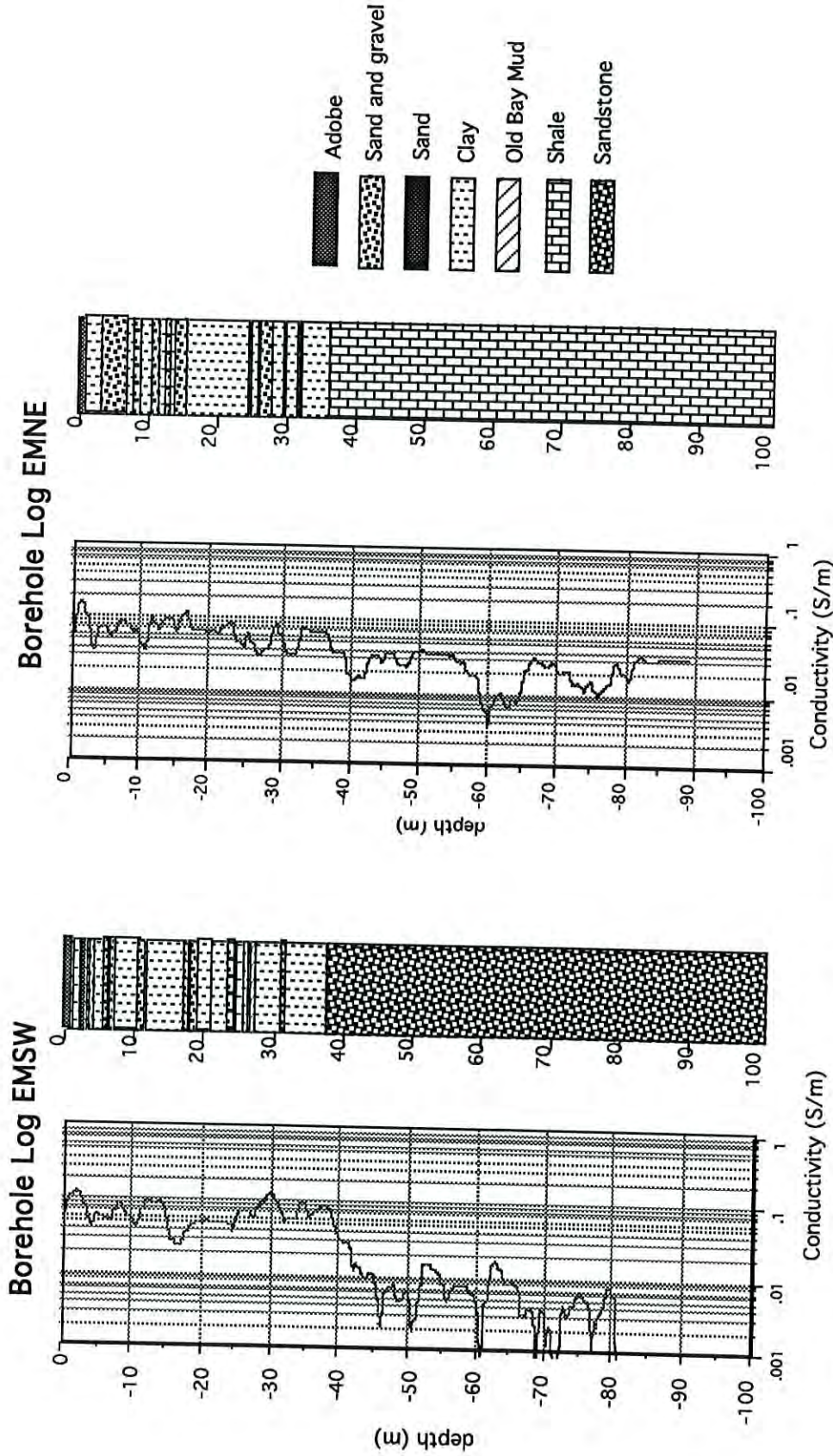


Figure 5.2 - Electrical conductivity and stratigraphic logs for the EMSW and EMNE wells at the Richmond Field Station. The stratigraphic logs were derived from the drill cuttings.

Borehole	Depth(m)	Year Drilled	Casing	Open Interval (m)	Remarks
OBS1	30	1986	4" PVC	at bottom	depth=20m
OBS2	30	1986	4" PVC	at bottom	
OBS3	30	1986	4" PVC	at bottom	
OBS4	30	1986	4" PVC	at bottom	
OBS5	30	1986	4" PVC	at bottom	
OBS6	30	1986	4" PVC	at bottom	
INJ	40	1986	6" PVC	26-30	grouted grouted steel-cased steel-cased
EXT	40	1986	6" PVC	26-30	
EMNE	90	1990	6" PVC	no open int	
EMSW	90	1990	6" PVC	no open int	
RES1	30	1990	-	no open int	
RES2	30	1990	-	no open int	
CAS1	30	1990	4" steel	at bottom	
CAS2	30	1990	4" steel	at bottom	
EMNW	70	1992	6" PVC	26-30	
EMSE	70	1992	6" PVC	26-30	
INJ1	70	1992	6" PVC	26-30	

Table D1 - Richmond Field Station well field.

D1 Borehole induction logs

Baseline borehole induction resistivity logs were recorded in most of the boreholes at Richmond during April 1992 using a Geonics model EM-39 logging instrument. The induction logs that were collected are listed as a function of the well location in table D-2 and are plotted in Figure D-1. Measurements were made at 0.05 m increments as the tool was moving upwards in the borehole. Although five of the wells are drilled to depths of 70 m or more, the induction logs were limited to a depth of 50 m by the length of the available logging cable. Several logs were done twice and typically these repeated to within 5 percent.

A second set of logging data was collected in June, 1992 after the salt water was injected. The only significant difference that was observed was in well INJ1 which is the salt water injection well. Figure D-2 shows both the pre- and post-injection logs that were measured in this well. The difference between the two logs indicates a change in resistivity due to the salt water in the vicinity of the injection well. The largest decrease is observed in a 4 m thick sandy-gravel aquifer at a depth of 26-30 m, where the well is perforated. In this zone the rock has decreased in resistivity from 15 ohm-m to 3.5 ohm-m. A second, thinner zone where the resistivity is different is present from 23 to 25 m depth. These two zones of low resistivity zone around well INJ1 are surprisingly large and suggests that the unconsolidated silts and sands have a fairly high permeability.

borehole	Ind logs	Water conduct
OBS1	yes	yes
OBS2	yes	yes
OBS3	yes	yes
OBS4	yes	yes
OBS5	yes	yes
OBS6	yes	yes
INJ	yes	yes
EXT	no	no
EMNE	yes	no
EMSW	yes	no
RES1	no	no
RES2	no	no
CAS1	no	no
CAS2	no	no
EMNW	yes	yes
EMSE	yes	yes
INJ1	yes	yes

Table D2 - List of the logging data collected during the 1992 Richmond experiment.

Except for well INJ1 we observed no significant changes in well log resistivity due to salt water injection. This includes well INJ, which is located only 5 m northeast of well INJ1. However there were variations noticed in the borehole fluid conductivity at depths from 26-30 m (see next section) which suggest that any perturbations in the resistivity of the open interval (26-30 m) in this well were most likely obscured by the presence of steel screening. Notice that no significant changes in resistivity were observed from 23 m to 25 m depth as had been in borehole INJ1.

D2 Borehole fluid conductivity logs

In addition to the induction logs we also measured the conductivity of the borehole water before and after salt water injection. These measurements are designed to improve the tracking of the salt water and also to provide knowledge of the in-situ groundwater conductivity.

In Figure D-14 the borehole water conductivity profiles measured after the injection are plotted for seven of the wells. Of these seven, high conductivity water (≈ 1 S/m) was found in only two of the wells, INJ1 and INJ. Both these profiles show the water

conductivity increasing towards the bottom of the well with values that approach the conductivity of the injected fluid. Because salt water is more dense than fresh water, this sort of stratification was expected with the salt water occupying the basal layer. (Note: the higher conductivity in INJ when compared to INJ1 is due to INJ1 being flushed out with fresh water after the injection was completed.) In all other wells the groundwater conductivity was the same before and after injection ($\approx 0.08\text{S/m}$).

ATTACHMENT 2
BEVC 1989

**Borehole to Surface Electrical Monitoring
of a Salt Water Injection Experiment**

By

Dimitri Bevc

B.A. (University of California) 1984

THESIS

Submitted in partial satisfaction of the requirements for the degree of

MASTER OF SCIENCE

in

ENGINEERING

MATERIALS SCIENCE AND MINERAL ENGINEERING

in the

GRADUATE DIVISION

of the

UNIVERSITY OF CALIFORNIA at BERKELEY

Approved:

..... *D.J. Morrison* *Sept 12 1989*
Chair *Alex Bech* Date *Sept 12, 1989*
..... *Paul A. Witherspoon* *Sept. 5, 1989*

Chapter One

Experimental Setting

The experiments took place in February 1988 and February 1989 at the University of California Richmond Field Station, an industrial area adjacent to San Francisco Bay and about six miles northwest of the Berkeley Campus. The site was chosen for its accessibility, suitable geological conditions and the availability of a supply of salt water for fluid injection. The well field is located in an open area 400 m north of San Francisco Bay.

Eight wells were drilled to depths ranging from 30 to 40 meters (Figure 1.1) through a section of unconsolidated clay and silt with intermittent lenses of sand and gravel. Analysis of the driller's logs shows that several of the clay horizons can be traced throughout the well field but that many sand and gravel bodies are lenticular connecting three or four of the wells at most (Pouch, 1987). A geologic section at well EXT is presented in Figure 1.2 (After Asch, 1986) as an illustration of the stratigraphy in the field area and the well construction. Pouch (1987) described the rocks as predominantly a deltaic sequence consisting of deposits from San Pablo and Wildcat Canyon Creeks.

Several geophysical methods have been used to characterize the geology of the field site. Among these methods are seismic, electrical resistivity (Wilt et al., 1987), time domain electromagnetics (Wilt and Zollinger, 1986) and a borehole induction log survey (Bevc, 1987). The data from these experiments are adequately interpreted by a four layer model. The surface layer is two meters thick and has a resistivity of 17 ohm-m when dry, and 5 ohm-m when saturated. This is underlain by a thin layer with conductivity thickness product of about 0.5 S and an 11 ohm-m to 13 ohm-m layer extending to a depth of 40 meters and representing the interbedded sequence of deltaic deposits. The whole sequence lies on top of a 50 ohm-m halfspace.

All the wells are cased with PVC plastic. Two of the wells, INJ and EXT, are 15.24 cm (6 inch) in diameter and were designed for fluid injection and withdrawal experiments; these wells have steel sections for current injection. As shown in Figure 1.2 there are metal pipe casing segments at 21.3 m to 22.9 m, at 38.7 m to 40.2 m and a metal screen segment between 30.5 m and 33.5 m. The latter was chosen to allow injection and withdrawal of fluids in the sand and gravel aquifers that are at this depth. The metal electrode segments are connected by individual cables to the current transmitter on the surface. The remaining six holes (OBS1-OBS6) are 10.16 cm (4 inch) diameter wells drilled to depths ranging from 30-35 meters. These wells are open at the bottom and designed for use in water level measurement, downhole water sampling, and subsurface electrical potential measurements.

Piezometric levels were measured in the wells at various dates. These measurements showed that under undisturbed conditions, flow in the vertically confined aquifer was from north to south and the average gradient of the piezometric level was about 0.003. Several pumping tests were carried out in different wells to calculate hydrologic properties of the aquifer. Values of drawdown from observation wells 1, 4, 5, and 6 due to pumping of Well INJ are shown on Figure 1.3 (Javandel, 1987). This figure shows that there is a distinct difference between transmissivity data obtained from Wells 1 and 6. The analysis of this data indicates that the transmissivity of the gravel formation at this location is largest in the west-east direction. Note that these curves represent a point measurement and are aliased in azimuth about the injection well so that they do not sample the bulk ground water flow in all directions.

Salt Water Injection and Extraction Procedure

Salt water for the two injection experiments was obtained from San Francisco Bay and pumped into a 50,000 gallon holding pond 200 meters south of the injection well. Salt and fresh water were pumped into the pond to adjust fluid conductivity. After mixing and settling to remove silt and mud, the water was passed through filters and pumped into the injection well. A total of 25,000 gallons of salt water was injected at an average flow rate of six gallons per minute for 72 hours. The conductivity of the native ground water and the injected salt water were monitored throughout the experiment with a conductance meter. Conductivity probes were located in the injection well just above the screen and at the bottoms of the observation wells.

The conductivity of the native ground water was measured to be 50 to 60 mS/m (20 ohm-m to 17 ohm-m) and the injected salt water was 1.3 S/m and 0.88 S/m (0.76 ohm-m and 1.13 ohm-m) for the first and second experiment, respectively. Since the injection zone is below the water table and the ground water resistivity is known, the resistivity of the intruded formation can be estimated as

$$\rho_{\text{anomalous}} = \rho_{\text{formation}} \left(\frac{\rho_{\text{salt water}}}{\rho_{\text{ground water}}} \right)$$

For a ground water resistivity of 17 ohm-m and a formation resistivity of 11 ohm-m, the intruded zone would have a bulk resistivity of 0.5 ohm-m for the first experiment and 0.75 ohm-m for the second experiment.

Assuming an aquifer thickness of 3 m and a porosity of 20 percent, it is easy to show that a 25,000 gallon (94.5 cubic meter) injection would result in a cylindrical

anomaly of 7 m radius under conditions of isotropic plug flow. No changes in ground water conductivity were measured at the observation wells 15 meters away.

Three days after injection was stopped, extraction was begun from the same well. The salt water was extracted at a rate of 20 gallons per minute for seven days until the outflowing fluid reached the same conductivity as the native ground water. This resulted in a total extraction of 200,000 gallons, eight times the amount injected.

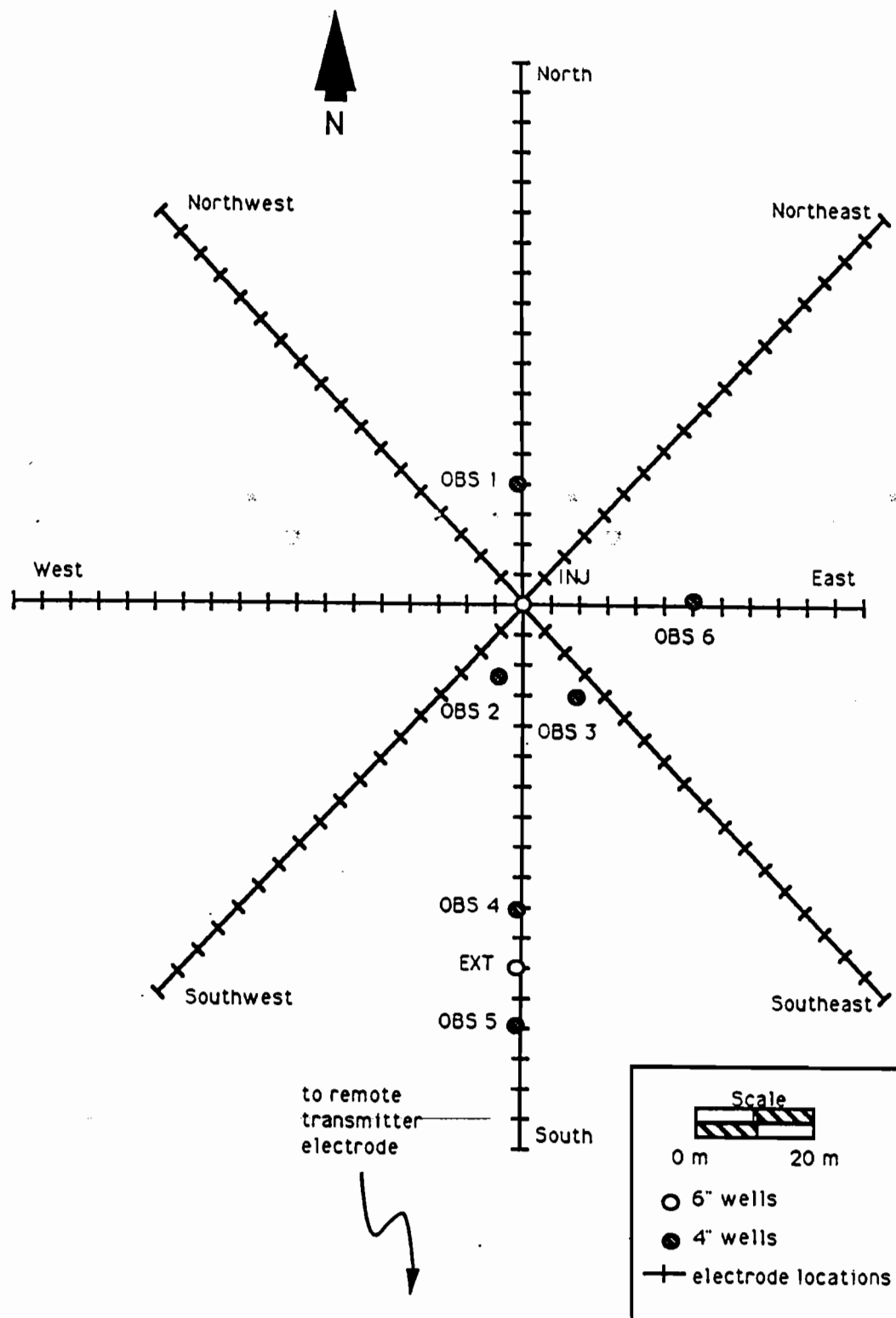


Figure 1.1. Plan map of the well field and resistivity array at the Richmond Field Station.

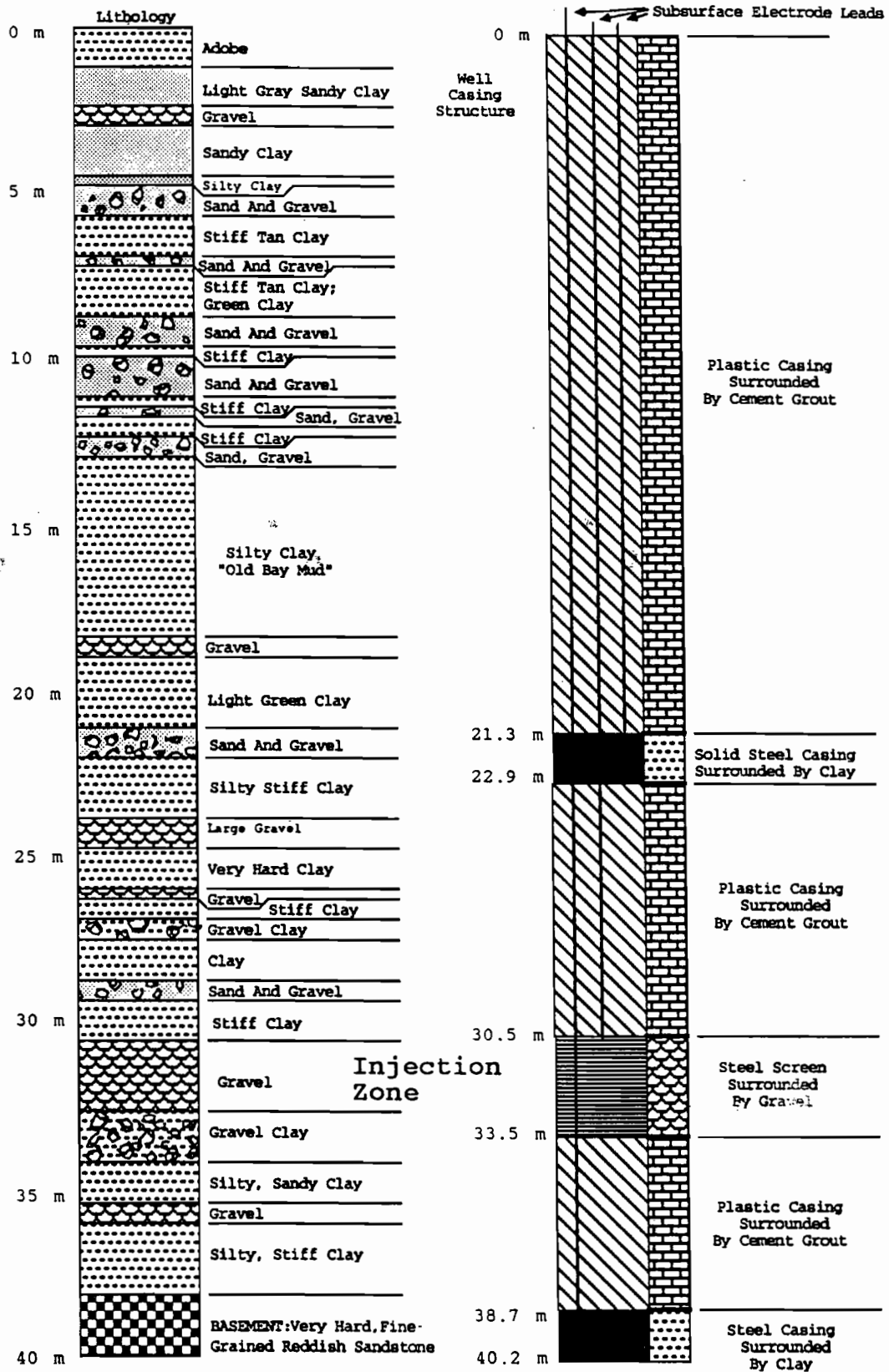


Figure 1.2. Stratigraphy and well construction at well EXT.

ATTACHMENT 3
POUCH 1987

Hydrogeologic Site Assessment of the Engineering Geoscience
Well Field at the Richmond Field Station, Contra Costa County,
California

Gregory W. Pouch

Engineering Geosciences

Department of Materials Science and Mineral Engineering

Hearst Mining Building

University of California, Berkeley

Berkeley, CA 94720

1987

ABSTRACT

The Engineering Geoscience group at the University of California at Berkeley has drilled an Injection, an Extraction, and six observation wells at the Engineering Field Station in Richmond (Richmond Field Station). The group plans to trace an injected slug of saltwater using electrical resistivity.

Analysis of driller's logs indicates that the unconsolidated sediments underlying the field station were deposited in a deltaic environment. In the lower alluvial sequence, depositional strike appears to be east-west. In the fluvial parts of the sequence, lenticular bodies of sand and gravel in a clay matrix serve as the main avenues of conduction, although storage in and leakage through the surrounding clays must be taken into account. There appear to be extensive layers which have been deposited under marine or quasi-marine conditions.

Hydraulic head measurements indicate that the wells are set in at least three different aquifer zones. Pump-test data confirm two of the zones and one pump test indicated significant leakage to the pumped aquifer. A third pump test indicated connection between the Sanitation Engineering Well Field 500' to the east and the southern three wells. The northern and southern wells are not in the same aquifer zone.

1. Introduction

The Richmond Field Station is located in the southeastern quarter of the Richmond Quadrangle (1:24 000), at approximately 37° 55' N, 122° 20' W. (see Figure 1.) The Engineering Geoscience Well Field is located in the field west of Building 300, the Sanitation Engineering Well Field is about 300 feet east of Building 300. (see Figure 2.) The ground surface at the Engineering Geoscience Well Field is about 17' above mean sea level.

The purpose of this investigation is to delineate the geologic and hydrologic conditions underlying the Engineering Geoscience Well Field, with particular regard to contaminant migration paths. This is of interest as part of a study by the Engineering Geoscience group at the University of California at Berkeley to test the feasibility of using surface and borehole-to-surface geophysics to track groundwater contamination (Morrison and others, 1986). The hope is to use electrical resistivity methods to track the movement of the electrically more conductive saltwater to be injected and recovered in the Engineering Geoscience wells. As leachate from municipal landfills, various holding ponds, and other sources often contains an anomalously high concentration of total dissolved solids, this experiment has the potential of assisting in the assessment and remediation of numerous groundwater contamination sites.

In the 1950's, the Sanitation Engineering group did an experiment at the Richmond Field Station on the migration of contamination; this resulted in at least twenty wells drilled and set in a gravel and sand layer which apparently correlates with the Maria gravel (see section on geology, Figure 11, and Appendix 1). The well casings of the Sanitation Engineering wells are severely rusted and it is unlikely that they are open only at their original perforations. Head measurements made in these wells could be misleading due to contact with other aquifer zones (see Davis and DeWiest, 1966, pp. 51-52). The location of the Sanitation Engineering Well Field is shown in Figure 2 and a map of the wells, the well logs, and other data gathered there is included in Appendix 2.

In August and September of 1986, the Engineering Geoscience group had two six-inch (INJ and EXT) and six four-inch (OBS 1 to 6) wells drilled by Smitty's Drilling of Oakland. (see Figure 3 for locations.) The designations of Extraction and Injection wells were based upon an assumed

regional groundwater flow to the south; in reality, all the wells could be used for either purpose. The original names are retained to avoid confusion. The driller's logs are presented as drafted stratigraphic columns in Figures A1-A8 and in Appendix 1, along with the interpreted correlations and inferred environments of deposition. The wells were drilled and constructed under the supervision of Ted Asch, who also took SP, resistance, and gamma-ray logs. (see Appendix 1.) Analysis of some of the geophysical logs confirms the driller's logs, which contain more useful data such as color of some units and occurrence of scattered gravel.

The locations of the wells can be seen in Figure 3, and the surveyed locations are listed in Table 1. Note that "north" refers to grid north determined by the line joining OBS 1, INJ and OBS 4; this closely corresponds to north as determined by Brunton compass. The origin for the coordinate system is the INJ (injection) well. No azimuth markers survive at the Richmond Field Station, so the actual geodetic azimuth is unknown. The horizontal control was obtained with a theodolite with three-wire level for bearings and distances, respectively. Vertical control was obtained by levelling.

Throughout this report, English units are used except where otherwise noted. 34.'20 means thirty-four and twenty hundredths feet. "Gradient to the east" means the east end is lower than the west end (east is downhill).

Table 1. Surveyed locations of wells at Richmond Field Station Engineering Geoscience Well Field.

Distances are in feet. Elevations are relative to mean sea level, as noted in the section on total head measurements.

Well	Northing	Easting	Elevation	Well
INJ	0.00	0.00	18.371	INJ
EXT	-203.40	1.20	18.351	EXT
OBS 1	55.10	0.00	18.314	OBS 1
OBS 2	-45.00	-28.30	18.843	OBS 2
OBS 3	-43.20	31.00	18.462	OBS 3
OBS 4	-124.70	0.00	18.236	OBS 4
OBS 5	-264.10	-0.80	18.236	OBS 5
OBS 6	2.60	99.70	17.784	OBS 6

2. Geology

The Richmond Field Station is located on the alluvial fan/delta built by Wildcat and San Pablo creeks. This is a semi-arid alluvial fan which extends from the Berkeley Hills down to San Pablo Bay (northern part of San Francisco Bay) and is semi-circular in plan view. While the area has been inhabited for some time, so that the contours are influenced by construction, it appears to be a typical fan, with radiating distributary channels and floodplains. The Bay shore is dominated by muds, although occasional gravel beaches and sand beaches occur.

Examination of driller's logs (Appendix 1, Figures A1-A8) indicates that the Richmond Field Station is underlain by deltaic deposits. This is particularly evident from the occurrence of layers which can be correlated across the entire well field and intervening zones in which a variety of clastic deposits cannot be correlated between adjacent wells. In particular, one can recognize a regressive sequence (coarsening upward) in OBS 4 between 90' and 95', where sand and gravel overlies brown clay which overlies gray clay, indicating an increase in energy with time (further onshore).

Evidence of fluvial deposition can be seen in OBS 5 between 82' and 87', where tan clay overlies sand and gravel which overlies coarse gravel (a classic point bar sequence), and at several other such sequences scattered throughout the well field. Gravel clay is also evidence of non-marine deposition: wave action strong enough to move gravel would winnow out clays. A more likely source is that the gravels were deposited in a river channel under high flow conditions during the winter rainy season and the clays were deposited under low flow conditions during the summer dry season. In addition, the numerous sequences where no correlations are seen probably represent fluvial sediments.

Figures 5-7 and 11 are stratigraphic correlation diagrams. Figures 5-9 are overlays for Figure 4a, which is an isometric drawing of the five northern wells (INJ, OBS 1, OBS 2, OBS 3, and OBS 6). Figure 8 shows the positions of the well screens and gravel packs and Figure 9 shows the relative proportions of fine and coarse material encountered in ten-foot vertical intervals. Figure 10 shows the graphic well logs of OBS 1, INJ, OBS 4, EXT, and OBS 5 and the intersection of the OBS 2-OBS 3 section with the north south line plotted in their correct positions along the north-

south line; Figure 11 is the corresponding correlation diagram. Figure 12 shows the positions of screens and gravel packs and the relative portions of coarse and fine materials in ten-foot vertical intervals. The symbols used on all correlation diagrams and graphic well logs are standard lithologic symbols, which are also shown on Figure 4b for convenience. In the geologic sections and interpreted well logs, feminine names denote inferred aquifer zones and masculine names denote inferred aquitard zones. Beds were named solely to facilitate discussion.

Correlations were drawn on the basis of maximizing the number and extent of horizontal sand and gravel layers. This is based on the assumption that the unconsolidated sediments have not been significantly deformed or tilted since deposition. Sands and gravels are rare enough that they are considered correlations. Clays were not correlated unless they were sandwiched by sand and gravel layers or appeared to have the same redox state (gray and green reduced clays were correlations, brown and tan oxidized clays were correlations) or some other distinctive feature such as the presence of gravel. Old Bay Mud was also considered grounds for correlation. White areas on the stratigraphic correlation diagrams were left where no correlations were obvious and probably represent fluvial deposits. These sediments are overwhelmingly dominated by clays. (see Figures 9 and 12.) In the fluvial portions of the sequence, sands and gravels occur as lenses set in a clay matrix.

The sequence from 55' to 83' where the sequence of the Tom Old Bay Mud, the Becky sand and gravel, the Ted clay (reduced to the south, oxidized to the north) and the Cindy sand and gravel occurs in all the wells except OBS 1 is almost certainly the result of marine (estuarine) deposition. In addition, sand and gravel layers seem to coalesce to the north while the extensive clay layers seem to pinch out northward. This would indicate that the paleo-shoreline was to the north of the sea, as it is presently.

OBS 6 has an excessive amount of clay. This could be due to simple chance, caving during drilling and logging of the caved debris or perhaps even soft-sediment deformation.

It should be emphasized that all the above geology is based on the driller's logs: cuttings were not saved during drilling, and, of course, visual inspection of the deposits for sedimentary features was impossible. These limitations should be born in mind when viewing the cross-sections and fence

diagrams. The continuity of certain deposits and the repetition of the same sequence in different wells, however, lend a fair amount of credence to the geologic interpretation.

Bearing in mind that the data on hand is limited to texture and occasionally color, the following geologic history is proposed. Deposition of the lower alluvial units (Lauren gravel, Mike gravel clay and others) to the north and possibly marine/possibly fluvial units to the south, (Maria gravel and others) began with initial subsidence of the Bay. A later sea level rise (possibly the Sangamon Interglacial highstand) resulted in deposition of the lower marine sequence (Tom, Becky, Ted, Cindy, unnamed clays, Jennifer). A drop in sea level or progradation of the shoreline resulted in deposition of an upper alluvial sequence (roughly between 24' and 56' near OBS 2 and OBS 3) with intertonguing marine (or at least rather extensive) deposits including the Lisa sand and gravel, which could be a beach/nearshore or channel deposit. The uppermost units (Brian to Kathy) could be the result of another era of marine deposition, or they could just be landfill.

This scenario is in general agreement with the ideal stratigraphic column of Atwater and others (1977) in which Holocene estuarine (Qhe) and alluvial deposits (Qha) overlie Pleistocene-Holocene (Wisconsin) alluvial (Qpha), terrestrial (Qpht) and eolian (Qphw) deposits which overlie Pleistocene (Sangamon) estuarine deposits (Qpe) which overlie and intertongue with Pleistocene alluvial deposits (Qpa) which rest on bedrock. The upper marine sequence would correspond to the Holocene estuarine deposits (Qhe), the upper alluvial deposits would correspond to the Pleistocene-Holocene alluvial sediments (Qpha) deposited during the low sea levels of the Wisconsin Glaciation, the lower marine sequence would correspond to the estuarine sediments (Qpe) deposited during world sea-level rise of the Sangamon Interglaciation, and the lower alluvial sequence would correspond to the late Pleistocene deposits (Qpa) of pre-Sangamon age.

The Lauren gravel is thickest in INJ (10') and OBS 6 (14'), thins to a 1' sand layer in OBS 1 to the north and a 1' gravel and sand layer in OBS 2 and OBS 3 at depths of 98', 95', 105', 101' and 103' respectively. This results in an east-west striking diamond shaped bar, which could be a channel deposit or a distributary mouth bar. The great thickness speaks against a subaerial river deposit, whose thicknesses rarely exceed the channels' depth. Although a river channel is possible,

an east-west mouth bar better explains the thickness and shape.

The Maria gravel is observed in OBS 5 (5' thick, 100.'5 deep) and EXT (7' thick, 101' deep) and seems to continue as a 1' sand layer at 107' and a 1' sand and gravel at 108.'5 in OBS 4. This was deposited in some high energy environment, possibly marine. It is only seen in the three southern wells, which lie on a north-south line. A connection to the Lauren gravel seems unlikely, although pump test results indicate a connection to the Sanitation Engineering Well Field "aquifer".

Bill Dietrich (pers comm., 1987) has expressed curiosity about the lack of sand in the stratigraphic section. This is a legitimate concern. It is possible that sands were not recognized in the cuttings, although the occasional sand layer/lens speaks against this. I feel it likely that the source regions (the Berkeley Hills) consist of rocks which do not weather to sand-sized fragments. Observations of stream cuts in the East Bay show a colluvium of clay with pebbles in it and no observed sand. Given the local geology, the absence of sand is not surprising.

It should be pointed out that the extensive gravel layers could be due to braided streams or fortuitous intersection of a channel deposit, although in most cases this seems unlikely. A very large area would need to be blanketed by sands and gravels to produce such layers, which, if sloping, would be very vulnerable to landslides and rainwash erosion; such an occurrence would be a very good source for a turbidite.

On the basis of the geologic correlations, it appears that groundwater flow at the Richmond Field Station will be channeled into the former river channels, distributaries and marine beach/nearshore deposits. This piping will result in complicated and tortuous flow paths in the channel and bar finger deposits, although flow in the marine (estuarine) parts of the sequence may approach that of ideal confined aquifers due to the lateral extent and uniformity of these deposits.

3. Hydrology

The hydrology of the Richmond Field Station is complex and is controlled by the geological framework within which flow occurs. The hydrologic data gathered comprises "static" water levels (head measurements), pump tests of the INJ and EXT wells, and continuous records obtained with

Richmond Field Station

Engineering Geoscience Well Field

Map of Engineering Geoscience Wells

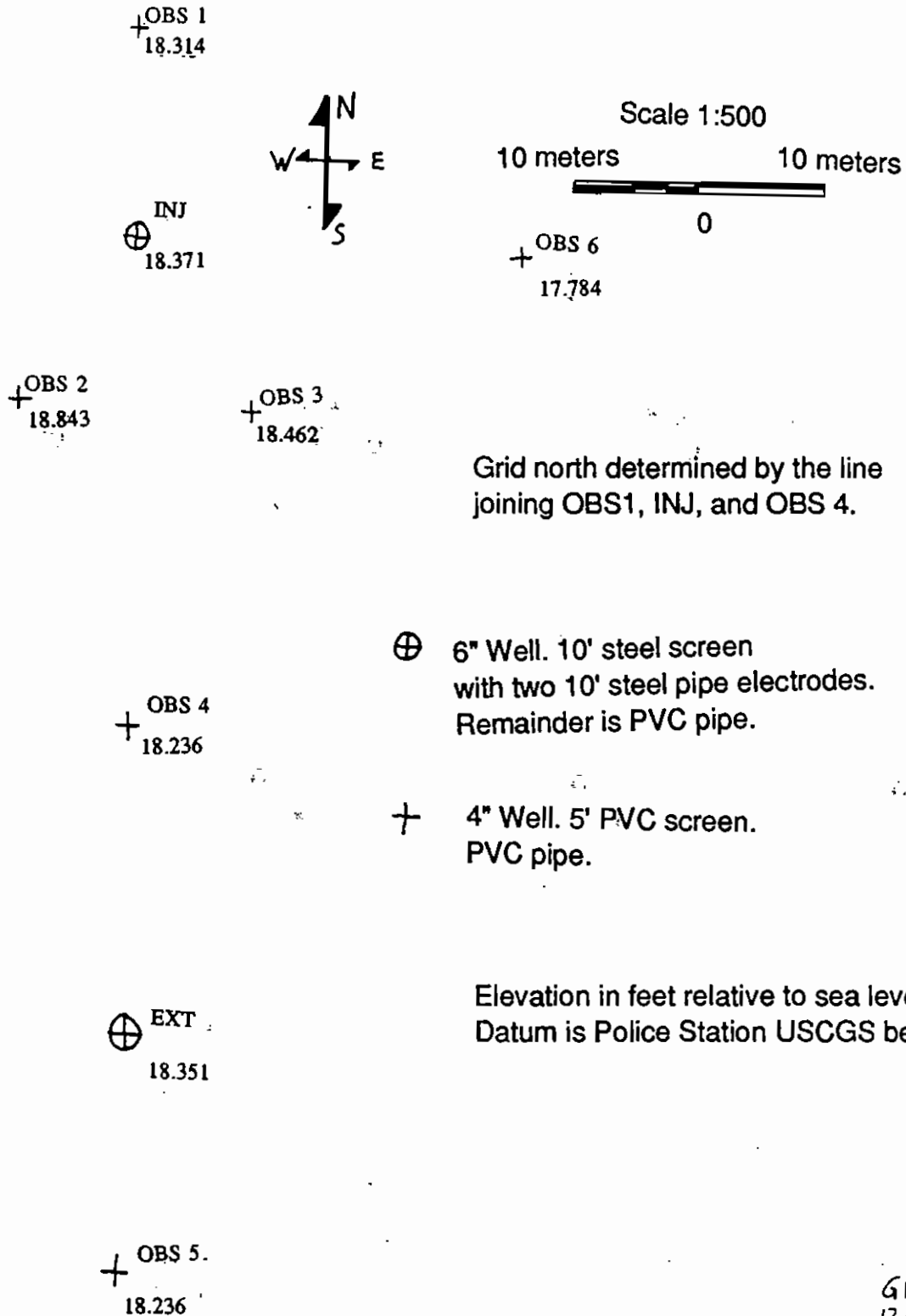


Figure 3

Richmond Field Station
Engineering Geoscience Well Field
West of RFS 300
Isometric Drawing
15° Projection Angle
Drafted at 1:240

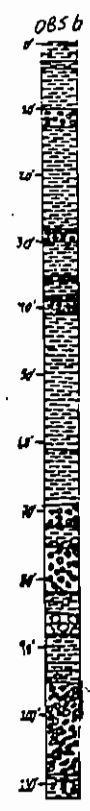
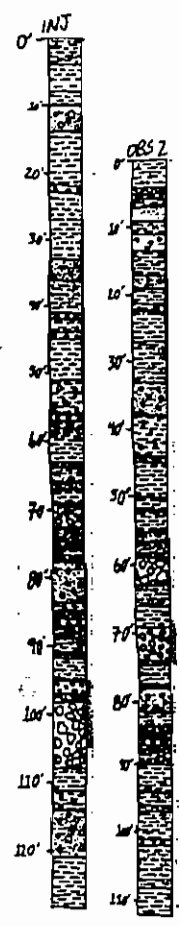
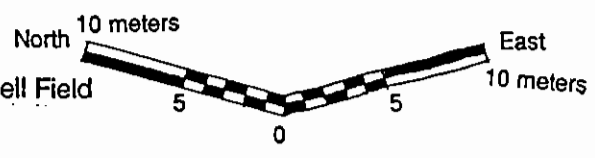
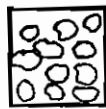
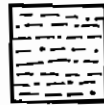


Figure 4a

Legend for Graphic Well Logs and Correlation Diagrams



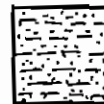
Gravel



Silty Clay



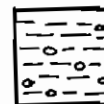
Sand



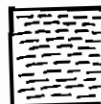
Sandy Clay



Sand and Gravel



Gravel Clay



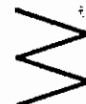
Clay



Old Bay Mud



Silt



Facies Change on
Correlation Diagrams

Figure 4b

+

Richmond Field Station
 Engineering Geoscience Well Field
 West of RFS 300
 Overlay for Figure 4a
 Stratigraphic Fence Diagram

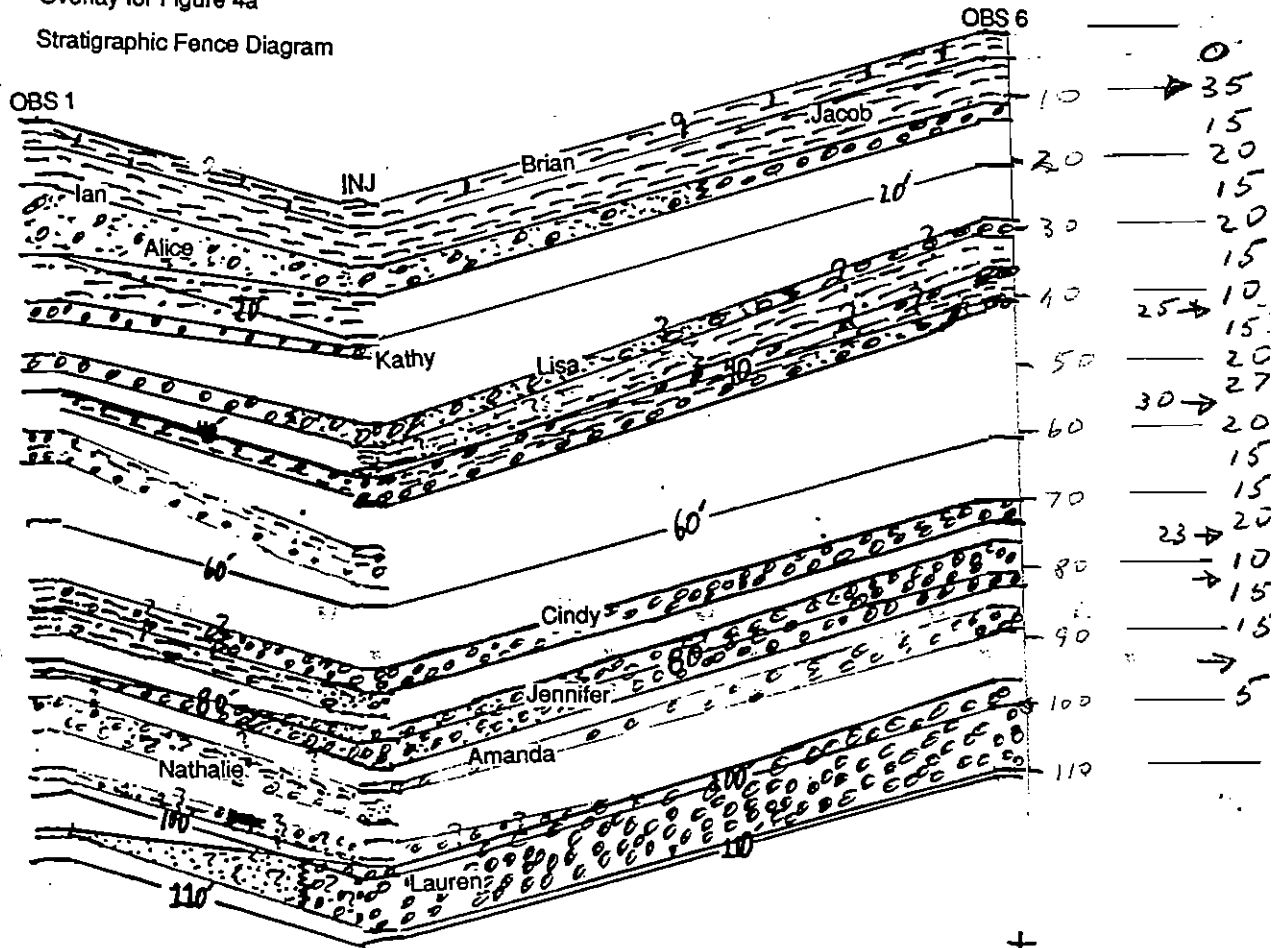


Figure 5

Greg Pouch
 6 April 1987

Richmond Field Station
 Engineering Geoscience Well Field
 West of RFS 300
 Overlay for Figure 4a
 Stratigraphic Fence Diagram

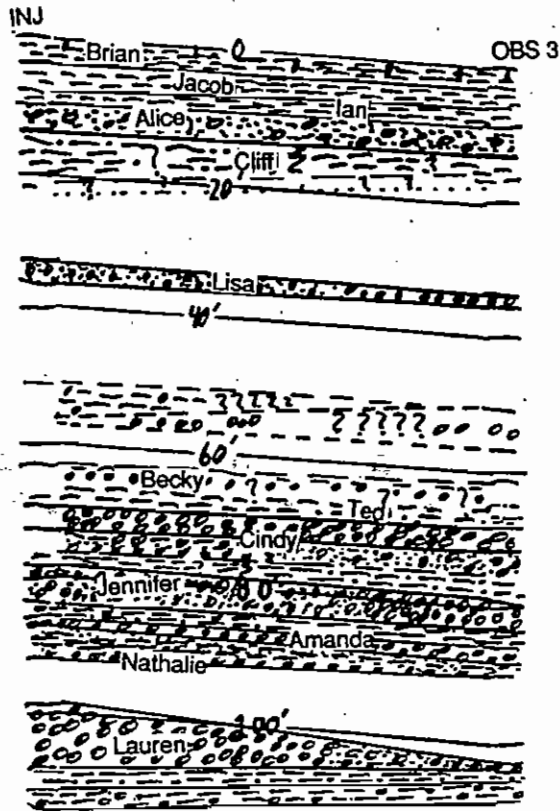


Figure 6

Greg Pouch
 Begun April 1987
 Completed Aug 1988

Richmond Field Station
Engineering Geoscience Well Field
West of RFS 300
Overlay for Figure 4a
Stratigraphic Fence Diagram

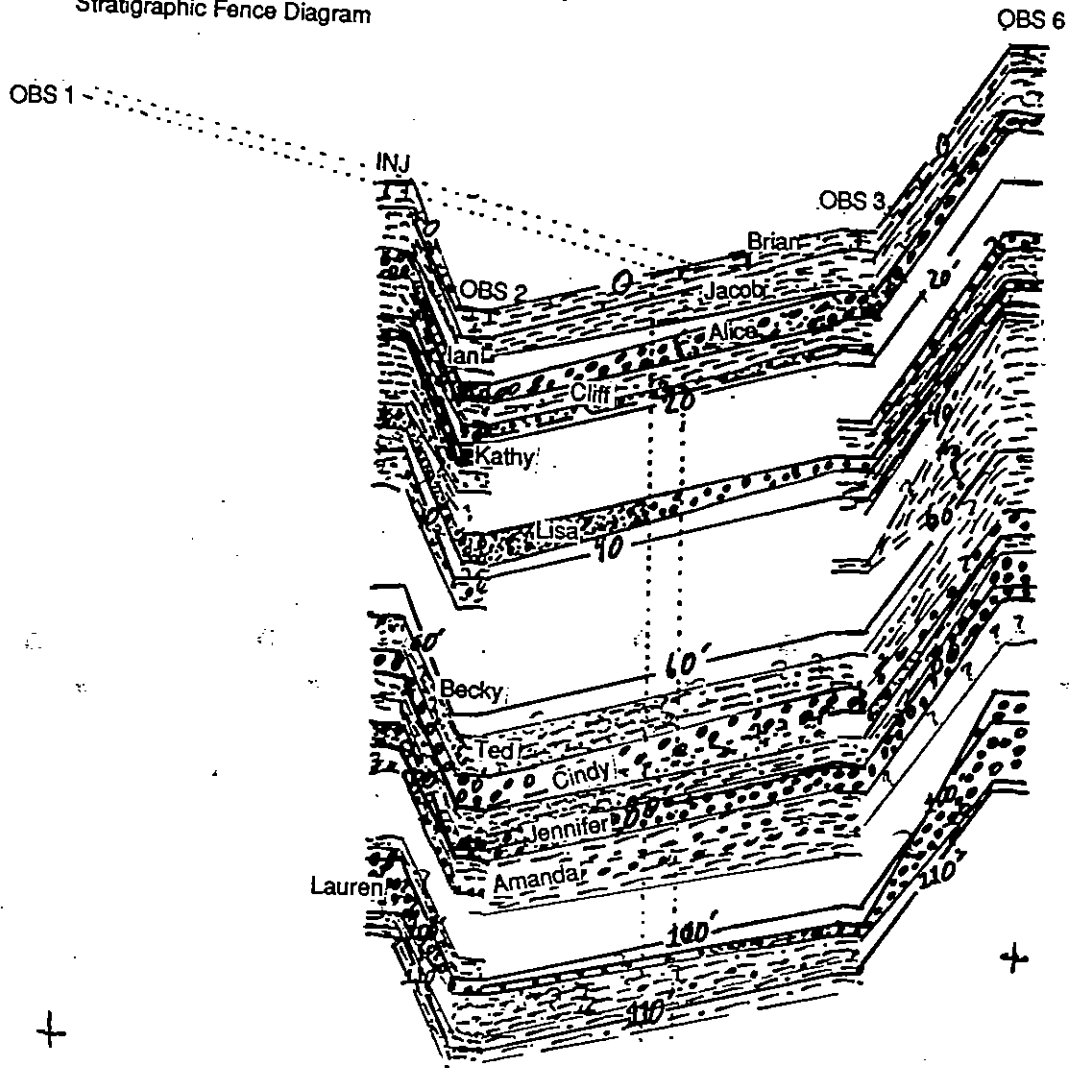


Figure 7

Greg Pouch
Began 6 April 1987
Completed 29 April 1987

+

Richmond Field Station
Engineering Geoscience Well Field
West of RFS 300
Overlay for Figure 4a

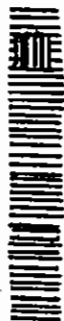
OBS 1

OBS 6

INJ

OBS 3

OBS 2



+

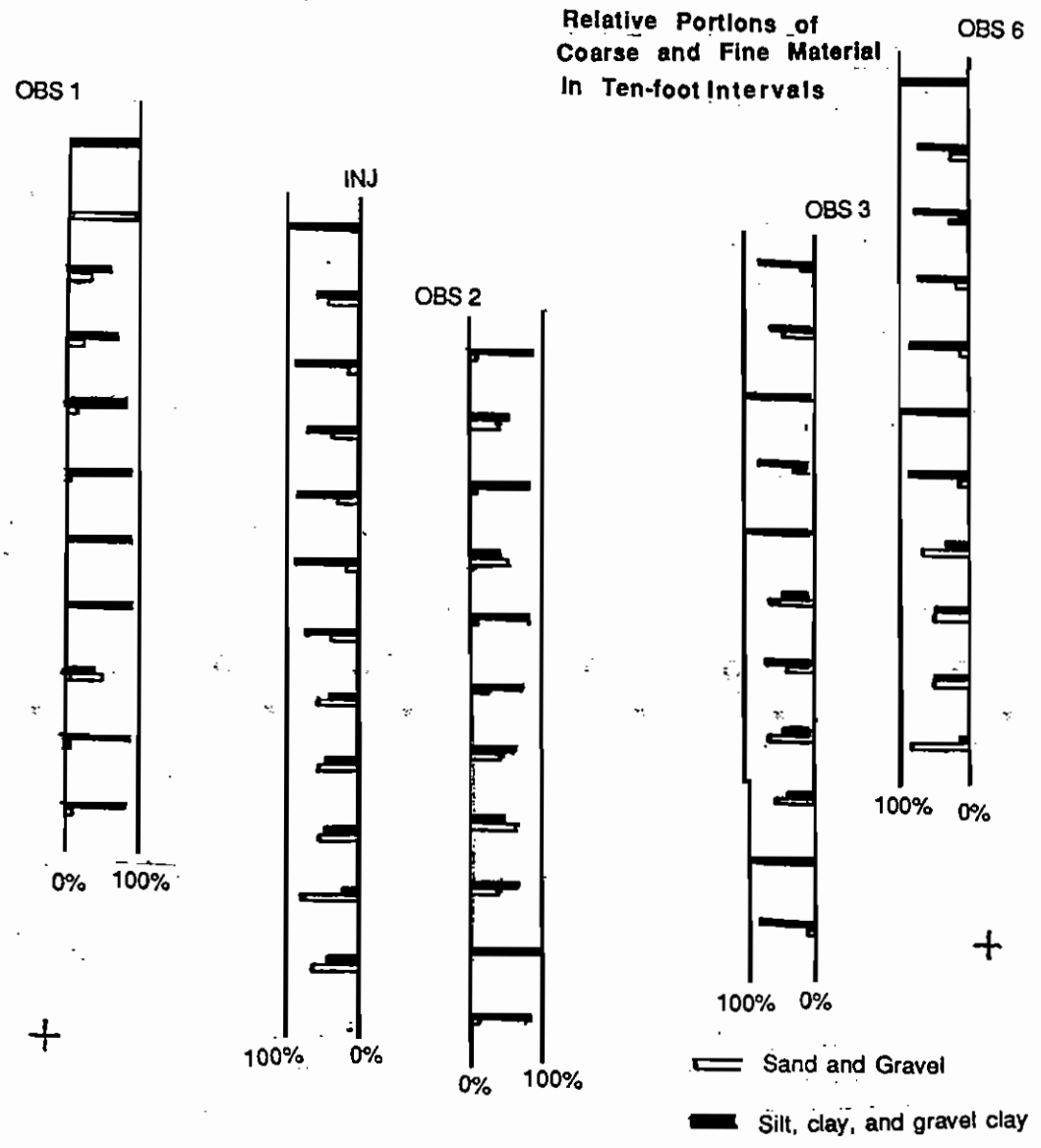
||| Screen

≡≡≡ Gravel Pack

Figure 8

+

Richmond Field Station
Engineering Geoscience Well Field
West of RFS 300
Overlay for Figure 4a



+

Figure 9

Richmond Field Station Engineering Geoscience Well Field

(west of Building 300)

Graphic Well Logs in North-South Section

South

North

Vertical Scale 1:240
Horizontal Scale 1:250
Vertical Exaggeration 1.04X

Datum is ground level
(about 17' above mean sea level).

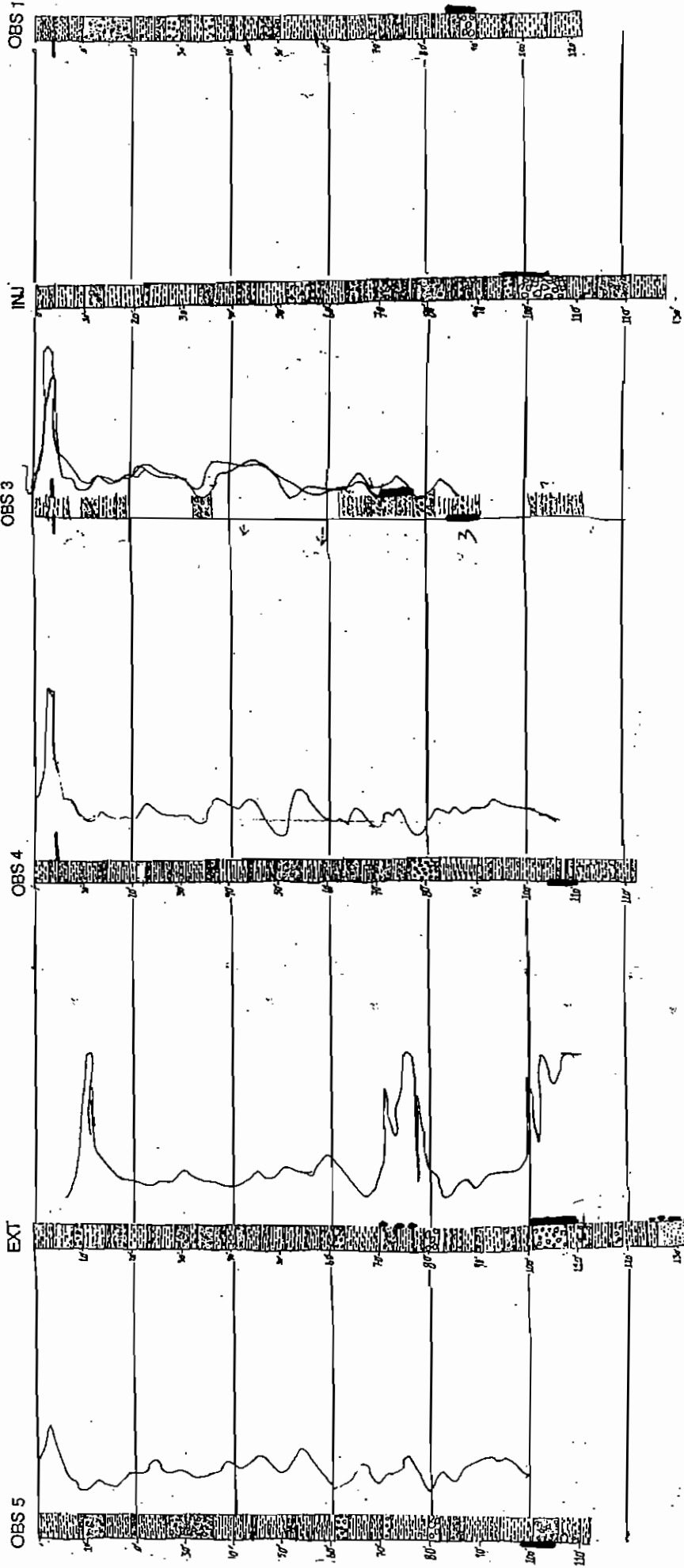
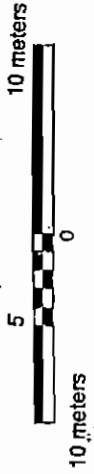


Figure 10j

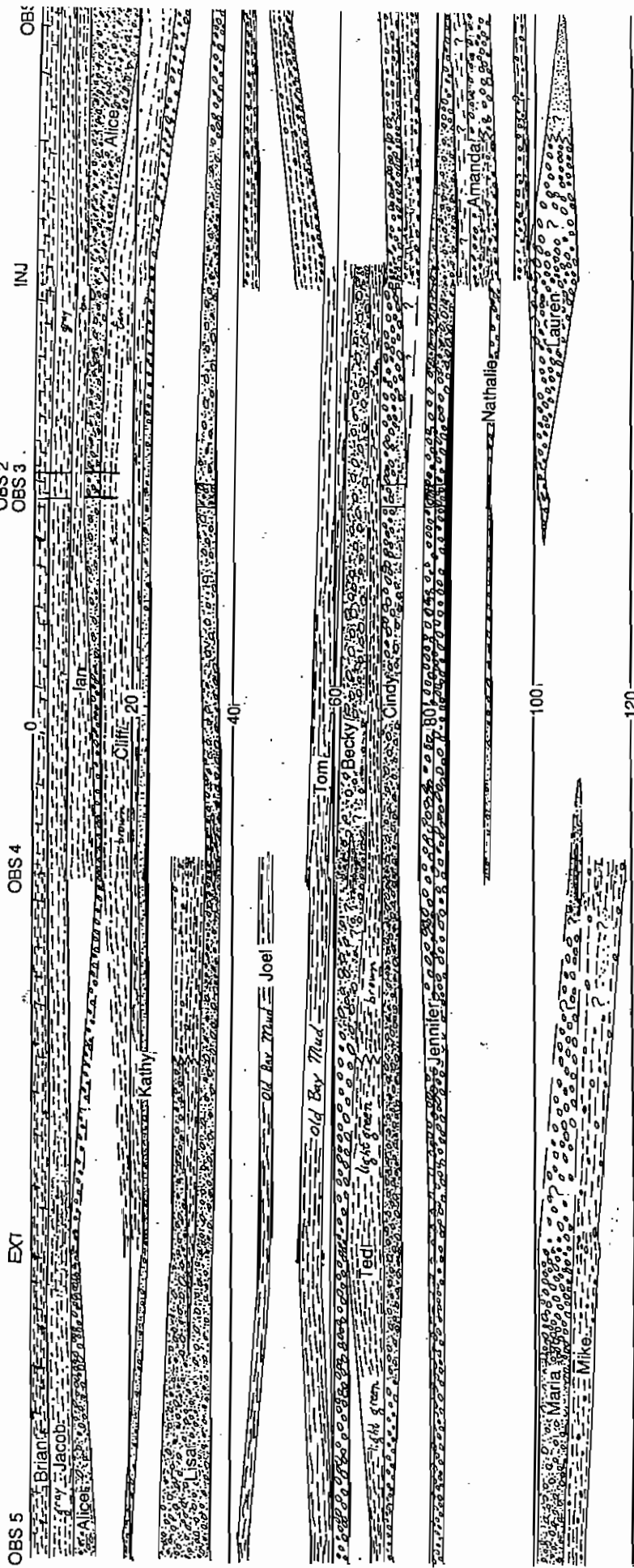
Richmond Field Station
Engineering Geoscience Well Field
 (west of Building 300)

Stratigraphic Cross-section

Vertical Scale 1:240
 Horizontal Scale 1:250
 Vertical Exaggeration 1.04X
 Datum is ground level
 (about 17' above mean sea level).



North



GP

Richmond Field Station Engineering Geoscience Well Field (west of Building 300)

Relative Portions of Coarse and
Fine Material in Ten-foot Intervals:



Screen
Gravel Pack

Silt, Clay, and Gravel Clay
Sand and Gravel

South

North

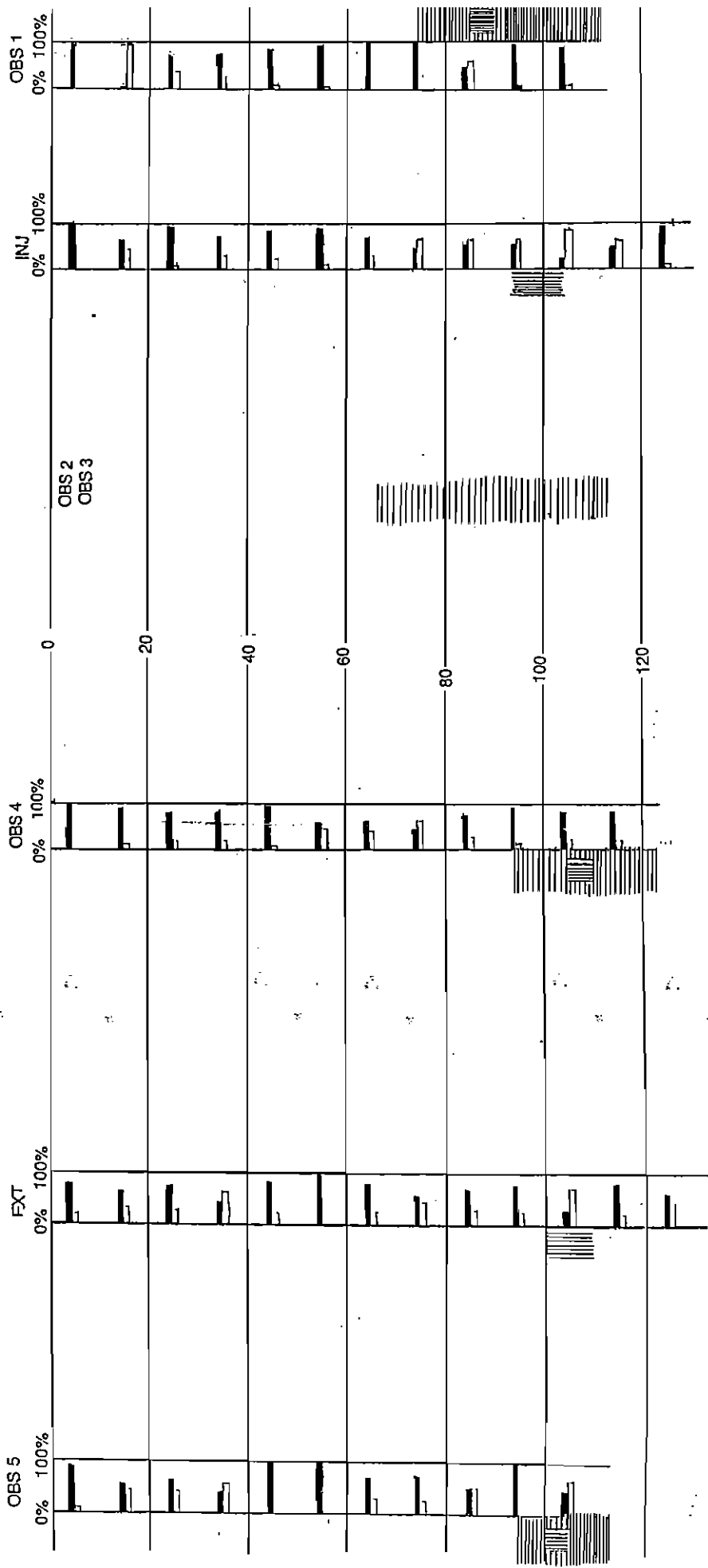


Figure 12:

GP

Drawdown Curve for Pumping of SE Production Well 7 July 1987

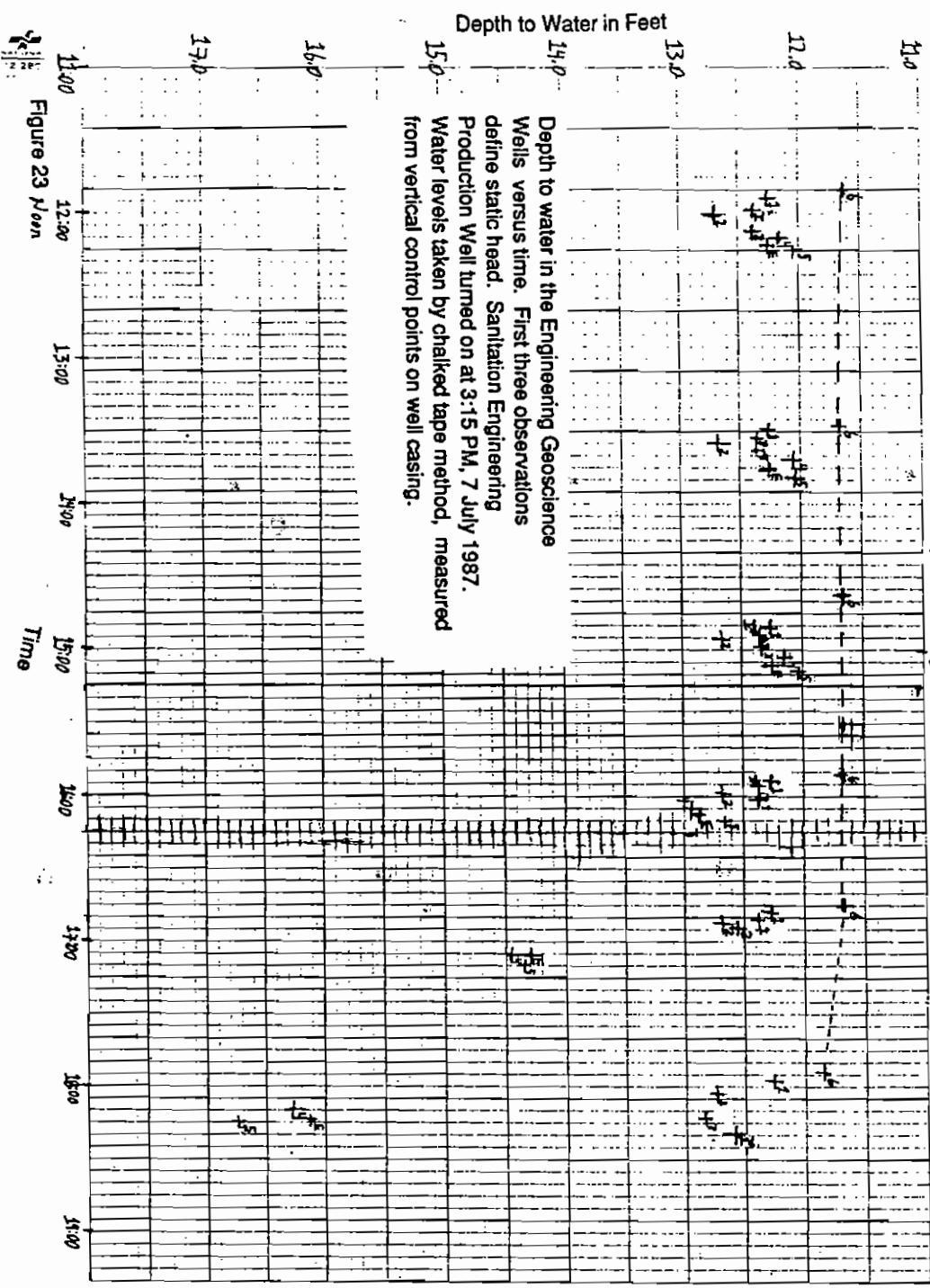


Figure 23 Moon

10 Squares to the Inch

ATTACHMENT 4
LIPPERT 1989

GMF
EARTH SCIENCES
Bldg. 31 Ext.6092
SEPT. 15,1989

MEMORANDUM

TO: PURCHASING, TOM PATOCK

FROM: D. LIPPERT

SUBJECT: DRILLING OF TEST WELLS AT RICHMOND FIELD STATION

WELLS NO. 1 AND 2

- WELLS TO BE DRILLED TO A DEPTH OF 100 FEET. WELLS TO BE OPEN AT BOTTOM HOLE, WITH FIRST 20 FEET TO BE 4 INCH I. D. SLOTTED PVC CASING BACK FILLED WITH GRAVEL. THE REST OF CASING (80 FEET) TO BE 4 INCH I. D. STEEL CASING, WITH NO I. D. DIFFERENCE IN BETWEEN STEEL CASING AND PVC. CASING TO EXTEND 2 FEET ABOVE GROUND LEVEL. WELL NO. 1, CEMENT UPPER 80 FEET WITH STANDARD DRILLING PRACTICES. WELL NO. 2 CEMENT UPPER 80 FEET WITH SAME CEMENTING PROCEEDURE AS USED WITH WELLS NO.3 AND 4.

WELLS NO 3 AND 4

WELLS TO BE DRILLED TO DEPTH OF 160 FEET. WELLS TO BE OPEN AT BOTTOM HOLE. STARTING AT BOTTOM HOLE, FIRST 2 FEET TO BE 4 INCH STEEL I. D. CASING, THEN 8 FEET OF 4 INCH I. D. PVC CASING, THEN 2 FEET STEEL CASING, 8 FEET PVC CASING, ETC. TOP SECTION(LAST SECTION) OF PVC CASING TO EXTEND 2 FEET ABOVE GROUND LEVEL. (LAST SECTION TO BE 10 FEET LONG)

CEMENTING: 90% CEMENT, 10% BENTONITE, MIXED WITH SALT WATER. FOR EVERY 100 LBS OF CEMENT ADD 10 LBS OF SALT AND MIX WITH STANDARD DRINKING WATER, SALT WILL BE FURNISHED BY LBL

WELLS 5 AND 6

WELLS TO BE DRILLED TO A DEPTH OF 300 FEET. WELLS TO BE CAPPED AT BOTTOM HOLE. CASING WILL BE 6 INCH I. D. PVC. CEMENT WITH STANDARD DRILLING PRACTICES. AFTER COMPLETION OF WELL, CASING TO BE PUMP DRY OF ALL FLUIDS. CASING TO EXTEND 2 FEET ABOVE GROUND LEVEL.

LOCATION OF WELLS IS ON ENCLOSED MAP.

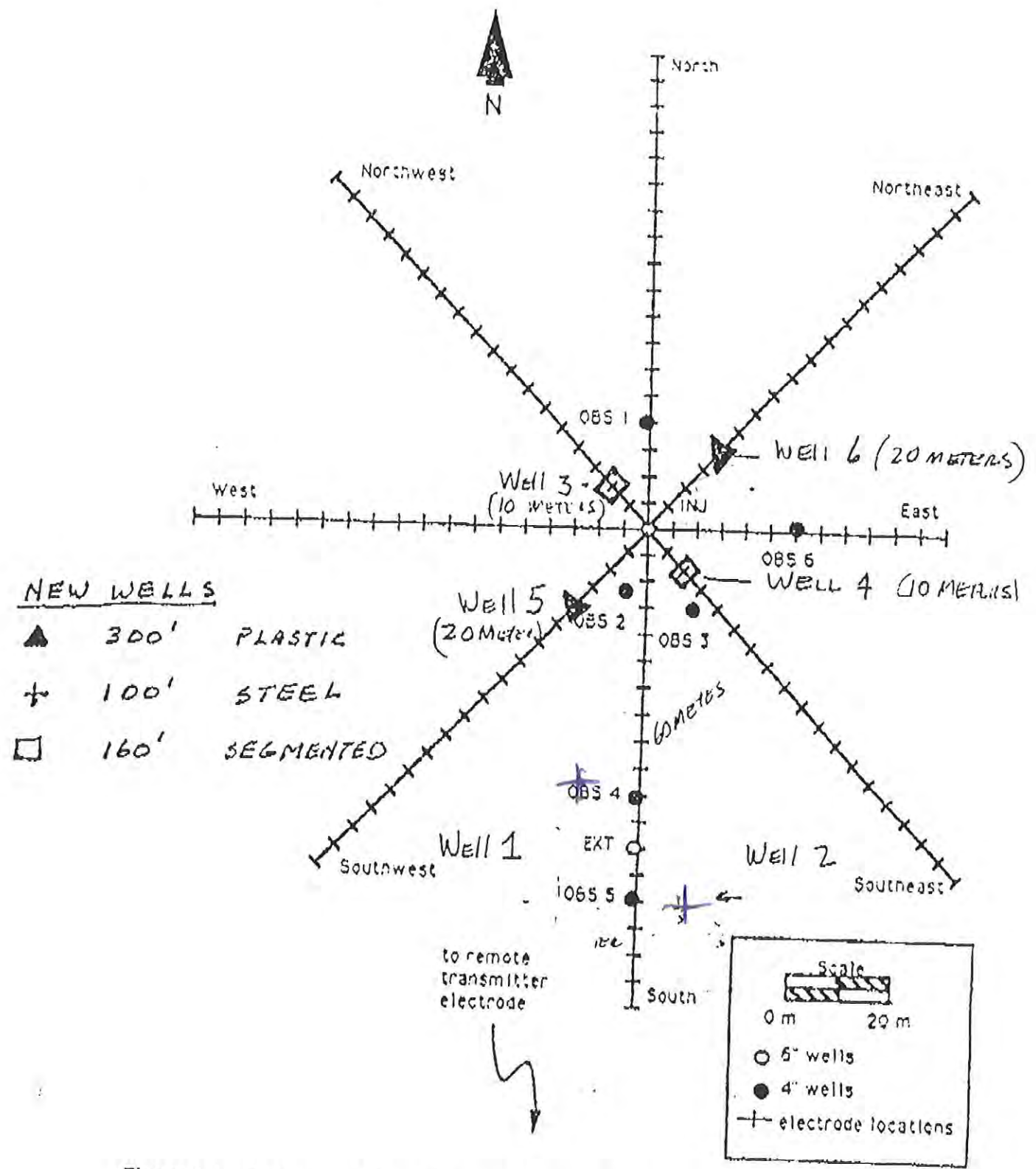
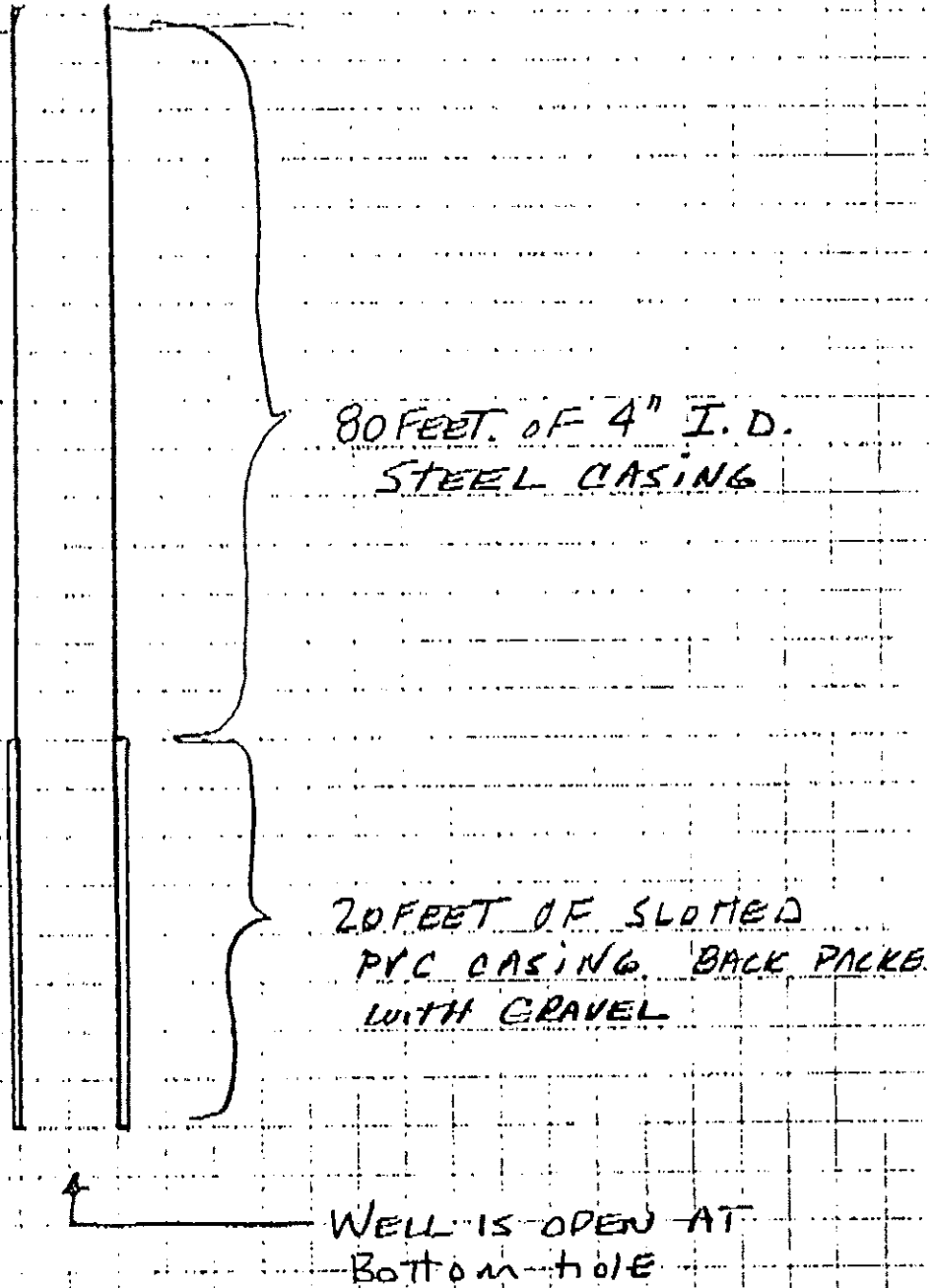


Figure 1.1. Plan map of the well field and resistivity array at the Richmond Field Station.

Wells No 1 & 2

Holes to be DRILLED 100 FEET
FOR 4" I.D. CASING:



Wells No 3 & 4

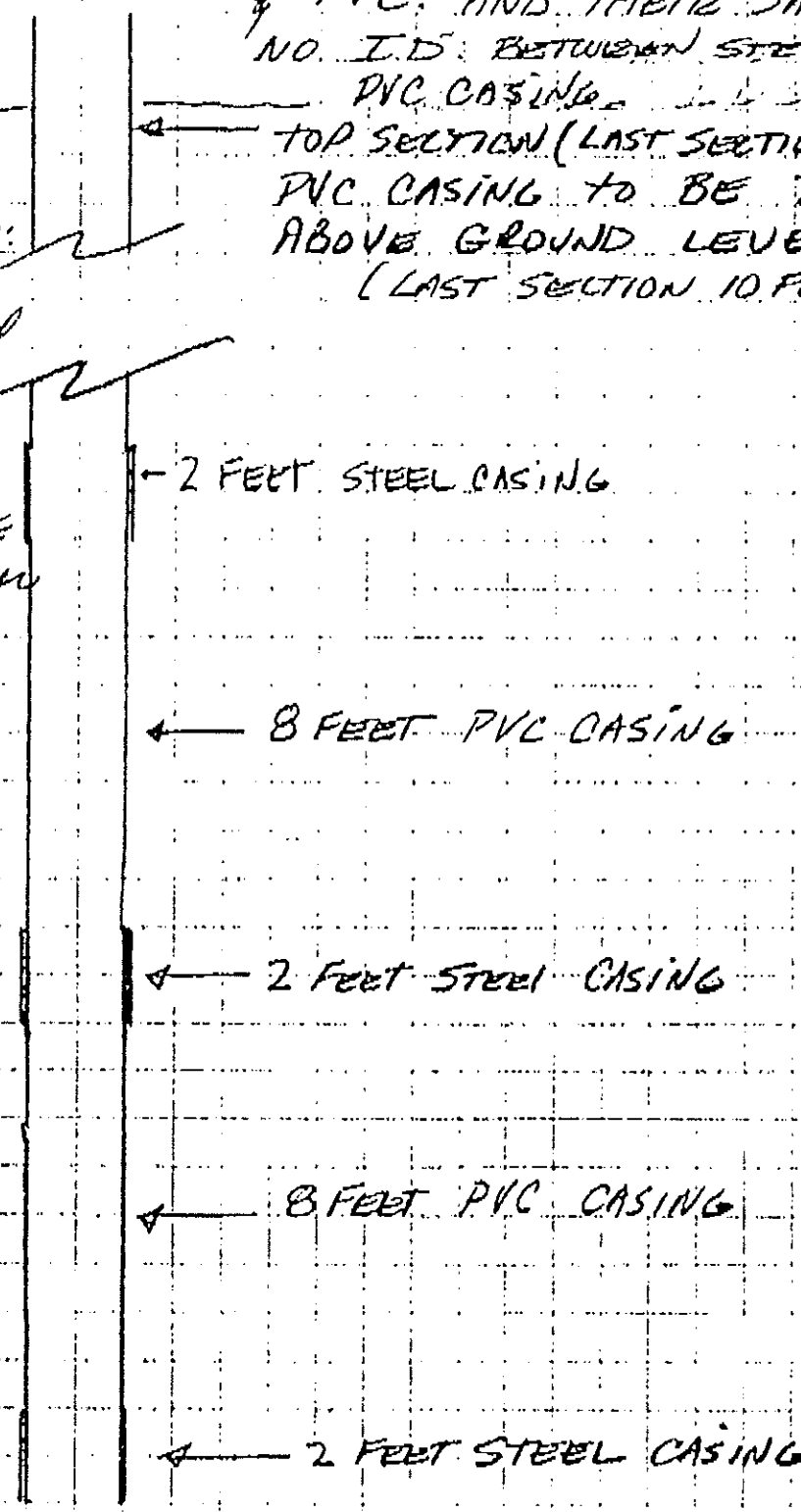
Holes to be drilled 160 FEET (Bottom hole

4" ID CASING BOTH STEEL & PVC. AND THERE SHOULD BE NO. I.D. BETWEEN STEEL AND PVC CASING.

TOP SECTION (LAST SECTION) OF PVC CASING TO BE 2 FEET ABOVE GROUND LEVEL (LAST SECTION 10 FEET LONG)

CEMENTING OF WELLS USING BENTONITE, GLASS G PORTLAND CEMENT.

16% BY WEIGHT OF CEMENT WITH BENTONITE MIXED WITH SACT WATER



← 2 FEET STEEL CASING

← 8 FEET PVC CASING

← 2 FEET STEEL CASING

← 8 FEET PVC CASING

← 2 FEET STEEL CASING

↑ Bottom hole OPEN

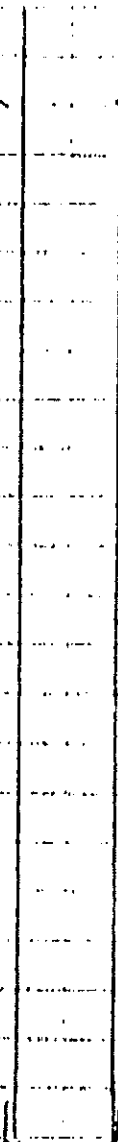
WELLS No 5 & 6

HOLES TO BE DRILLED 300 FEET

MATERIAL: 6" ID PVC CASING.

CEMENTED WITH STANDARD
DRILLING PRACTICES.AFTER CEMENTING CASING TO BE
PUMP DRY.

≈ 2 FEET ABOVE GROUND LEVEL

WELL IS CLOSED AT
BOTTOM HOLE.

MEMO FROM . . .

Pitcher Drilling Co.

P.O. BOX 50367, PALO ALTO, CA 94303

PHONE: (415) 328-8910

1/18/90

TO: Mr. Alex Becker

SUBJECT: Richmond Field Station #3426706

Enclosed are copies of the logs for the above captioned job
per your request.

Pitcher Drilling Co.

PO. BOX 50367, PALO ALTO, CA 94303
PHONE: (415) 328-8910

RICHMOND FIELD STATION

Hole #1

0 - 100 Alluvium

Running sand at 70'. Probably an aquifer - hole
tended to cave there.

Pitcher Drilling Co.

P.O. BOX 50367, PALO ALTO, CA 94303
PHONE: (415) 328-8910

RICHMOND FIELD STATION

Hole #2

0 - 100 Alluvium

Did not encounter sand problem although there was a sand layer between 75 - 80'.

Pitcher Drilling Co.

PO. BOX 50367, PALO ALTO, CA 94303

PHONE: (415) 328-8910

RICHMOND FIELD STATION

Hole #5

- | | | | |
|-----|---|-----|--|
| 0 | - | 114 | Alluvium mostly silty clay & silty sand with occasional gravels. |
| 114 | - | 132 | Shale medium hard. |
| 132 | - | 150 | Sandstone layer - very hard. |
| 150 | - | 170 | More shale softer than sandstone. |
| 170 | - | 300 | Shale & sandstone - very hard. |

After alluvium, shale at 114 was not too hard. Sandstone layer from 132 - 150 was the hardest layer of rock in the hole. From 170 - 300 consistent bedrock. Drilling averaged 1 to 1.5' per hour of drilling.

Pitcher Drilling Co.

PO. BOX 50367, PALO ALTO, CA 94303
PHONE: (415) 328-8910

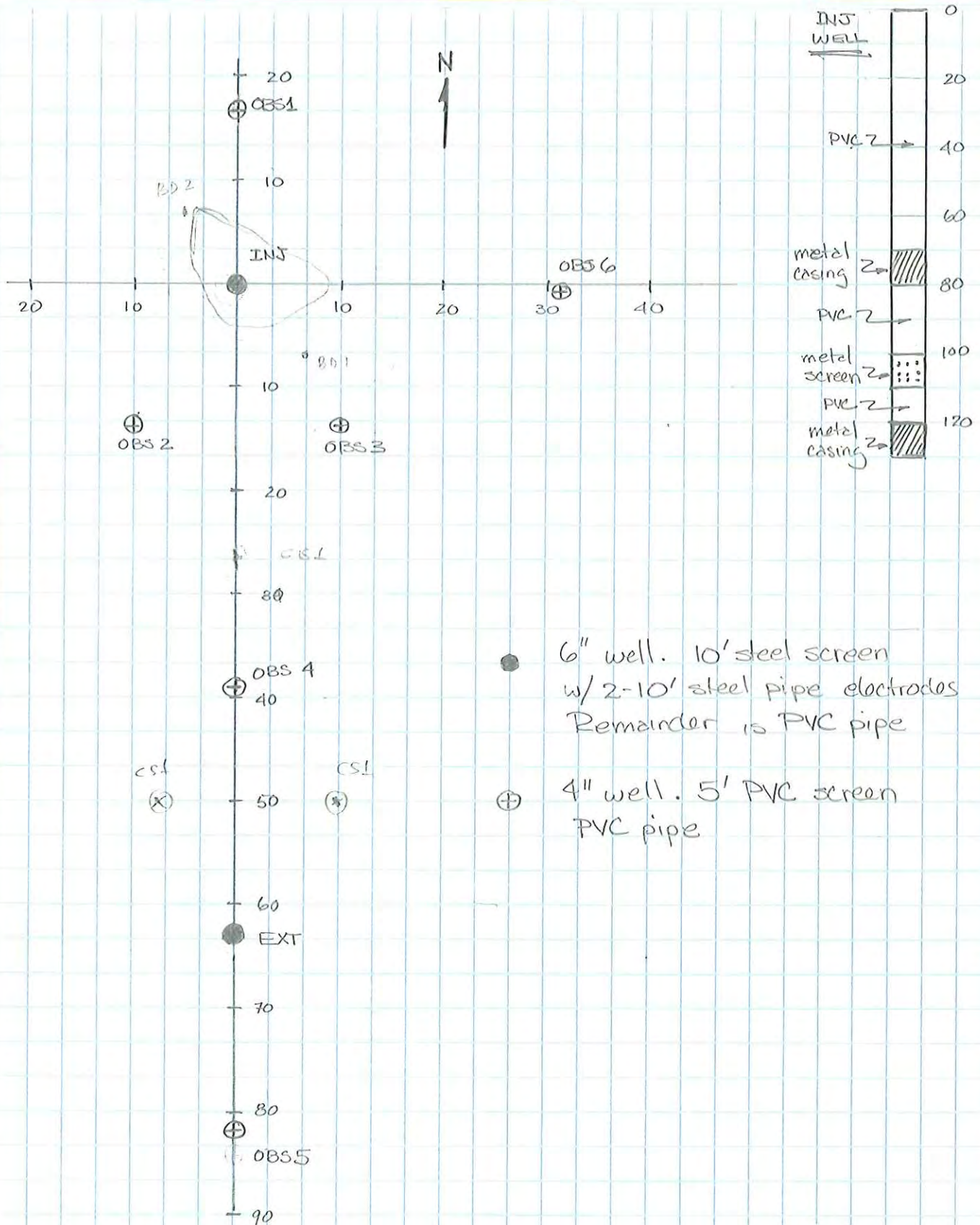
RICHMOND FIELD STATION

Hole #6

0	-	104	Silty clay with occasional gravels & some sand layers.
104	-	118	Shale - Medium hard.
118	-	134	Medium hard to hard shale with sandstone layers.
134	-	199	Sandstone - very hard.
199	-	210	Shale layer - drill rate doubled.
210	-	228	Hard sandstone.
228	-	238	Intermittent sandstone - shale layers.
238	-	300	Sandstone - hardest drilling of hole. Less than 1' per hour.

Hole #6 had harder rock than #5. Drill rate was almost twice as slow in bedrock on hole #6. Sandstone was more prevalent also.

SUBJECT Richmond Well Field



ATTACHMENT 5
THE EFFECT OF SALT IN CONCRETE ON COMPRESSIVE STRENGTH, WATER
VAPOR TRANSMISSION, AND CORROSION OF REINFORCING STEEL, U.S. NAVAL
CIVIL ENGINEERING LABORATORY

603376

2 of 3

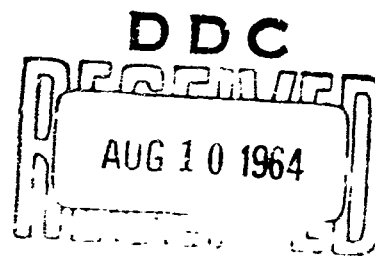
*614
he ~ 300
926 ~ 5000*

Technical Report

R 306

THE EFFECT OF SALT IN CONCRETE
ON COMPRESSIVE STRENGTH, WATER
VAPOR TRANSMISSION, AND CORROSION
OF REINFORCING STEEL

22 July 1964



U. S. NAVAL CIVIL ENGINEERING LABORATORY

Port Hueneme, California

THE EFFECT OF SALT IN CONCRETE ON COMPRESSIVE STRENGTH, WATER
VAPOR TRANSMISSION, AND CORROSION OF REINFORCING STEEL

Y-R007-05-01-012

Type C Final Report

by

Donald F. Griffin and Robert L. Henry

ABSTRACT

The purpose of this investigation was to determine the effects of sodium chloride and sea-water salts separately in concrete. The investigation covered the effects of salt on the compressive strength and water vapor transmission (WVT) of concrete, as well as the corrosive effects of salt on mild reinforcing steel. Variables included water-cement ratio, salinity of mixing water, and diameter and thickness of the specimens. The test environments included 20, 50, and 75 percent RH at 73.4 F.

The data presented herein supports the general conclusion stated in a previous report, namely, that at a mixing-water salinity of approximately 25 grams of salt per kilogram of solution, compressive strength is increased, WVT is minimized, and corrosion of mild steel is not significant.

Copies available at OTS \$1.25

Qualified requesters may obtain copies of this report from DDC.
The Laboratory invites comment on this report, particularly on the
results obtained by those who have applied the information.

CONTENTS

	page
INTRODUCTION	1
COMPRESSIVE STRENGTH	1
Sodium Chloride Series	1
Sea-Water Series	1
Wall Specimens	2
WATER VAPOR TRANSMISSION	2
Sodium Chloride Series	2
Sea-Water Series	7
Wall Specimens	8
WVT Hysteresis	8
Vented Cups	8
CORROSION OF STEEL	12
Corrosion-Detection Probe	12
Sea-Water Series	12
Depth-of-Cover Series	22
Experimental Walls	22
GENERAL SUMMARY	26
FINDINGS AND CONCLUSIONS	26
REFERENCES	27
APPENDIXES	
A — Mix Design Data	29
B — Experimental Walls	32
C — Corrosion-Detection Probe	39
DISTRIBUTION LIST	41
LIBRARY CATALOG CARD	45

INTRODUCTION

The purpose of this task was to determine the effect of sea-salt spray on portland cement concrete and to determine the permissible amounts of salt in concrete when it is mixed. Specifically, it was desired to establish the separate effects of sodium chloride and sea-water salts in concrete on strength, water vapor transmission (WVT), and corrosion of mild reinforcing steel.

This report reviews the findings presented in previous reports^{1, 2} and coordinates all information developed throughout the investigation. The wet-cup system is discussed in greater detail in References 3 and 4. For convenience, the mix design data in Reference 1 is included here as Appendix A. References 1 and 2 reported the results of series of tests from 360 to 520 days age. The present report extends the results of these tests up to 1000 days age and includes some data for additional series of tests.

COMPRESSIVE STRENGTH

Sodium Chloride Series

Some rather uniquely shaped curves of compressive strength versus salinity of mixing water were obtained previously¹ using NaCl. In order to verify the characteristics of these curves, two additional series of tests were performed. Plots of these data confirm the previous findings even though a different brand of cement (Victor) was used in place of the brand first used (Colton). Selected example curves of each water-cement ratio (W/C) for the Victor cement are presented in Figure 1. The data show that, for maximum compressive strength, the optimum salinity of mixing water is between 18 and 36 gm/kg for the W/C ratios used — 0.444 or 0.702.

Sea-Water Series

The effect of sea water on compressive strength of concrete also resulted in some rather unusual curves of strength versus salinity of mixing water.¹ Consequently, these tests were repeated with the same brand and type of cement except that a W/C of 0.444 was used instead of 0.702, and the salinity range was extended

from about 63 to about 88 gm/kg. Sea water with a salinity of 31.32 gm/kg and distilled water were proportioned by weight to obtain salinities less than 31.32 gm/kg. Sea-Rite salt, a simulated sea-salt mixture containing elements found in natural sea water in quantities greater than 0.004 percent, was added to sea water to obtain greater concentrations.

Figure 2 shows an example of the results of these tests. In general, all of the curves are similar to and verify the previous curves and findings. Although there were variations of compressive strength with increased sea-water salinities, there is a general increase in strength of concrete with age and with increasing salinities of mixing water up to about 88 gm/kg. This is true for Figure 2 as well as for the previous work. A report⁵ recently published in England is in complete agreement with this finding.

Wall Specimens

Twelve small reinforced concrete walls were cast, the characteristics of which are described in Appendix B. One side of each wall and one-half of the cylinders for each wall (sea side) have received sea-water spray for a few minutes each day since cast (3 years). The other side of each wall and the other one-half of the cylinders for each wall (land side) received no spray.

Compressive strength values for the entire series, including two additional ages not previously reported, are presented in Table I. Compressive strength values from Table I were plotted versus age in Figure 3. Although the land-side curve is above the sea-side curve for each aggregate, indicating greater strengths for the land-side cylinders (except for the GMR high W/C ratio curve which is coincident for land and sea side), curves for both sides show increasing strength with time. The effect of poor-quality aggregate on strength of concrete can be seen in Figure 3 by comparing the GMR concrete strength to the SG and ENG concrete strengths.

WATER VAPOR TRANSMISSION

Sodium Chloride Series

Water vapor transmission (WVT) is defined as the rate of migration of water through a material, the units of which are grains per square inch per day, using a system like the wet cup shown in Figure 4.

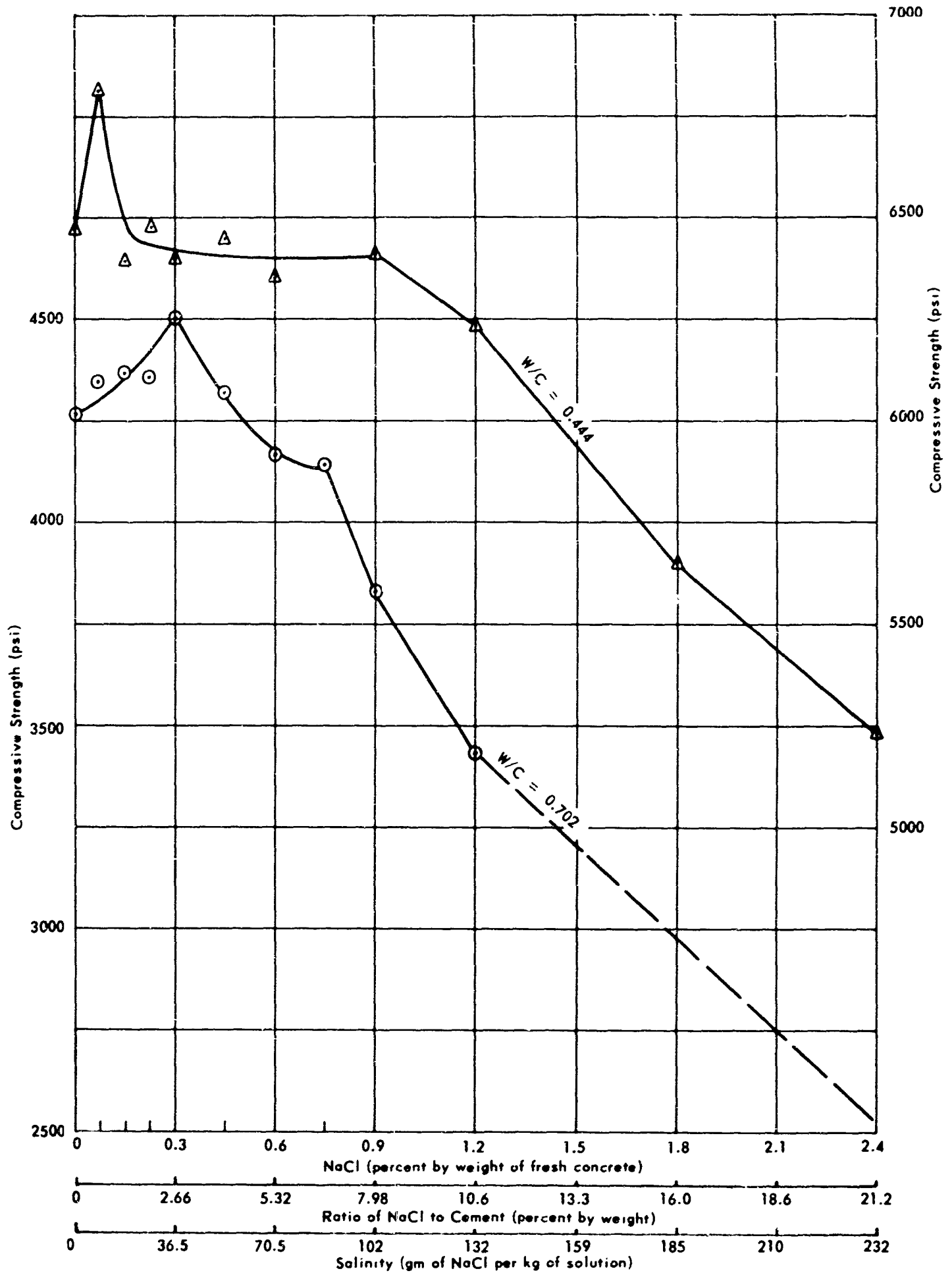


Figure 1. Compressive strength versus NaCl content for Victor cement at 14 days age.

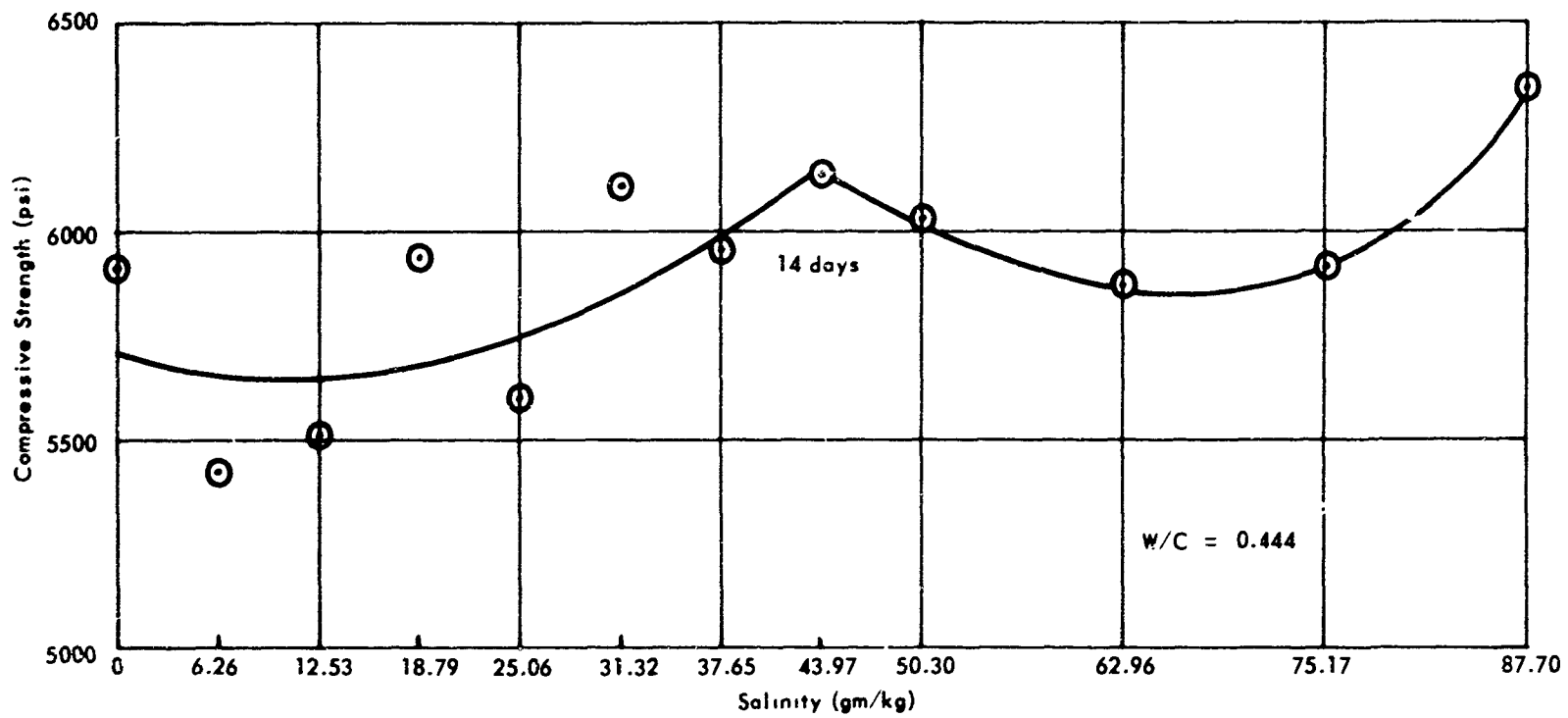


Figure 2. Compressive strength versus salinity of mixing water (sea water).

Table I. Compressive Strength of Wall Specimens

Aggregate Type ^{a/} and W/C	Compressive Strength (psi) Age of 3-in.-dia by 6-in. concrete cylinders (days)						
	28d ^{b/}	56d	112d	224d	448d	728d	975d
SG, 0.702							
Land Side	3330	4420	5250	4450	5990	5200	6090
Sea Side		4390	5060	4940	4600	5190	5620
SG, 0.444							
Land Side	6590	7990	7990	8140	8500	8030	9270
Sea Side		7410	7390	8460	7880	8180	8240
ENR, 0.702							
Land Side	3120	4490	4600	4510	4780	4920	6370
Sea Side		3240	5230	4550	4670	4660	4930
ENR, 0.444							
Land Side	6150	7110	7820	8150	8850	9230	9330
Sea Side		7600	7610	8110	8280	8370	8570
GMR, 0.702							
Land Side	1630	1990	2230	2040	2400	2360	2550
Sea Side		1960	2430	1980	2190	2390	2630
GMR, 0.444							
Land Side	3610	4670	4550	4840	6050	5800	6380
Sea Side		4460	5180	4880	5240	5310	5470

a/ See Appendix A.

b/ Each value is average of four fog-cured cylinders; other values are averages of three field-cured cylinders.

Note: C-Type II cement.

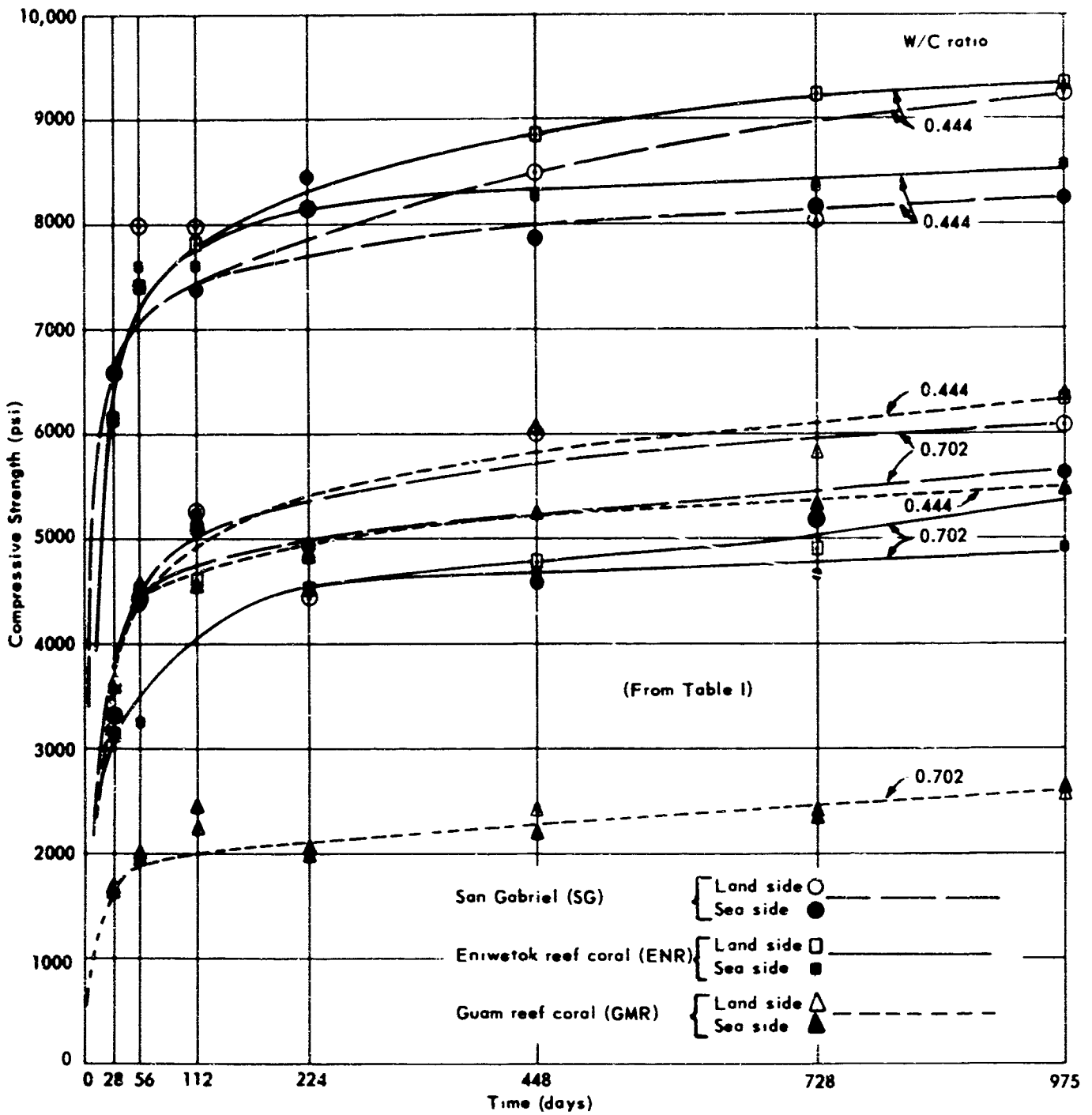


Figure 3. Compressive strength versus age of walls (from Table I).



Figure 4. Wet Cup assembled with corrosion probe added.

For the NaCl series previously reported, continued observations of the WVT values have shown no significant numerical changes. Still valid are the facts that WVT reaches a minimum value at a mixing water salinity of about 70 gm/kg, and that with further increases in salinity, the WVT values remain virtually constant.

Sea-Water Series

The values of WVT previously reported for varying salinities of mixing water using sea water have shown no changes after approximately 950 days of test.

For additional data on WVT with higher salinities of mixing water (using up to 87.70 gm/kg of sea water in the concrete), two new series of specimens were cast, and wet-cup specimens were made.

Wet cups from the first series of 12 batches ($W/C = 0.444$) and wet cups from the second series of eight batches ($W/C = 0.702$) were placed in the 20 percent RH environment, and values for WVT were obtained. Values of WVT from both

series are plotted in Figure 5 along with a curve reprinted from Reference 1 for comparison. Previous findings, that WVT decreases with an increase in strength and that WVT decreases with an increase in salinity to approximately 25 gm/kg and thereafter levels off with further increases in salinity, are verified. Being of like design, the two top curves are compatible enough to present virtually the same results.

Wall Specimens

The WVT values for wet-cup specimens fabricated at the time the walls were cast show no changes after extending the test period from 360 days to 800 days.

WVT Hysteresis

Hysteresis is herein defined as a reduction in WVT caused by aging or by previous exposure of the specimen.⁶ After a test period of approximately 950 days, WVT values were computed as listed in Table II.

Figure 6 is a plot of WVT versus salinity of mixing water, with separate curves for each thickness in each RH room. The salinity at which the curves become nearly horizontal, i.e., where the WVT is not significantly changed by increased salinities, is approximately 19 gm/kg. This salinity is in fairly close agreement with the finding previously reported;¹ although the curves of Figure 6 are generally of the same order, they are lower on the WVT scale. The data wholly supports the definition of hysteresis; i.e., the WVT rate is reduced when the specimen is first exposed to an environment different from the test environment.

Vented Cups

In order to assure equal total pressure both internal and external to the wet cup, vents were installed in two cups and omitted in two cups as previously reported. After approximately 500 days age, WVT values of the four specimens were calculated to be:

1. Two 1-inch-thick specimens, one with and one without vent; WVT for each = 0.490 grains per square inch per day.
2. One 2-inch-thick specimen, with vent; WVT = 0.401 grains per square inch per day.
3. One 2-inch-thick specimen, without vent; WVT = 0.347 grains per square inch per day.

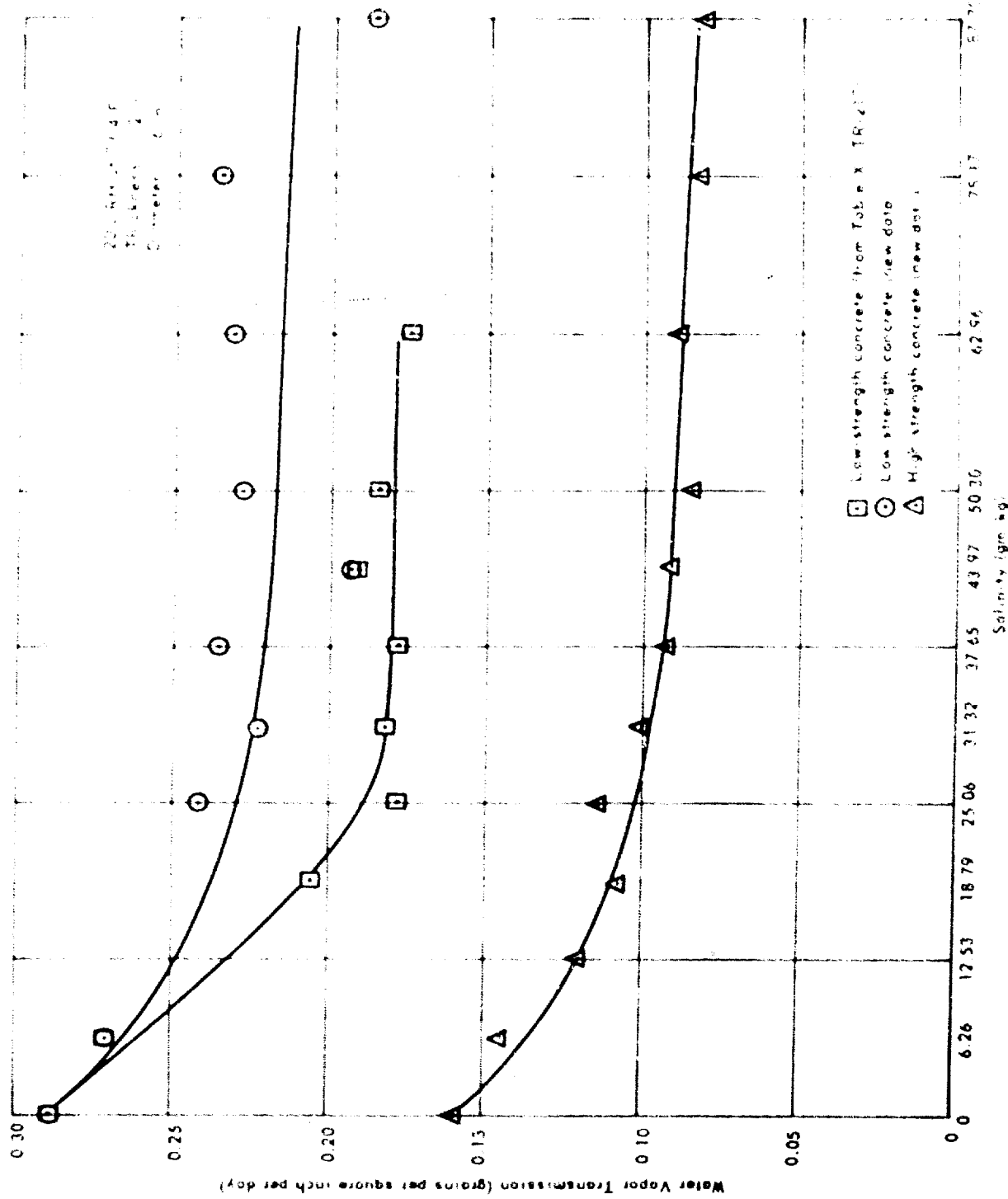


Figure 5. Water vapor transmission versus salinity of mixing water (sea water) — strength comparison.

Table II. WVT Versus Salinity of Mixing Water for 4-Inch-Nominal-Diameter Concrete Specimens With W/C = 0.702 (Sea Water and C-Type II Cement)

Batch No.	Cup No.	Sea-Water Concentration (% by weight)	Salinity (gm/kg)	$\frac{a}{b}$ (in.)	RH at 73.4 F (%)	W/t ^{b/}	WVT ^{c/}
S3L-2	U415-D	20	6.26	3.050	20	0.098	0.135
S3L-2	U415-C	20	6.26	1.507	20	0.154	0.213
S3L-4	U481-D	60	18.79	3.070	20	0.090	0.125
S3L-4	U481-C	60	18.79	1.500	20	0.122	0.170
S3L-6	U570-D	100	31.32	3.057	20	0.076	0.106
S3L-6	U570-C	100	31.32	1.501	20	0.118	0.164
S3L-8	U639-D	140	43.97	3.076	20	0.083	0.116
S3L-8	U639-C	140	43.97	1.490	20	0.124	0.172
S3L-10	U705-D	200	62.96	3.082	20	0.066	0.091
S3L-10	U705-C	200	62.96	1.481	20	0.124	0.172
S3L-2	U415-A	20	6.26	3.073	50	0.058	0.080
S3L-2	U415-B	20	6.26	1.516	50	0.088	0.123
S3L-4	U481-A	60	18.79	3.032	50	0.042	0.058
S3L-4	U481-B	60	18.79	1.494	50	0.069	0.096
S3L-6	U570-A	100	31.32	3.047	50	0.041	0.057
S3L-6	U570-B	100	31.32	1.514	50	0.069	0.096
S3L-8	U639-A	140	43.97	3.051	50	0.042	0.059
S3L-8	U639-B	140	43.97	1.511	50	0.069	0.095
S3L-10	U705-A	200	62.96	3.057	50	0.039	0.054
S3L-10	U705-B	200	62.96	1.522	50	0.078	0.108
S3L-2	U416-F	20	6.26	3.033	75	0.055	0.077
S3L-2	U416-E	20	6.26	1.527	75	0.085	0.118
S3L-4	U482-F	60	18.79	3.009	75	0.049	0.068
S3L-4	U482-E	60	18.79	1.516	75	0.065	0.090
S3L-6	U571-F	100	31.32	3.010	75	0.046	0.064
S3L-6	U571-E	100	31.32	1.536	75	0.063	0.087
S3L-8	U640-F	140	43.97	3.021	75	0.039	0.055
S3L-8	U640-E	140	43.97	1.568	75	0.058	0.081
S3L-10	U706-F	200	62.96	3.011	75	0.033	0.046
S3L-10	U706-E	200	62.96	1.510	75	0.063	0.087

a/ Length of flow path (or thickness of specimen).

b/ Slope of straight-line portion of graph of water loss, grams versus time in days; 950-day record.

c/ Grains per sq in. per day (1 gram = 15.43 grains).

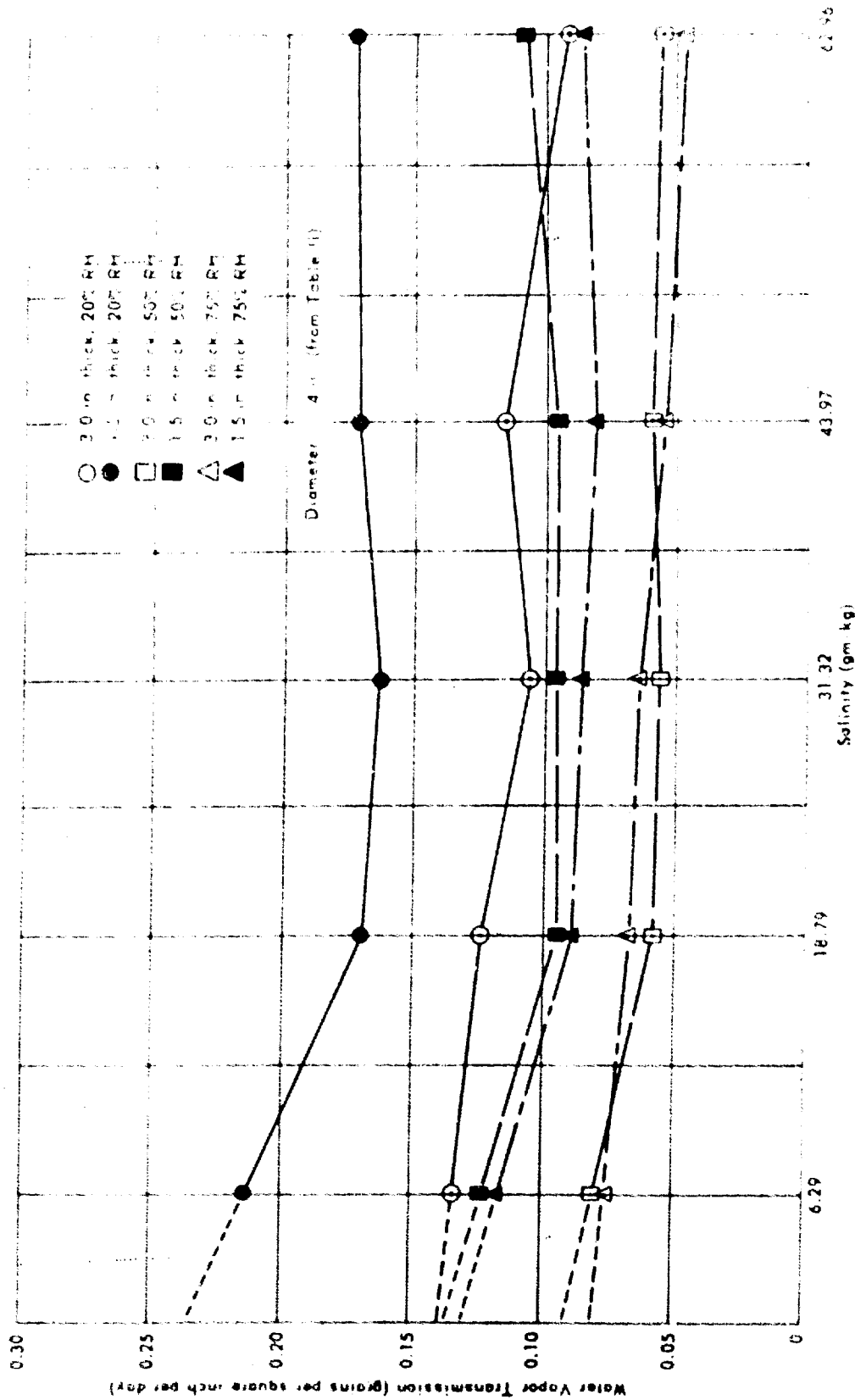


Figure 6. Water vapor transmission versus salinity of mixing water (sea water) — hysteresis.

Since these WVT differences are slight, it may be concluded that there are apparently no significant differences between the vented and unvented cups or between the 1- and 2-inch-thick specimens. If a total pressure change had occurred within the wet cups of this task, this total pressure change did not significantly affect the true WVT rates as reported.

CORROSION OF STEEL

Corrosion-Detection Probe

A complete description of the detection probe used in this task is presented in Appendix C.

Sea-Water Series

The data from the series of wet cups (like that shown in Figure 4) with probes previously reported^{1, 2} remained unchanged to 860 days age, but did not reveal what might occur with higher salinities and higher-strength concrete. To obtain more information, two new series of concrete wet cups (each cup with a probe) were prepared — one high-strength (W/C = 0.444) and one low-strength (W/C = 0.702).

Twelve high-strength concrete wet-cup specimens with probe were prepared and placed in the 20 percent RH room. Probe readings were taken periodically and plotted versus time in days. These curves are presented in Figure 7 for each salinity of mixing water. From these plots the corrosion rate was calculated in mils per year (MPY), using the following equation:

$$\text{MPY} = \frac{(\Delta D) M (365)}{(\Delta T) (1000)} \quad (1)$$

where ΔD = change in dial divisions (probe reading) between data points, microinches (the 1000 converts this to mils)

ΔT = elapsed time between data points in days (the 365 converts this to years)

M = multiplier (for the probes of this task M = 2)

$\Delta D/\Delta T$ = slope of curves in Figure 7

which reduces to:

$$\text{MPY} = 0.730 (\text{slope})$$

The maximum corrosion rates for the high-strength concrete are presented in Table III. The maximum rate is determined by using the maximum slope of the curve during the life of the test, and the maximum rate was chosen because the slope varied throughout the life of the test for most of the specimens.

Figure 8 is a plot of maximum corrosion rate versus salinity for the high-strength series. The points plotted in the figure are observed corrosion rate values; whereas, the curve drawn in the figure is a least-squares fit to the polynomial equation,

$$Y = A + Bx + Cx^2 + Dx^3 \quad (2)$$

with a correlation coefficient, r , of 0.81. The product moment correlation coefficient, r , was computed to indicate the degree of correlation between the observed data and the computed curve. The curve in Figure 8 (high-strength concrete) develops a significant corrosion rate at lower salinities and continues at a slower rate of increase than the curve in Figure 9 (low-strength concrete). Figure 8 confirms that the most favorable salinity in high-strength sea-water concrete for the maximum corrosion rate is evidently beyond 87.70 gm/kg.

An extrapolation of the theoretical least-squares curve from a salinity of 87.70 gm/kg out to 156.65 gm/kg indicates that the point of maximum corrosion rate should occur at a salinity of approximately 119 gm/kg (dashed line in Figure 8). This is presented for interest only as there are no supporting data.

Eight low-strength concrete wet-cup specimens, each with probe, were prepared and placed in the 20 percent RH room. These have the same design as those reported in Table IV and Figure 9 except that the salinity was extended to 87.70 gm/kg. Probe readings were plotted against time in days for each salinity as shown in Figure 10. From these plots the corrosion rate in MPY was calculated using Equation 1. The maximum corrosion rates for the low-strength concrete are presented in Table V.

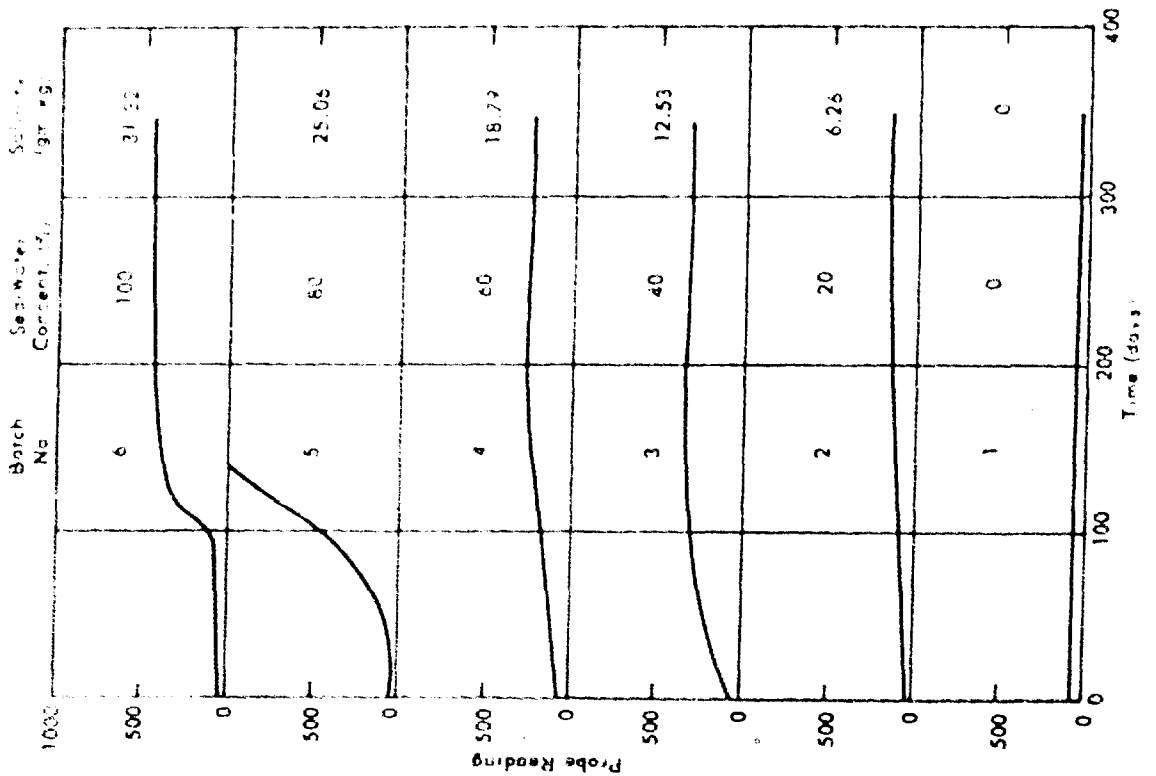
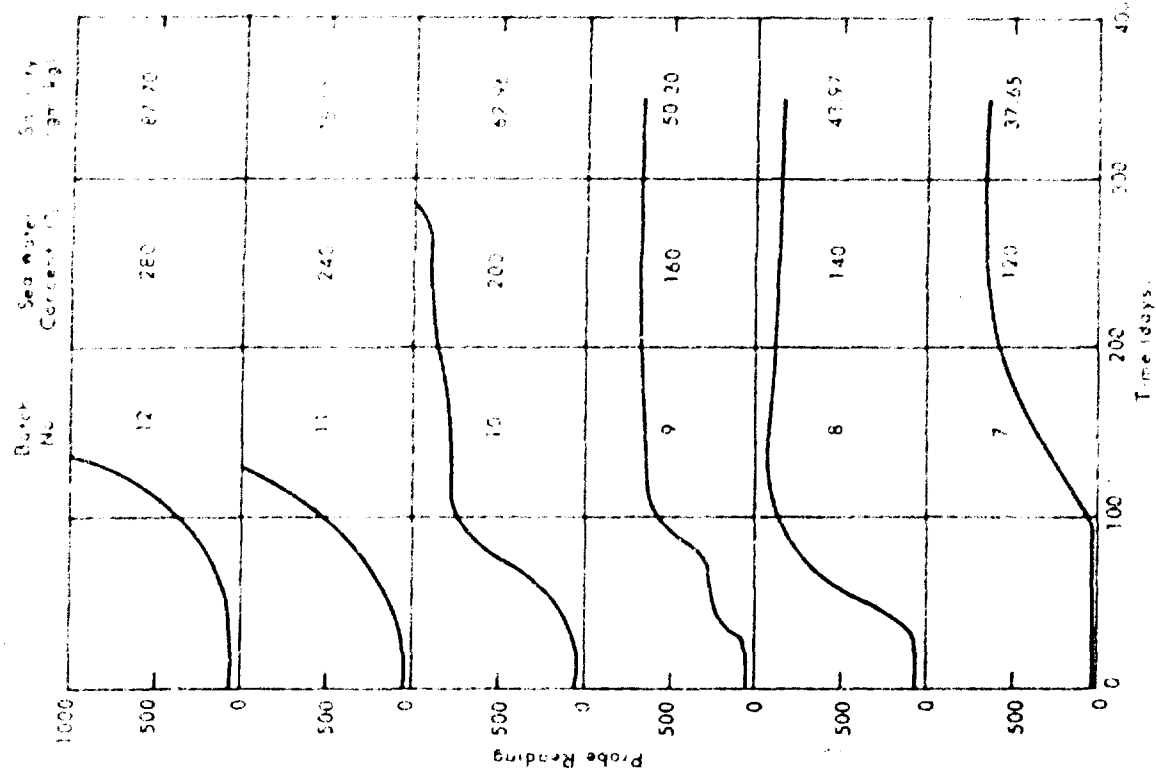


Figure 7. Probe reading versus time in days — high-strength concrete (W/C = 0.444).

Table III. Maximum Corrosion Rate of Steel in Concrete Versus Salinity of Mixing Water for W/C = 0.444 (Sea Water and C-Type II Cement)

Batch No.	Cup No.	Sea-Water Concentration (% by weight)	Salinity (gm/kg)	Time to Begin Corrosion (days)	Maximum Corrosion Rate (mils per yr)
SIH-1-C	Y67	0	0	none	0
SIH-2-C	Y98	20	6.26	28	0.3
SIH-3-C	Y129	40	12.53	29	1.1
SIH-4-C	Y160	60	18.79	28	0.9
SIH-5-C	Y191	80	25.06	28	9.8
SIH-6-C	Y239	100	31.32	28	8.8
SIH-7-C	Y270	120	37.65	74	4.6
SIH-8-C	Y301	140	43.97	31	11.7
SIH-9-C	Y332	160	50.30	28	9.4
SIH-10-C	Y363	200	62.96	33	12.6
SIH-11-C	Y394	240	75.17	30	10.7
SIH-12-C	Y425	280	87.70	46	16.3

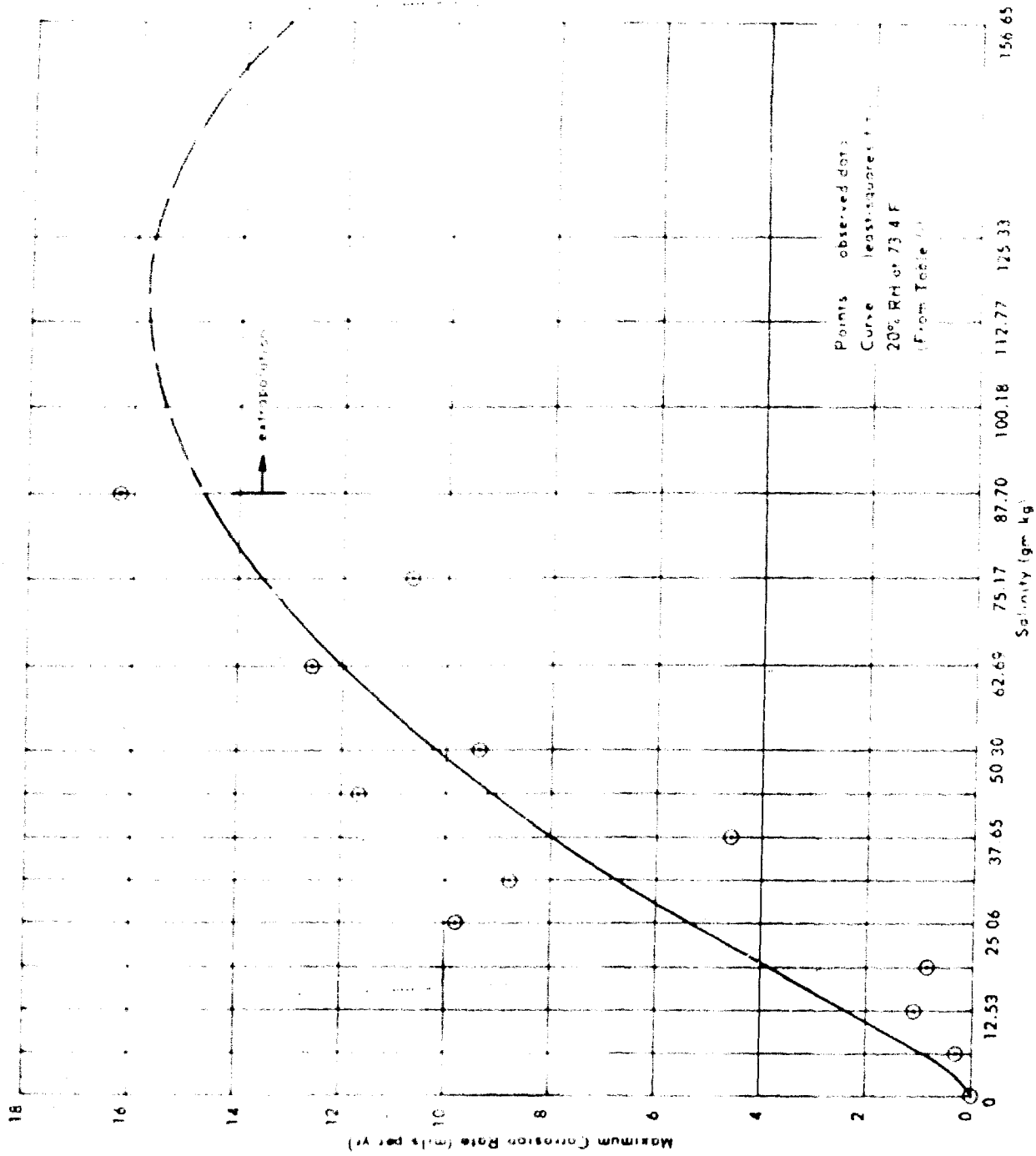


Figure 8. Corrosion versus salinity of mixing water — sea water and high-strength concrete (W/C = 0.444).

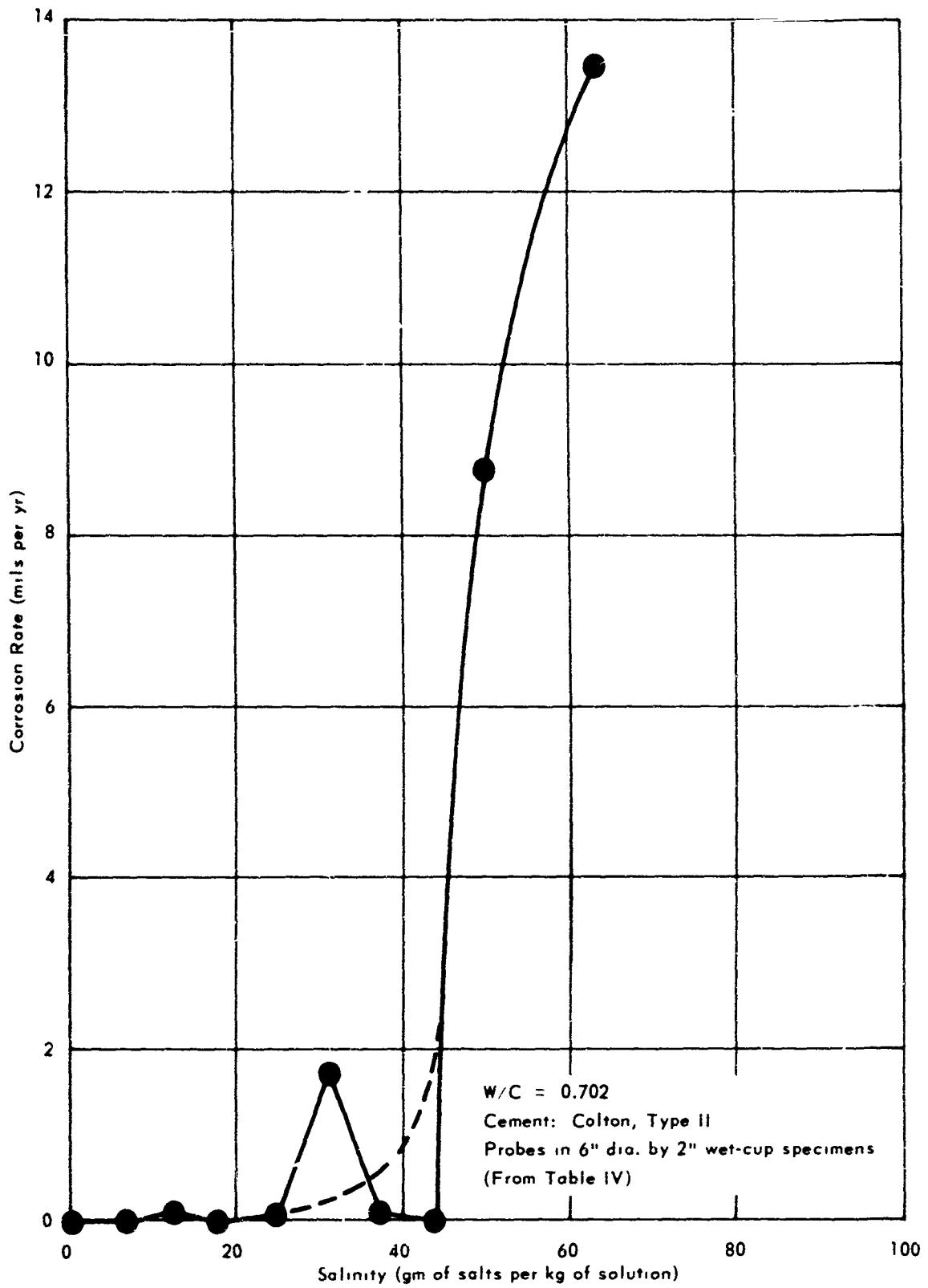


Figure 9. Corrosion versus salinity using sea water (reprinted from TR-217).

Table IV. Sea-Water Concentration Versus Corrosion of Steel in Concrete for W/C = 0.702 (Reprinted From TR-217)

Cup No.	Sea-Water Concentration (% by weight)	Salinity (gm/kg)	Time to Begin Corrosion (days)	Maximum Corrosion Rate (mils per yr)
U306	0	0	none	—
U414	20	6.26	none	—
U447	40	12.53	25	0.1
U480	60	18.79	none	—
U514	80	25.06	193	0.1
U569	100	31.32	360	1.7
U605	120	37.65	60	0.1
U638	140	43.97	none	—
U671	160	50.30	25	8.8
U704	200	62.96	315	13.5

Table V. Maximum Corrosion Rate of Steel in Concrete Versus Salinity of Mixing Water for W/C = 0.702 (Sea Water and C-Type II Cement)

Batch No.	Cup No.	Sea-Water Concentration (% by weight)	Salinity (gm/kg)	Time to Begin Corrosion (days)	Maximum Corrosion Rate (mils per yr)
S3L-5-C	Y611	80	25.06	15	0.7
S3L-6-C	Y612	100	31.32	22	10.1
S3L-7-C	Y613	120	37.65	76	12.7
S3L-8-C	Y614	140	43.97	16	16.0
S3L-9-C	Y615	160	50.30	146	5.7
S3L-10-C	Y616	200	62.96	61	18.7
S3L-11-C	Y617	240	75.17	56	42.2
S3L-12-C	Y618	280	87.70	16	23.8

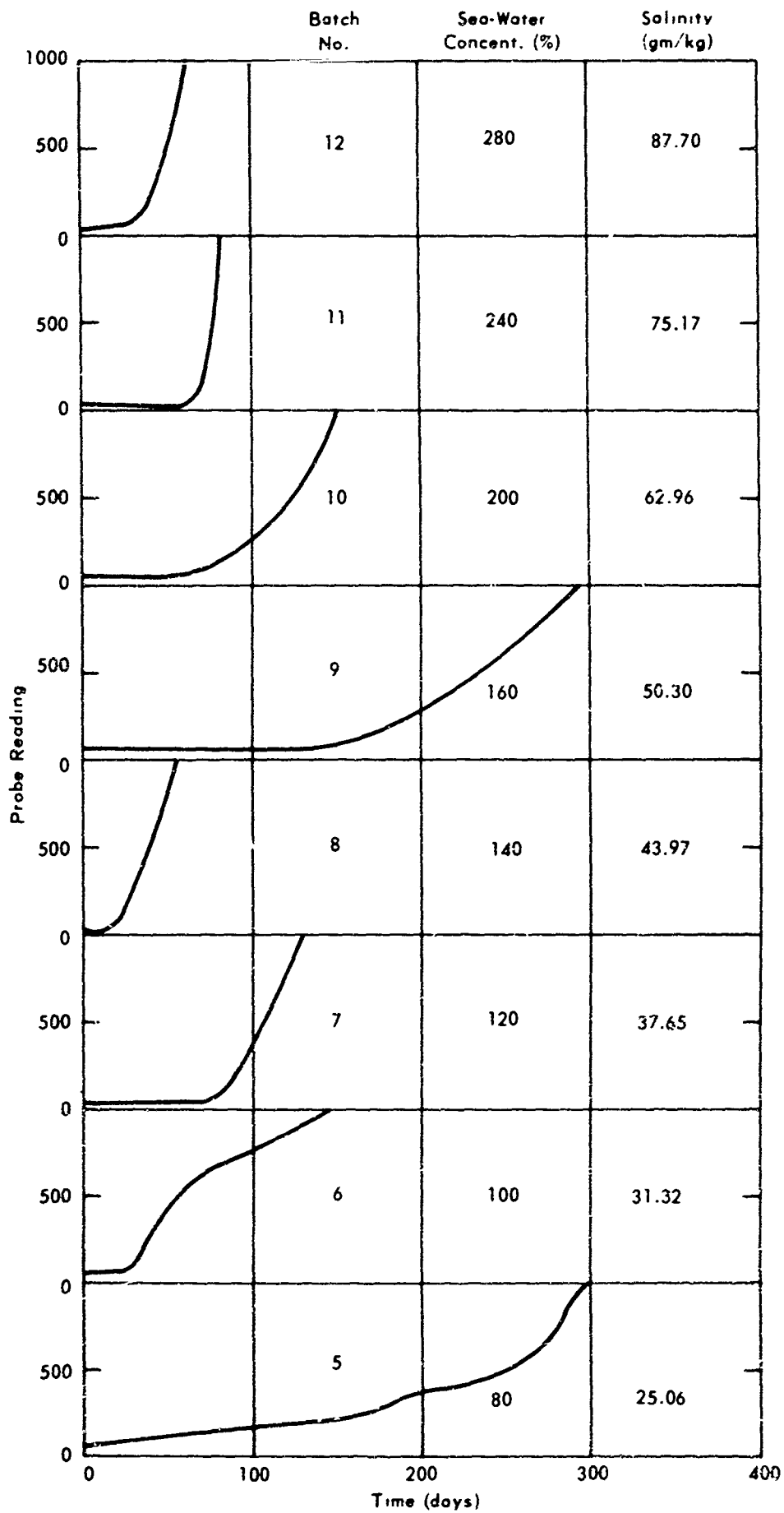


Figure 10. Probe reading versus time in days — low-strength concrete (W/C = 0.702).

The corrosion data in Tables IV and V were each subjected to the least-squares method of curve fitting. The r value for each set of data was computed to be 0.89 and 0.67, respectively. Then the two sets of data were both fitted to the same curve by the least-squares method. The r value for the combined data set was 0.70.

An analysis of the variance of each set of data with the computed curve was conducted using the F-test:

$$F = \frac{s_1^2}{s_2^2} = \frac{58.7}{19.4} = 3.02$$

where s_1^2 = variance of new data about the curve

s_2^2 = variance of old data about the curve

and where $F_{95(7.9)} = 3.29$

$F_{05(7.9)} = 0.27$

which indicates that there is no significant difference in the variances at the 90 percent confidence level.

With this degree of confidence, the data points from Tables IV and V were plotted (Figure 11) as maximum corrosion rate versus salinity for the low-strength series. The points in the figure are observed corrosion-rate values; whereas, the curve represents the least-squares fit of Equation 2, with r value of 0.70.

An extrapolation of the theoretical least-squares curve in Figure 11 (like that in Figure 8) indicates that the point of maximum corrosion rate should occur at a salinity of approximately 100 gm/kg. Again, this extrapolation has no data to support it, but is presented for interest.

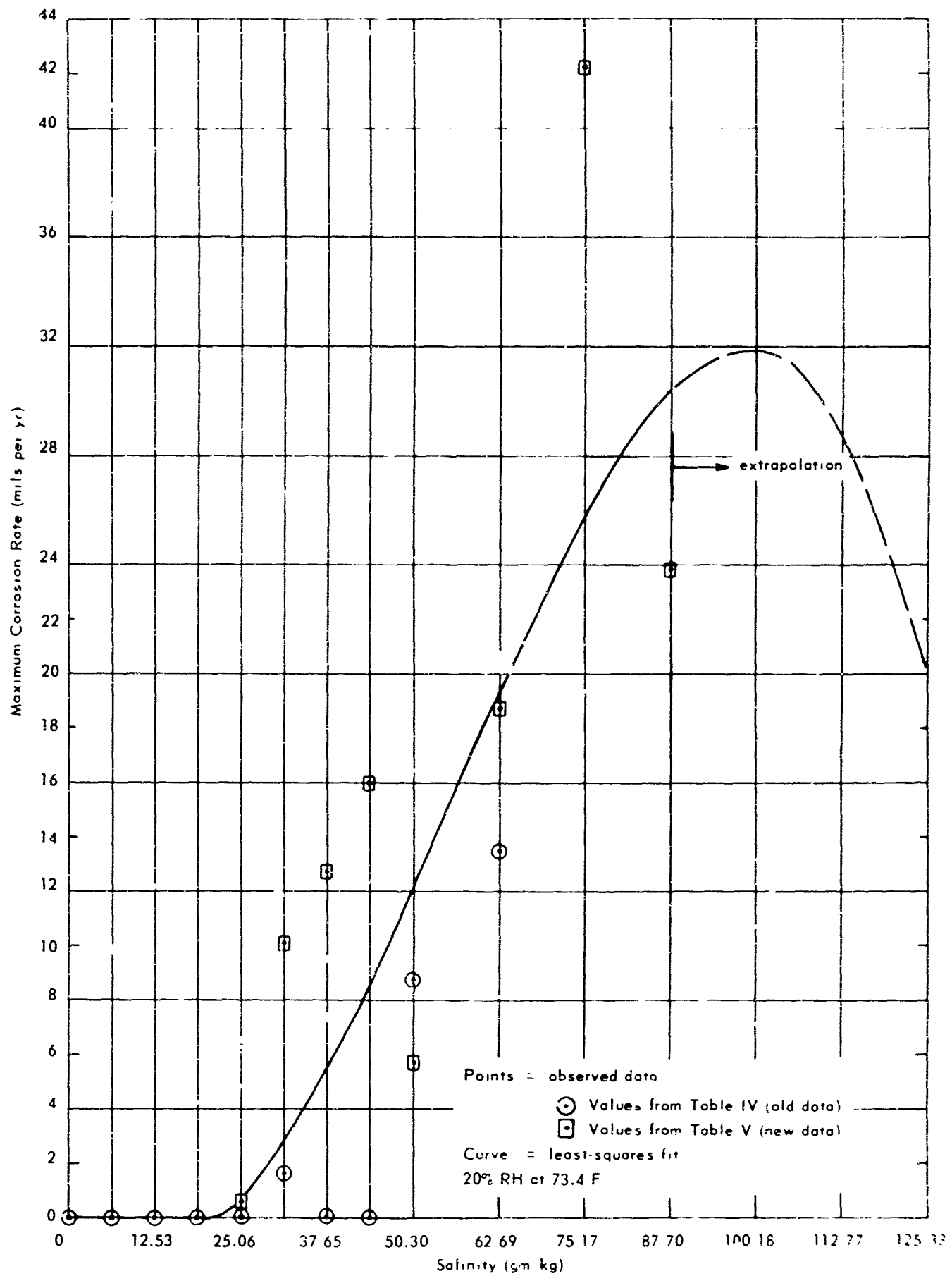


Figure 11. Corrosion versus salinity of mixing water — sea water and low-strength concrete (W/C = 0.702).

Figure 11 agrees with the findings as indicated in Figure 9 in that no significant corrosion occurs up to a salinity of approximately 25 gm/kg; thereafter the rate of increase of the maximum corrosion rate for the low-strength concrete is about 1 MPY for every 2 salinity units. Figure 8 shows that the rate of increase of the maximum corrosion rate for the high-strength concrete is about 1 MPY for every 5 salinity units. This indicates that the high-strength concrete offers 2-1/2 times more resistance to corrosion of mild steel than does the low-strength concrete. This indication also adds support to the extrapolated information that the point of maximum corrosion rate demands a higher salinity for the high-strength concrete (119 gm/kg) than for the low-strength concrete (100 gm/kg).

Depth-of-Cover Series

A series of 6-inch-thick concrete specimens of two different strengths ($W/C = 0.444$ and 0.702) were prepared as wet cups with probes. Measuring from the bottom surface of the specimen, the probes had concrete cover depths of 1, 2, 3, 4, and 5 inches. These cups have been stored in 50 percent RH at 73.4 F for approximately 1000 days with no significant or measurable corrosion occurring. This is to be expected since the salinity of the mixing water is zero.

Experimental Walls

A very complete description of the walls is reprinted in Appendix B. One side of the walls has been sprayed daily with sea water for approximately 3 years.

When the walls were 22 months old, the first observable cracks appeared in the vertical end faces of Walls 1, 2, and 10. Walls 2 and 10 are low-strength SG and ENR, respectively, with welded steel and 1-inch cover (thinner walls). Wall 1 is high-strength GMR with tied steel and 1-inch cover. Figure 3 shows that at the age of approximately 660 days the low-strength SG and ENR and the high-strength GMR concrete all had compressive strengths ranging from 4500 to 6000 psi. This range was even smaller at lower ages. Since these three designs began to show deterioration at approximately the same time, they appear to have somewhat the same resistance to deterioration. It would be expected that the thin-wall low-strength GMR design would show cracking also, but it has not. The thicker less-resistant and the thinner more-resistant designs have not shown cracking. The sprayed face of each of the walls has shown varying degrees of spalling.

Figure 12 shows the cracks in Walls 1, 2, and 10 after 34 months of testing, or 12 months after the cracks first formed. The sprayed surfaces of the walls face south. Over this 12-month period, the propagation rate of the crack development in each face shown in Figure 12 is:

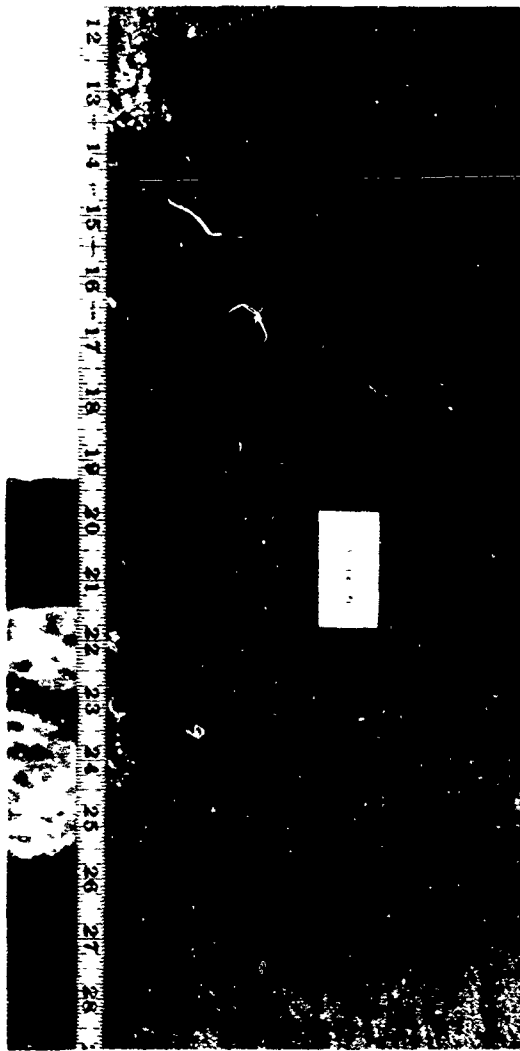
Wall	Propagation Rate (inches per month)
No. 1 East	3/4
No. 1 Front	1
No. 2 East	1
No. 2 West	1-1/16
No. 10 East	1-1/12
No. 10 West	1 1/3

Apparently the repeated wetting and drying of the wall surface sprayed with sea water assisted the movement of salts into the concrete, causing the steel to corrode. The basic cause of this corrosion (oxidation) is the instability of the iron in its refined form. The oxide of iron requires a greater volume than the original metal occupied thereby inducing tensile forces in the surrounding concrete causing the concrete to expand. Since concrete has a very low tensile strength, its failure by cracking serves to relieve the tensile forces. Even the smallest cracks propagate additional corrosion and further cracking by exposing the metal to outside elements. As would be expected, the cracks thus far developed in the end faces of the walls are in the same plane as the steel grid. One reason the top faces have not developed cracks, as the end faces have, is that each side face receives about half as much sunshine as the top face. The same is true of the front faces, except for the front face of Wall 1 adjacent to the east end face (Figure 12) which did develop a 10-inch-long crack.

These wall exposure tests and the compressive-strength tests (Figure 3) verify the finding that high-quality aggregate and high-strength concrete are essential if reinforced concrete structures are to resist the deteriorating effect of sea water and sea salts.



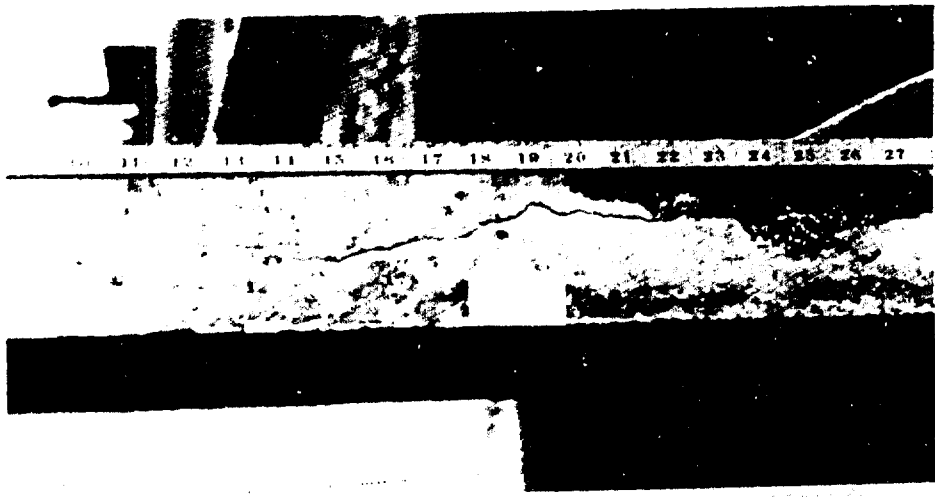
East end of Wall 1



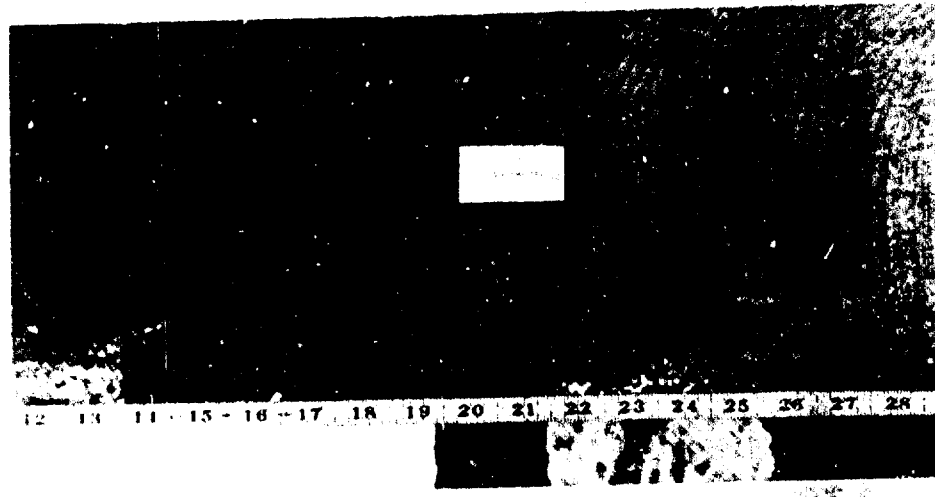
Sprayed surface adjacent
to east end of Wall 1



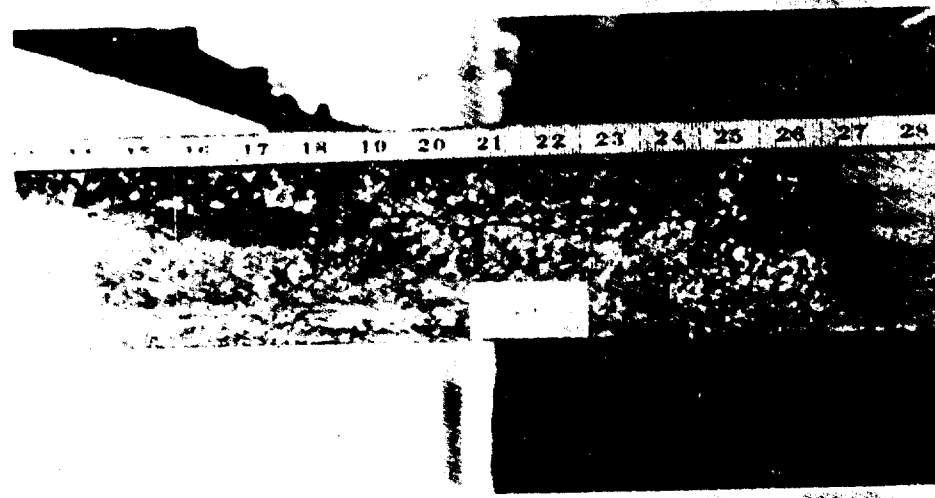
East end of Wall 2



East end of wall 1



Sprayed surface adjacent to east end of wall 1



East end of wall 1

GENERAL SUMMARY

The new and additional data as reported herein has not changed the findings last reported^{1, 2} but has expounded and generally verified them, with the following exception.

Some salt may be beneficial to concrete in some respects. Although the new and additional data have not changed the findings about strength or WVT of concrete, the corrosion rates are affected slightly by the findings of the new high-strength series of specimens with probe. It is not possible to state what is or is not a significant corrosion rate in practice (actual construction), based on limited laboratory tests alone. But it can be stated that, within the bounds of this investigation, the higher the concrete strength the lower the salinity necessary to have a significant corrosion rate occur.

FINDINGS AND CONCLUSIONS

It is a general conclusion that a small amount of sea-water salts may be beneficial to concrete if rigid controls are exercised. At a mixing-water salinity of approximately 25 gm/kg, strength is improved, WVT is minimized, and for the low-strength concrete of this investigation corrosion of mild steel is negligible.

Compressive Strength

1. Maximum compressive strength occurs between salinities of 18 and 36 gm/kg for concrete incorporating NaCl in the mixing water.
2. Depending upon the age of concrete, relatively high salinities of NaCl can occur before strengths become less than those for zero salinity.
3. Natural sea water does not deteriorate plain concrete; strength is generally increased with salinities up to nearly three times that of natural sea water.

Water Vapor Transmission

1. With increasing NaCl salinity of mixing water up to 70 gm/kg, and of sea water up to a range of 19 to 31 gm/kg, WVT is reduced to its minimum for all thicknesses studied. With further increasing salinities, WVT is almost constant.
2. With increasing salinities, the effect of the thickness of the specimen becomes much more pronounced; thicker specimens show much greater reductions in WVT than do thinner specimens.

3. With or without salts (NaCl or sea-water salts), WVT varies inversely with compressive strength.
4. Without salts, thinner concrete specimens have somewhat higher WVT rates than do thicker specimens. Indications are that 6 inches may be a limiting thickness beyond which greater thicknesses do not further decrease WVT significantly.
5. Concrete made with poor-quality aggregate (GMR) shows higher WVT rates than concrete made with high-quality aggregate (SG and ENR), other factors being equal.
6. This investigation does not confirm nor does it completely negate an earlier finding³ that an ambient RH of 20, 50, or 75 percent at 73.4 F has no significant effect on WVT compared with experimental variability.

Corrosion

1. The electrical-resistance corrosion-rate detection probe appears to be a reliable device for measuring the corrosive effect of concrete on mild reinforcing steel.
2. Concrete with NaCl in the mixing water shows an optimum salinity of about 70 gm/kg for maximum corrosion of mild steel.
3. When sea water is used in concrete mixing water, the salinity at which mild steel develops a significant corrosion rate appears to vary directly with the W/C. Within the limits of this investigation, for concrete with a low W/C, the maximum corrosion rate increased rapidly at lower salinities. For higher salinities the rate of increase of the maximum corrosion rate was 2-1/2 times slower for concrete with a low W/C.

REFERENCES

1. U. S. Naval Civil Engineering Laboratory. Technical Report R-217, The Effect of Salt in Concrete on Compressive Strength, Water Vapor Transmission, and Corrosion of Reinforcing Steel, by D. F. Griffin and R. L. Henry. Port Hueneme, California, 12 November 1962.
2. Griffin, D. F., and R. L. Henry. "The Effect of Salt in Concrete on Compressive Strength, Water Vapor Transmission, and Corrosion of Reinforcing Steel," American Society for Testing and Materials, Proceedings, Vol 63, 1963, pp 1046-1078.
3. U. S. Naval Civil Engineering Laboratory. Technical Report R-130, Water Vapor Transmission of Plain Concrete, by D. F. Griffin and R. L. Henry. Port Hueneme, California, 16 May 1961.

4. Griffin, D. F., and R. L. Henry. "Integral Sodium Chloride Effects on Strength, Water Vapor Transmission, and Efflorescence of Concrete," *Journal of American Concrete Institute*, No. 6 (December 1961), pp 751-772.
5. Cement and Concrete Association. TRA/374, *The Workability and Compressive Strength of Concrete Made With Sea Water*, by J. D. Dewar. London, December 1963.
6. ASTM Committee C-16, "Water Vapor Transmission Testing," *Bulletin of ASTM, Materials Research and Standards*, Vol 1, No. 2 (February 1961), pp 117-121.
7. U. S. Naval Civil Engineering Laboratory. Technical Report R-057, *Evaluation of Condensate Return Line Corrosion Testers*, by J. M. Hayhoe and N. L. Slover. Port Hueneme, California, 13 March 1961.

Appendix A
MIX DESIGN DATA

Table A-1. Summary of Concrete Mix Design Data
(Reprinted From TR-217)

A. Characteristics of Materials

Cements: Colton, Type II; Colton, Type III; Victor, Type III.

Aggregates: 1. SG or San Gabriel, a reference aggregate from the Irwindale Pit of Consolidated Rock Products Co., Calif.

2. ENR or Eniwetok Atoll reef coral from Eniwetok Islet, Marshall Islands; a good-quality coral consisting of 95 percent coralline limestone.

3. GMR or Guam reef coral from Apra Harbor, Guam, the Marianas; a poor-quality coral consisting of 96 percent cellular coral or porous coralline rock.

4. Specific characteristics:

Item	SG		ENR		GMR	
	C	F	C	F	C	F
Bulk Sp Gr (oven-dry)	2.66*	2.63*	Overall Avg 2.49 2.49		Weighted Avg L: 2.16 H: 2.11**	
24-hr abs, percent	1.6*	1.8*	2.32	2.32	20.0*	7.6*
Comparative general physical condition, percent by weight	Reference aggregate, approx. 100 percent good		73 Good 25 Fair 2 Poor	73 25 2	49 Good 45 Fair 6 Poor	45 45 10

* Determined by Task Engineers.

Data without (*) taken from NCEL TN-335A.

** L = W/C ratio of 0.702.

H = W/C ratio of 0.444.

Note: San Gabriel aggregate was used unless otherwise indicated.

Table A-1. Summary of Concrete Mix Design Data (Cont'd)

5. Grading: Pounds retained on each sieve per 6.0± cu-ft batch

Sieve	SG		ENR		GMR	
	H	L	H	L	H	L
3/4 in.	19.7	16.5	0	0	0	0
3/8 in.	197.6	196.6	202.0	193.8	179.6	172.4
No. 4	125.1	121.0	116.4	110.0	103.4	98.0
No. 8	72.5	85.9	67.2	77.8	59.8	69.6
No. 16	65.9	82.9	61.2	75.2	54.4	67.0
No. 30	72.5	83.5	67.2	76.0	59.8	67.6
No. 50	59.2	76.2	55.2	69.4	49.0	61.8
No. 100	33.1	38.7	30.6	35.4	27.2	31.2
Pan	13.3	18.7	12.2	17.0	10.8	15.2
Total	658.9	720.0	612.0	654.6	544.0	582.8

Water: Port Hueneme tap water at 73.4 F.

Chemical analysis (ppm): hydroxide (0.0); carbonate (0.0); bicarbonate (137.0); chlorides (62.0); calcium (38.0); magnesium (14.6); sulphate (465.0); sodium and potassium (219.0).

Slump: Designed for 3 in.

B. Batch of 1.0± cu ft consisted of the following:

Mix Design Factors	SG		ENR		GMR	
	H	L	H	L	H	L
W/C	0.444	0.702	0.444	0.702	0.444	0.702
Water (lb) ^{a/}	11.7	11.7	13.4	13.8	13.4	13.8
Cement (lb)	26.4	16.7	30.1	19.7	30.1	19.7
Cement Factor ^{b/}	7.62	4.81	8.65	5.66	8.65	5.66
Aggregate (lb)	109.9	120.0	102.0	109.0	90.7	97.2

^{a/} The quantity of water added at the mixer was corrected for moisture present in the aggregate and moisture required for absorption.

^{b/} Sacks per cu yd of concrete.

Appendix B

EXPERIMENTAL WALLS (All the material in this appendix is reprinted from TR-217)

Experimental Walls

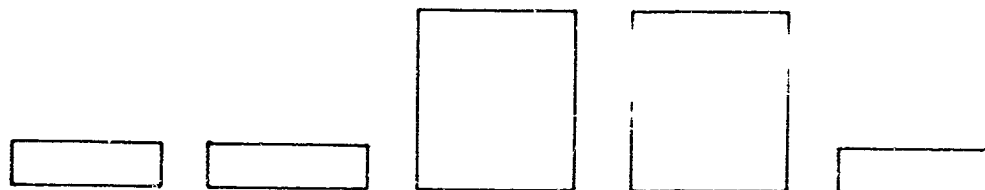
In order to simulate a marine environmental exposure such as that encountered by a building on a tropic atoll, small walls of reinforced concrete were built and sea-water spray was applied daily. The details of the concrete mixes and their ingredients are shown in Table A-1, Appendix A.

The variables to be investigated are shown in Table B-1. The three types of aggregate described in Table A-1 and two water-cement ratios (0.444 and 0.702) were used, and two different reinforcing-steel arrangements were employed. Each of the steel arrangements had the same grid spacings. The only difference in arrangement was that in one case the mild-steel bars were insulated from each other with electricians' plastic tape and tied together with nylon fishing cord, as shown in detail in Figure B-1. In the other arrangement all steel bars were tack-welded together at the point of contact. These arrangements were to permit the investigation of corrosion of individual steel bars as compared to the corrosion of an interconnected grid of steel bars. Two depths of steel cover were also included as variables, the depth being measured from the outer surface of the concrete to the nearest surface of the steel. It was desired to eliminate all external entries, such as tie-wire and bolt holes, through the concrete to the steel as unknown variables; therefore, concrete blocks for the particular kind of concrete to encase the steel grids were precast with wire loops embedded in each block for securing the steel grids. These are shown in Figure B-2. In this way there were no steel wires going from the steel grid through the concrete to the outside. The use of spacer blocks was avoided for the same reason, and the grids were held in place vertically by means of temporary holding devices which may be seen in Figure B-3.

It was desired to hold the W/C for the high-strength concretes equal throughout and that for the low-strength concretes equal throughout. It was further desired to design all concretes for identical consistencies as measured by the slump test. This required a greater amount of water and cement for the coral aggregate concretes than for the San Gabriel aggregate concrete.

if

Table B-1. Var




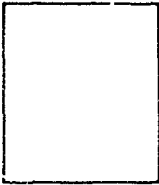




Wall Configuration (Plan View)					
Statistical Factors					
Wall Number	1	2	3	4	5
Aggregate ^{a/}	GMR	SG	ENR	SG	ENR
Strength ^{b/}	Hi	Lo	Lo	Hi	Hi
Steel Arrangement ^{c/}	T	W	T	W	T
Depth of Steel (cover)	1"	1"	6"	6"	1"
Wall Thickness	3-1/2"	3-1/2"	13-1/2"	13-1/2"	3-1/2"
Casting Date (1961)	15 May	8 May	11 May	8 May	11 May
Cylinder Test Dates	10 Jul '61	3 Jul '61	6 Jul '61	3 Jul '61	6 Jul '61
	5 Sep '61	28 Aug '61	31 Aug '61	28 Aug '61	31 Aug '61
	26 Dec '61	18 Dec '61	21 Dec '61	18 Dec '61	21 Dec '61

^{a/} See Table I

^{b/} Hi = High W/C = 0.444
 Lo = Low W/C = 0.702

^{c/} T = Tied (and steel contacts insulated)
 W = Welded

4-1. Variables for Experimental Walls

							
5	6	7	8	9	10	11	12
NR	GMR	ENR	SG	GMR	ENR	GMR	SG
Hi	Lo	Hi	Lo	Lo	Lo	Hi	Hi
T	W	W	T	T	W	W	T
1"	1"	6"	6"	6"	1"	6"	1"
1/2"	3-1/2"	13-1/2"	13-1/2"	13-1/2"	3-1/2"	13-1/2"	3-1/2"
May	15 May	11 May	8 May	15 May	11 May	15 May	8 May
Jul '61	10 Jul '61	2 Aug '62	30 Jul '62	6 Aug '62	2 Aug '62	6 Aug '62	30 Jul '62
Aug '61	5 Sep '61	11 May '63	8 May '63	15 May '63	11 May '63	15 May '63	8 May '63
Dec '61	26 Dec '61	10 Jan '64	8 Jan '64	15 Jan '64	10 Jan '64	15 Jan '64	8 Jan '64

While the slump test has for a number of years appeared to be an excellent measure of consistency for San Gabriel aggregate concrete, coral aggregate concretes do not respond quite so uniformly to the slump test. Although distribution of aggregate by percentage was approximately the same for all batches, the coral concretes appeared too harsh, compared with the San Gabriel aggregate concrete. The slumps in inches for the various concretes used in the walls are tabulated below:

Wall No.	Min	Avg	Max	W/C	Aggregate
6, 9	4-1/2	6-1/2	8	0.702	GMR
2, 8	1	2	3	0.702	SG
3, 10	1-1/2	5	6-1/2	0.702	ENR
1, 11	1/2	1-1/2	3	0.444	GMR
4, 12	3	3-1/2	4-1/2	0.444	SG
5, 7	3	4-1/2	6	0.444	ENR

The apparent harshness of the coral concretes was further demonstrated in the construction of walls when the forms were stripped at 7 days age. For example, Figure B-4 shows a typical San Gabriel concrete wall immediately after the forms were stripped and Figure B-5 shows a typical coral concrete wall after the forms were stripped. Although the apparent consistencies were the same, the coral concretes did not flow down into the foundation of the wall as well as did the San Gabriel concrete. This occurred even though the spud vibrator was applied internally to the concrete as well as externally to the form.

During the first 7 days of curing, the forms of each wall remained in place, and burlap was placed across the top of the walls for moisture retention. The burlap was kept wet by means of water spray. On the 7th day, after the forms were stripped from each wall, the voids, as shown in Figure B-5, were filled in with appropriately designed fresh concrete. On the 8th day each wall was rubbed down with mortar employing the same fine sand that had been used in the concrete mix for each particular wall. The walls were then completely wrapped in burlap, which was kept soaking wet. On the 28th day after placing, the walls were stripped of burlap, and 3-inch-diameter by 6-inch concrete cylinders for determining compressive strength were placed along the walls as shown in Figure B-6. When the last walls to be cast (GMR) had achieved an age of 30 days, the first application of sea water was made to the seaward side of each wall on 15 June 1961 for a 5-minute interval once each day at 0830. The sea water was obtained from the NCEL sea-water well.

When the GMR walls were 29 days old, the first set of monthly photographs was taken for the purpose of a statistical evaluation of time-dependent deterioration. On 7 July 1961, considerable efflorescence was noted on Walls 6, 9, and 11. Outside of this, no deterioration of the walls has been noted as of June 1962. The tests will continue.

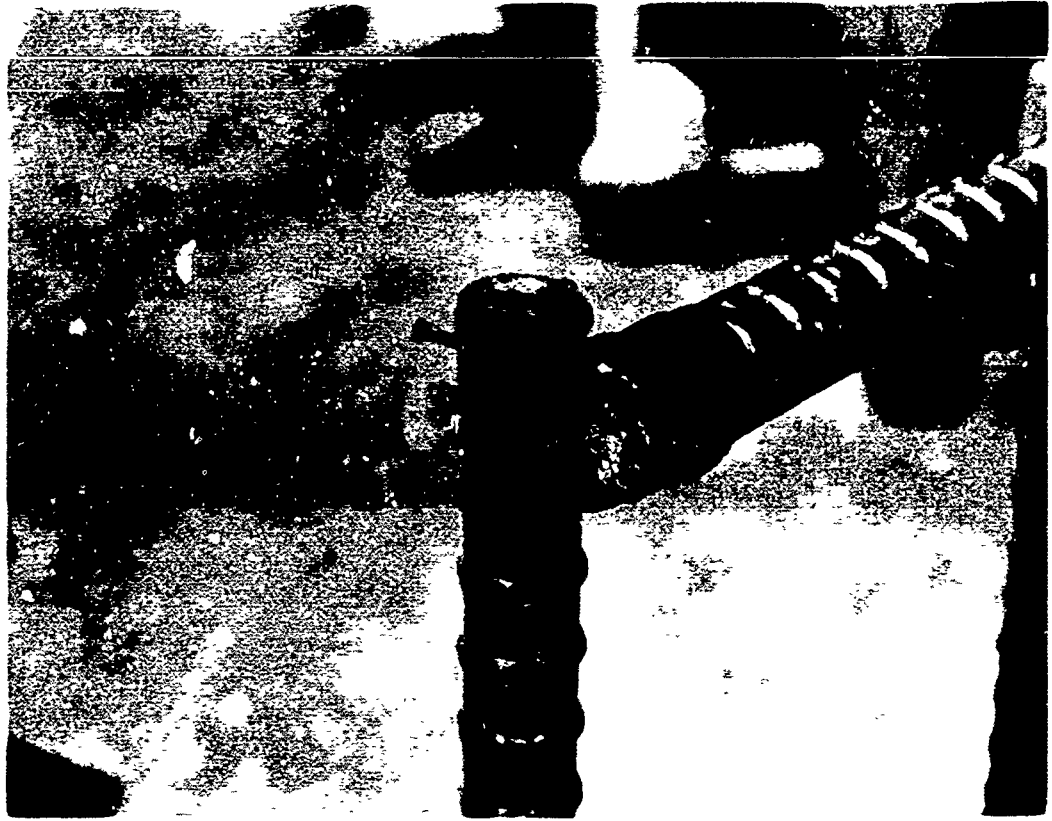


Figure B-1. Details of steel insulation.

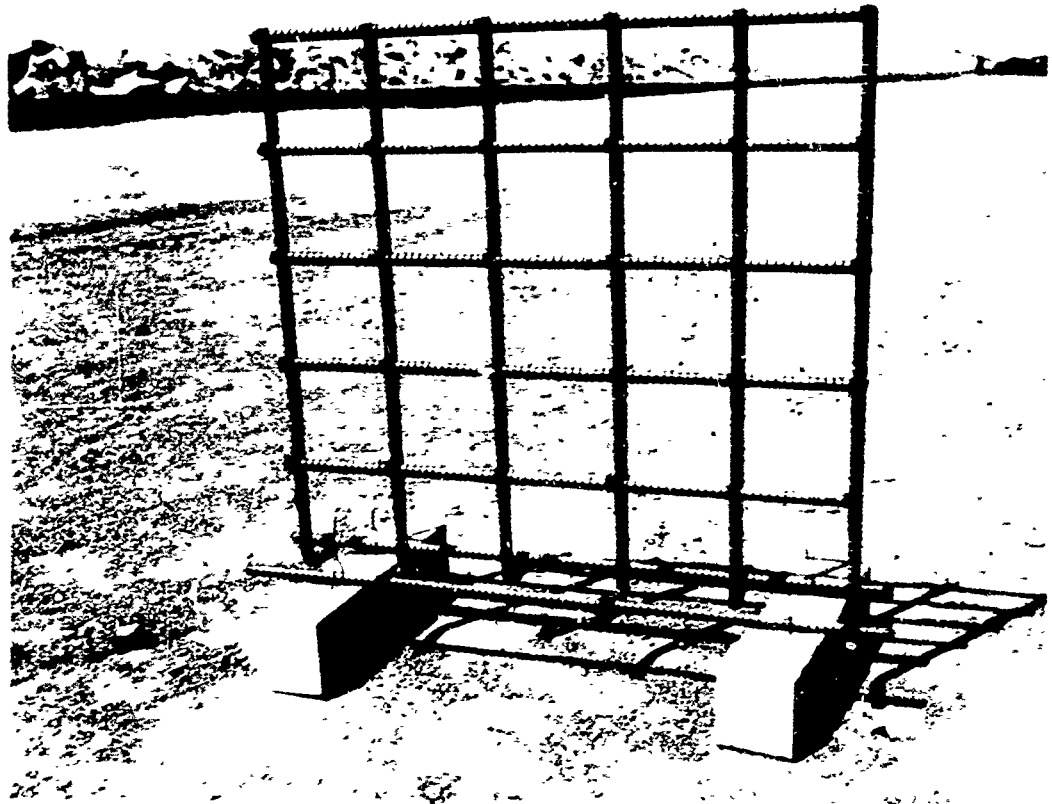


Figure B-2. Concrete supports for steel grids.

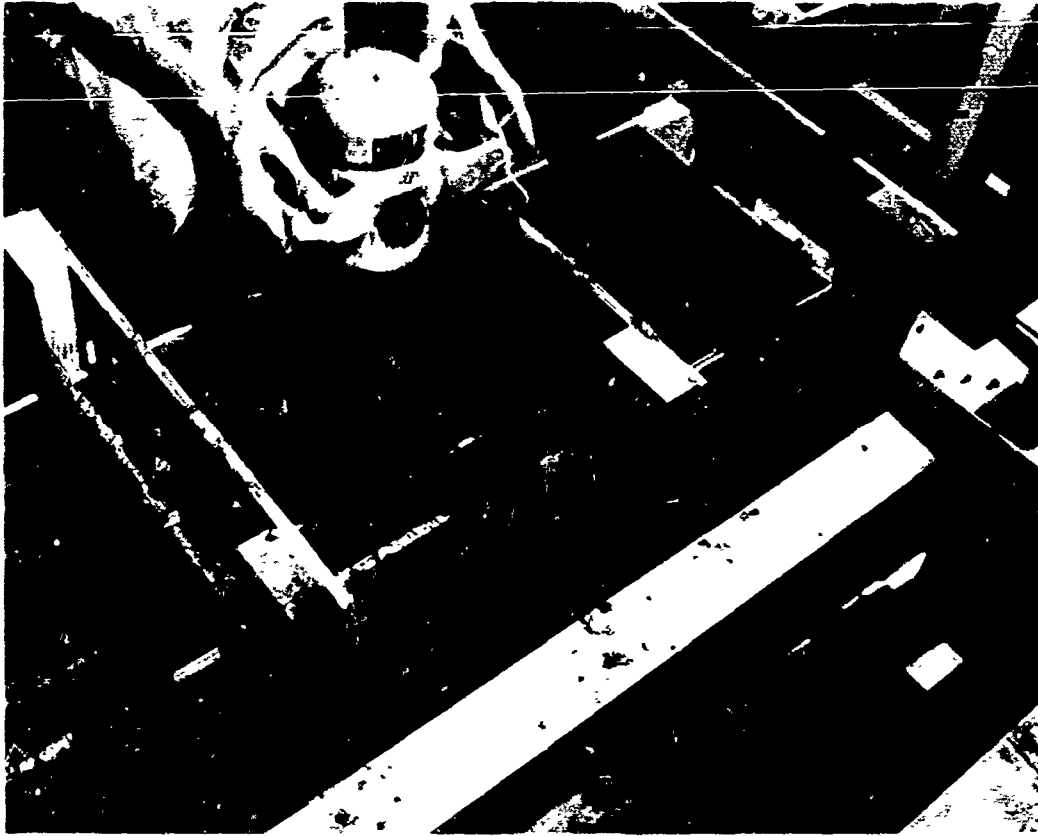


Figure B-3. Temporary devices for holding steel grids in forms.

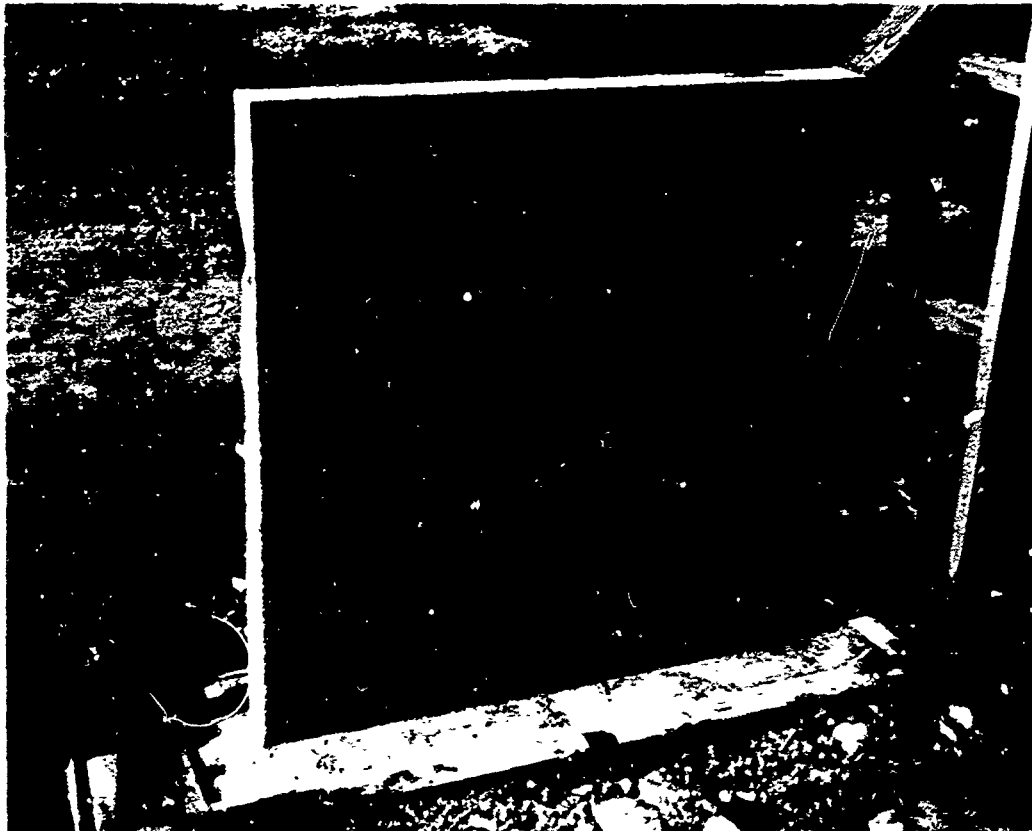


Figure B-4. San Gabriel wall after stripping forms.



Figure B-5. Coral concrete wall after stripping forms.



Figure B-6. Overall view of experimental walls.

Appendix C

CORROSION-DETECTION PROBE (All the material in this appendix is reprinted from TR-217)

Corrosion-Detection Probe

The use of a Corrosometer, an electrical-resistance corrosion-rate detection probe and metering device, to measure directly the degree of corrosive environment of reinforcing steel occurred to the authors. The efficacy of the Corrosometer and probes as a corrosion-detection device had been investigated previously.⁷ Consequently, probes fabricated of mild steel of the type shown in Figure C-1 were obtained for this purpose. The phenolic-resin potting cylinder shown in this figure was made just long enough to extend about 1/2 inch into the concrete. The probes were inserted into the fresh concrete through a hole in the wall of the cylindrical steel mold of the concrete cylinder. In order to do this, a cap was fastened across the top of the cylinder immediately after the concrete was cast. The cylinder was laid on its side, the plug unscrewed from the hole, and the probe inserted. The cylinder was then replaced in its as-cast position and placed in the fog room. The exterior end of the probe was protected by a small rubber sheet fastened around it.

The operation of the Corrosometer is based on the fact that the electrical conductivity of most metals is very great, while the conductivity of nonmetals is negligible by comparison. As the corrosion process converts metal into nonmetal, the electrical resistance of a piece of metal thus increases. The Corrosometer circuit utilizes this change of resistance to indicate the extent of penetration in an exposed metal specimen as corrosion proceeds on its surface.

The resistance of this exposed specimen is not measured directly by the Corrosometer circuit. Instead, a second specimen, made from the same metal or alloy, is connected in series with the first and the two specimens are made part of a bridge circuit. The second specimen is covered with a highly corrosion-resistant coating and so retains its original cross section and resistance. The ratio of the resistance of the exposed specimen to that of the covered specimen is then determined. Changes in this resistance ratio are translated directly into units of corrosion by the meter circuit.

By using a circuit which measures only the ratio of the two resistances, the measurements are made essentially independent of the current used to energize the bridge. Likewise, because temperature changes affect the resistance of both exposed

and covered elements in the same manner, the resistance ratio and the meter reading are independent of the temperature of the environment. It is this self-compensating feature of the bridge arrangement that permits the high degree of precision and sensitivity attained by the Corrosometer.

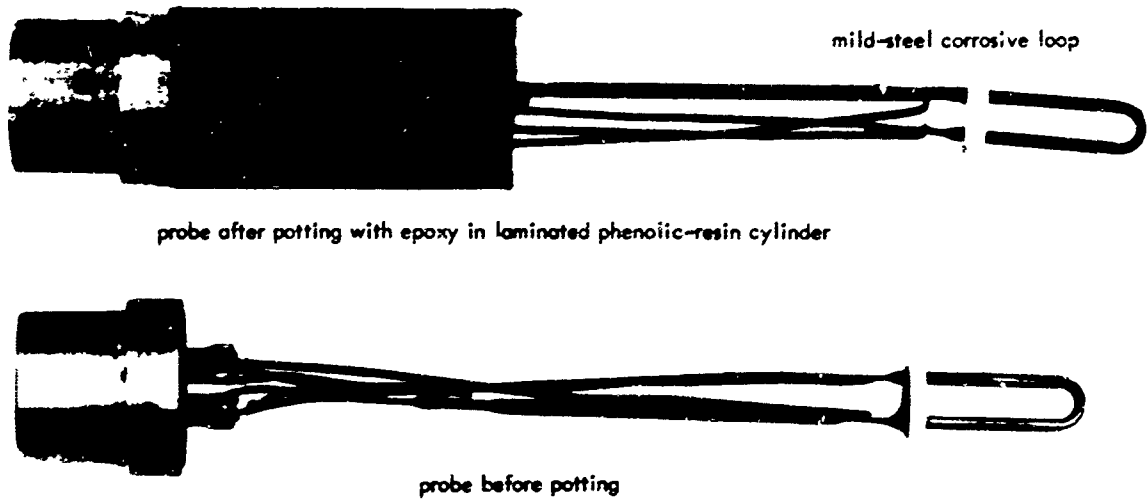


Figure 13. Electrical-resistance corrosion-rate detection probe.

Figure C-1. Electrical-resistance corrosion-rate detection probe.

ATTACHMENT 6
RESPONSE TO COMMENTS
